Final Thesis

by Rk S

Submission date: 04-Dec-2025 06:26AM (UTC+0530)
Submission ID: 2834904397
File name: Final_Thesis.pdf (6.78M)
Word count: 27948
Character count: 159301

CHAPTER 1

INTRODUCTION

1.1 General Introduction

Automotive suspension system is among the most important subsystems that help to maintain stability, ride comfort and safety of a vehicle. The leaf spring is one of its many parts used as a load bearing and energy absorbing component of the vehicle, being used to carry the static load of the vehicle as well as absorbing shocks and vibrations caused by irregularities in the road surfaces. The leaf spring has been in commercial and heavy vehicle applications over the decades due to its simple design and self-damping property [1].

These springs are traditionally made out of high-carbon or alloy steels, which are sufficiently strong and stiff yet have a number of limitations [2]. The reason is that the high self-weight of steel contributes a lot to the unsprung mass of the vehicle leading to high fuel consumption and low vehicle ride quality [1-3]. Moreover, their reliability and cost-effectiveness are limited by a high level of corrosion, short fatigue in cyclic loading, and frequent maintenance.

Over the past few years, the automotive industry has shifted evidently towards lightweight structural design in a bid to enhance fuel economy, payload capacity and dynamic performance and achieve greater emissions standards. The

change is centered on the materials and structural concepts that provide superior specific strength, corrosion resistance, and durability and are lighter [4].

As a result, researchers have thus explored the use of complex material structures such as fiber-reinforced polymers (FRP), metal-matrix composites (MMCs) and more recently, functionally graded material (FGMs) as alternative material replacements of conventional steels. They are highly stiff-to-weight ratio, more fatigue-resistant materials, and may alter the design of suspensions through the establishment of custom mechanical and damping characteristics.

1.2 Need for Light weight and High-Performance Leaf Springs

This is because reducing unsprung mass has been found to be very effective in enhancing the performance, fuel economy of the vehicle, as well as passenger comfort. Other components like the leaf spring provide contact between the chassis and the wheels and add a lot of mass. The decrease of the weight of these components results in tangible improvements in the quality of the ride, handling, and braking. The lighter parts also reduce vibration to the body of the vehicle. One of the engineering goals of a commercial and heavy-duty automobile is to optimize weight without sacrificing strength [1]. These suspension systems operate under dynamic constant loading.

Traditional steel leaf springs, which have been in existence a long time, have a number of drawbacks. Their density is very high about 7.8 g/cm^3 that doubles the weight of the vehicle and it negatively impacts fuel consumption [2]. They also have a tendency to corrode, have low fatigue strength and require periodic maintenance so

that they do not start cracking in cyclic stresses. Besides, the rigidity of steel does not allow it to be flexible to the current design techniques, which aim at flexible energy-absorbing behave our and utilization of less material.

In order to eliminate these drawbacks, studies and industrial activities have focused on lightweight metallic materials, especially alloy of aluminium. These alloys are significantly lighter than steel, which allows them to achieve a huge mass reduction without losing sufficient stiffness and strength after heat treatment (approximately a third of the density of steel is required) [5]. They are also well corrosive resistant and highly reusable and satisfy the performance and environmental requirement.

Late progress on metal-matrix composite (MMC) technology has widened structural applications of lightweight alloys. The incorporation of ceramic particles or fibre in the metallic matrix forms composites that have a high ratio of strength to weight. This is also better in the elastic modulus and wear and fatigue resistance [6, 7]. The above characteristics have rendered aluminium-based metal-matrix composites (AMCs) suitable to substitute steel in load and suspension components. Examples here are the leaf springs where it is important to have stiffness and resilience and durability over a long period. The current trend of replacing the conventional steel with lightweight metallic and composite suspension system is a balance between the sustainability, performance and fuel economy in the next generation car manufacturer.

1.3 Motivation

The current demand of strong, lightweight, and energy-efficient materials has transformed the modern design of transportation. There is an increasing demand in the automotive and aerospace sectors to use components with low mass and high fatigue and wear resistance, to enhance the total durability and fuel efficiency [8].

The technology in India is in accordance with the vision of the country industrial growth, which has been launched in the year 2014 by the Hon. Prime Minister Shri Narendra Modi through the Make in India campaign. By boosting the manufacturing industry contribution in the GDP of India by at least 25 percent against about 16 percent, and encouraging local design and cutting-edge material development, the program focuses on ensuring that India becomes a global manufacturing destination [9]. Global Manufacturing Competitiveness Index (2018) by the World Economic Forum classified India in the 30 th position globally. India is expected to develop further in the fields of engineering and technology based upon innovation such as development of materials research that will enhance self-dependence (Atmanirbhar Bharat) and less dependence on foreign parts.

In this context, the creation of light-metal composites is technologically as well as strategically of importance. Yet, in spite of the fact that monolithic aluminium alloys have a high mass saving over steel, their wear and fatigue behaviour under cyclic loads is poor [10]. Ceramic reinforcement, including boron carbide (B4C) is a potent way to enhance hardness, tensile strength, and tribological behaviour by increasing load-transfer efficiency and alleviating localised deformation [11]. Al 7075 is one of the most common aluminium alloys exhibiting

high specific strength, good heat-treatability as well as machinability, hence is a good matrix in advanced composites [12].

However, metal-matrix (homogeneous) composites have non-uniform distribution of stress in bending thus causing early fatigue failure. A solution can be found in the Functionally Graded Material (FGM) concept whereby reinforcement concentration changes on a layer-by-layer basis, that is, a higher stiffness on the surface and a higher ductility on the neutral axis [8].

The thesis aims at designing and manufacturing a layer-graded Al 7075/ B_4C composite leaf-spring plate by utilizing a less expensive stir-casting and gravity-die methodology. It focuses on the creation of an indigenous, lightweight, and high-performance suspension component that would outperform the traditional materials in terms of attaining high stiffness and stress distribution as well as fatigue resistance. This development is part of the vision of self-reliant state-of-the-art manufacturing in India in the Make in India and Atmanirbhar Bharat programs [9].

1.4 Material and Conceptual Background

1.4.1 Composite Materials

Composite materials are engineered by combining two or more distinct constituents so that the resulting material exhibits properties superior to those of the individual components. These constituents differ significantly in their physical, chemical, and mechanical characteristics; however, when combined, they form a material system whose performance is tailored for specific engineering applications [13, 14].

Several natural materials around us demonstrate the concept of composites.

For example, wood is a natural composite consisting of a lignin matrix reinforced with cellulose fibres, which provide strength and stiffness [15, 16]. Similarly, bone is a biological composite in which a collagen matrix is reinforced with hydroxyapatite crystals, resulting in a combination of toughness and rigidity [17].

Composite materials differ fundamentally from mixtures, alloys, and solid solutions. Unlike alloys, where constituents dissolve into one another at the molecular level, composites retain their individual identities. The matrix and reinforcement coexist but do not chemically merge; instead, they synergistically contribute to the overall mechanical and functional performance of the final material [18, 19]. Microscopic examination clearly reveals the distinct phases, confirming the heterogeneous nature of composites.

In any composite, one constituent acts as the matrix, which is usually a continuous and ductile phase responsible for binding the reinforcement. The other constituent acts as the reinforcement, which may appear as particles, fibres, whiskers, or platelets, and is embedded within the matrix to enhance properties such as strength, stiffness, hardness, and thermal stability [20, 21]. Typically, the matrix offers ductility, toughness, and thermal conductivity, while the reinforcement provides high strength, low thermal expansion, and improved rigidity [22].

Based on the nature of matrix and reinforcement, composites can be broadly classified into categories such as fibre-reinforced composites, particle-reinforced composites, and structural composites, which are discussed in the subsequent sections

1.4.2 Classification of Composites

Composites can be broadly classified into the following two categories:

1. **Based on Reinforcement**
2. **Based on Matrix**

The classification based on reinforcement is illustrated in Figure 1.1, while the classification based on matrix is shown in Figure 1.2.

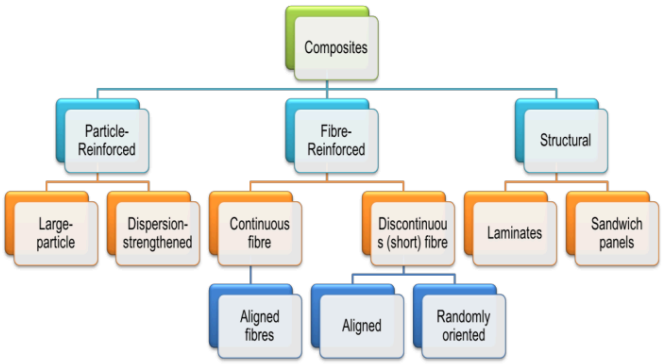

Figure 1.1: Classification based on reinforcement

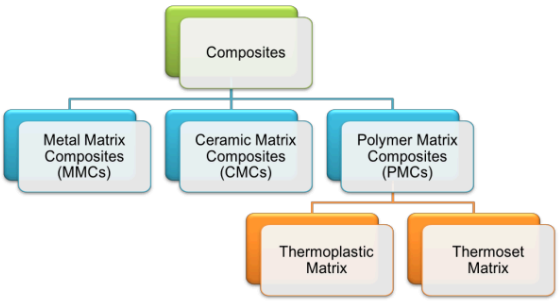

Figure 1.2: Classification based on Matrix

1.4.3 Metal Matrix Composites (MMCs) and Their Engineering Significance

Metal Matrix Composites are a class of advanced materials in which a metallic matrix is reinforced with ceramic particles, whiskers, or fibres to achieve superior mechanical and functional properties compared to monolithic metals. Typical matrix materials include aluminium, magnesium, titanium, copper, and their alloys, while common reinforcements consist of silicon carbide (SiC), aluminium oxide (Al_2O_3), boron carbide (B_4C), titanium carbide (TiC), and carbon fibres. The combination of a ductile metal matrix and a stiff, hard reinforcement phase provides MMCs with an exceptional balance of strength, toughness, and thermal stability [23-24].

MMCs possess some benefits over traditional metals such as improved specific strength, high stiffness-weight ratios, higher wear resistance, lower coefficient of thermal expansion as well as a higher fatigue performance. These features render MMCs especially appealing to be used in structural and functional applications where it is required to work with high loads, high temperatures, or abrasive environments. Compared to polymer matrix composites, MMCs do not degrade during thermal cycling and have excellent dimensional stability, which is why they are used in parts that experience intermittent mechanical and thermal loads [25].

Aluminium-based metal matrix composites out of existing MMC systems have also gained a large industrial interest because of low mass density, high thermal conductivity, and the ability to co-exist with a large variety of ceramic reinforcements [24-25]. The Aluminium MMCs are customizable, with reinforcement type, size and volume fraction, so that the engineers can create

materials with very specific uses of performance. Consequently, AMCs have wide applications in aerospace fittings, automotive brake rotors, pistons, connecting rods, bicycle frames, defence armour systems and high-performance electromechanical components [26].

The other significant benefit of MMCs is that they can offer a graded distribution of reinforcements using highly developed processing pathways, including centrifugal casting, stir casting, powder metallurgy, and additive manufacturing. This has allowed the creation of Functionally Graded Materials (FGMs), with the concentration of reinforcement spatially graded in order to create location-dependent characteristics. This graded structure decreases interfacial stresses, increases impact resistance, and increases load transfer between layers, is especially important in components i. e. leaf spring, turbine blade, armour plates, biomedical implants.

Overall, MMCs are important in the ensuring engineering practice because of their enhanced mechanical behavior, high thermal, and design flexibility. Their flexibility to graded architectures also increases their possibilities when it comes to the applications of the optimum stiffness, strength and fatigue behaviour. This renders MMCs, in particular the aluminium-based systems the most convenient materials to develop lightweight and high-performance automotive suspension components like the functionally graded Al7075/B_4C leaf spring that will be discussed in the current research work.

1.4.4 Aluminium Matrix Composites (AMCs)

Aluminium Matrix Composites (AMCs) are a class of advanced materials in which a

lightweight aluminium or aluminium-alloy matrix is reinforced with a secondary phase such as ceramic particles, fibers, or whiskers. Depending on the geometry and distribution of the reinforcement, AMCs are broadly classified as particulate reinforced, fiber-reinforced, or laminar composites. Among these, particulate reinforced AMCs are most widely developed because they combine near-isotropic behaviour with economic scalability for bulk components.

The key advantages of AMCs include:

- Low density leading to a high specific strength and stiffness compared with steels or bronzes.
- High elastic modulus and enhanced fatigue resistance, enabling weight reduction without sacrificing mechanical integrity.
- Superior wear and corrosion resistance, attributed to the hard, stable ceramic phase embedded in the aluminium matrix.
- Excellent thermal stability and dimensional control, making them suitable for elevated-temperature service conditions such as engine, brake, and suspension components.

These properties collectively make AMCs ideal candidates for automotive, aerospace, and defence applications that demand a combination of light weight and high performance.

1.5 Discrete Boron Carbide Reinforced Aluminium 7075 Composite FGM for Leaf Spring Applications

1.5.1 Aluminium 7075

The selection of a suitable matrix material is a critical step in the development of metal matrix composites (MMCs), particularly for structural applications such as automotive leaf springs. Aluminium is one of the most abundant elements in the Earth's crust (approximately 8 wt.%), making it readily available and economically viable for large-scale engineering use. Owing to its excellent formability, high strength-to-weight ratio, good flexural strength, durability, and corrosion resistance, aluminium and its alloys are widely employed in transportation, aerospace, and mechanical systems where lightweight design is essential.

Table 1.1: Classification of Aluminium Alloy Series Based on Major Alloying Elements

Series Number	Description (Major Alloying Element)
1xxx Series	Pure aluminium alloys (≥ 99% Al), excellent corrosion resistance and electrical conductivity.
2xxx Series	Aluminium–copper alloys; high strength, heat-treatable, used in aerospace applications.
3xxx Series	Aluminium–manganese alloys; good workability and corrosion resistance, non-heat-treatable.
4xxx Series	Aluminium–silicon alloys; improved wear resistance and lower melting point, used in welding and casting.
5xxx Series	Aluminium–magnesium alloys; high strength-to-weight ratio, excellent corrosion resistance.
6xxx Series	Aluminium–magnesium–silicon alloys; heat-treatable, good formability and extrudability.
7xxx Series	Aluminium–zinc alloys; very high strength, used in aerospace and high-performance structural parts.
8xxx Series	Other aluminium alloys (e.g., Al–Li, Al–Fe, Al–Ni), developed for specialized applications.

Aluminium can be alloyed with several elements, including zinc, silicon, magnesium, manganese, and copper, to tailor its mechanical and thermal properties. These alloys are classified into series based on their primary alloying element, as shown in Table 1.1. Among them, the 7xxx series, where zinc is the principal alloying element, offers exceptionally high strength and hardness after heat treatment [27]. Aluminium 7075, a representative alloy of this series, is therefore an excellent candidate for high-performance components such as leaf springs, where weight reduction, stiffness, and fatigue resistance are crucial.

1.5.2 Boron Carbide (B4C) as Reinforcement

For a particular matrix material in composite, reinforcement selection is based on its compatibility and adaptability with the matrix. The suitable reinforcement for the various matrix materials is shown in Table 1.2.

Table 1.2: Common Reinforcements and Compatible Metal Matrices in MMCs

Reinforcement Type	Compatible Metal Matrices
Boron fibre (including coated)	Titanium, Aluminium
Alumina particulates (Al_2O_3)	Magnesium, Aluminium
Boron carbide particulates (B_4C)	Magnesium, Aluminium
Silicon carbide particulates (SiC)	Magnesium, Aluminium
Silicon carbide whiskers (SiCw)	Magnesium, Aluminium
Alumina fibres	Magnesium, Aluminium
Alumina–silica fibres	Aluminium
Silicon carbide fibres (SiCf)	Titanium, Aluminium
Graphite fibres	Aluminium, Magnesium, Copper

Common reinforcements employed in AMCs include silicon carbide (SiC), alumina (Al_2O_3), titanium carbide (TiC), and boron carbide (B_4C). The mechanical improvement in AMCs arises from several strengthening mechanisms:

- **Load-transfer mechanism**, in which applied stresses are efficiently transferred from the ductile matrix to the stiff ceramic particles.
- **Orowan looping**, where dislocations bypass the hard reinforcement particles, increasing yield strength.
- **Grain refinement**, produced by particle-stimulated nucleation during solidification, enhancing hardness and fatigue life.

Among the available reinforcements, B_4C is particularly attractive because of its extremely high hardness, low density (2.52 g/cm^{-3}), and strong interfacial compatibility with aluminium alloys, providing an optimal strength-to-weight ratio for dynamic components.

1.6 Fabrication Approach

Several fabrication techniques exist for AMCs, including powder metallurgy, squeeze casting, in situ reaction, and liquid-state methods. Among these, stir casting has emerged as the most cost-effective and industrially scalable route for producing particulate reinforced AMCs. The process involves mechanical stirring of preheated ceramic particles into a semi-solid aluminium melt, ensuring reasonably uniform dispersion before casting into a desired mould. The simplicity, adaptability to conventional foundry equipment, and suitability for large components make stir casting particularly appropriate for manufacturing automotive parts such as brake rotors, connecting rods, and leaf springs [28].

1.6.1 Functionally Graded Materials (FGMs)

Functionally Graded Materials (FGMs) are a special class of composite materials in which the composition or reinforcement content varies gradually through the thickness, resulting in a continuous change in microstructure and properties across the section as shown in figure 1.3. This gradation concept was first proposed in the 1970s for polymeric materials and later implemented in metals and ceramics in Japan during the 1980s. Natural structures such as bamboo, bone, and teeth exhibit similar graded architectures that inspired the design of engineered FGMs for improved multifunctional performance.

In FGMs, the compositional or microstructural gradient may follow linear, exponential, or power-law distributions, enabling the material to meet localized performance requirements such as high strength on one surface and high toughness or damping on the other. This smooth transition eliminates sharp interfaces common in conventional laminated composites and provides better mechanical continuity under thermal or mechanical loading.

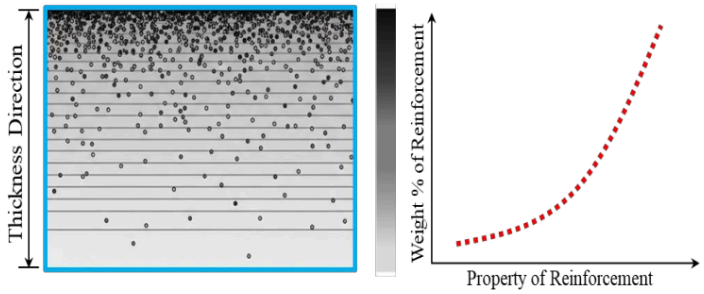

Figure 1.3: Schematic representation of a functionally graded material showing gradual variation of reinforcement content through thickness.

1.6.2 Benefits of FGMs

FGMs exhibit several distinct advantages over traditional composites:

- **Reduced interfacial stress:** The smooth variation of composition minimizes stress concentrations and delamination at layer boundaries.
- **Enhanced mechanical and thermal compatibility:** Gradual transition between metal and ceramic phases improves bonding, reduces residual stresses, and enhances wear and fatigue resistance.
- **Improved service reliability:** The material can withstand severe thermal or mechanical gradients, resulting in longer fatigue life and stable dimensional performance.
- **Tailored property distribution:** Local mechanical, thermal, or electrical properties can be customized for specific functional zones (e.g., high stiffness on outer layers, high damping at the core).

Table 1.3: Comparison of FGMs and conventional composites (interfacial bonding, stress gradient, fatigue performance, and cost)

Aspect	Functionally Graded Materials	Conventional Composites	Key Citations
Interfacial Bonding	Continuous composition gradient eliminates sharp interfaces; superior damage tolerance; reduced delamination and debonding.	Sharp interfaces create stress discontinuities; prone to debonding, delamination, and lower interfacial stability.	[29-31]
Stress Control	Graded modulus redistributes stresses; minimizes edge singularities and peak stresses at holes/notches.	Abrupt stiffness changes cause high stress concentrations at ply drops and layer boundaries.	[32-34]
Fatigue Performance	Lower interfacial stress amplitudes delay crack initiation and slow propagation; enhanced high-cycle fatigue life.	Early fatigue damage at interfaces; rapid accumulation of matrix cracking and delamination.	[35-37]
Cost & Manufacturing	Higher cost; specialized processes (AM, graded PM, centrifugal casting); complex QC and gradient verification.	Lower cost; mature processes (RTM, stir casting, lay-up); easier QC and scalability.	[38-40]

These benefits make FGMs particularly valuable for high-performance components requiring strength, wear resistance, and thermal stability, such as those found in automotive suspensions and aerospace systems. A detailed comparison of FGMs and conventional composites has shown in table 1.3.

1.6.3 Applications of FGMs

FGMs are increasingly used in engineering systems that demand a smooth transition of properties, such as stiffness, toughness, thermal resistance, or biocompatibility - to withstand multi-functional loading environments. Their ability to combine the advantages of ceramics and metals makes them suitable across a wide range of industries [41-42].

• *Aerospace:*

FGMs are used in thermal barrier coatings, turbine blades, rocket propulsion chambers, and re-entry vehicle nose cones, where gradual thermal resistance is essential.

• *Automobiles & Mechanical Engineering:*

Applications include brake rotors, cutting tools, wear-resistant liners, and leaf spring plates with tailored stiffness gradients, enhancing fatigue life and load distribution.

• *Defence:*

Used in armour plates, projectile structures, and blast-resistant components requiring a ceramic–metal property transition.

• *Nuclear Energy:*

FGMs provide enhanced performance in reactor control rods, shielding layers, and high-temperature structural components due to their tolerance to thermal shocks and neutron flux.

• *Energy Conversion Systems:*

Applied in corrosion resistant lining of reactors, vessels that need to withstand the heat and catalytic structures where graded chemistry enhances wear.

• *Chemical and Process Industries:*

Used for corrosion-resistant reactor linings, heat-resistant vessels, and catalytic structures where graded chemistry improves durability.

• *Electronics & Optics:*

FGMs permit graded dielectric substrates, optical lenses; thermal stress reduced electronic packages, and infrared domes.

• *Biomedical & Biomaterials:*

The FGMs have found extensive use in orthopedic implants, dental prostheses, and bone-like structures, where the biocompatible outer shells give way to cores made of tough metals.

• *Commodities & General Engineering:*

The FGMs have been used in cookware, wear-resistant surfaces, sporting goods and structural components that need functional transitions that are customized.

The large area of the use of FGMs has demonstrated in figure 1.4. Such wide-ranging applications indicate that FGMs fill the discontinuity between brittle ceramics and ductile metals, with the provision of multidisciplinary mechanical, thermal, and functional functionality.

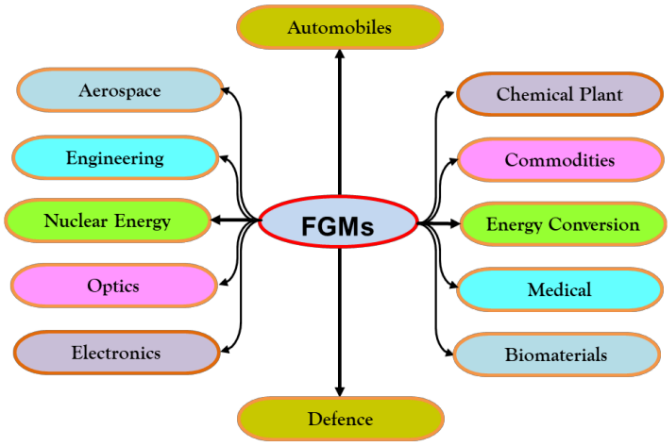

Figure 1.4: Applicable fields for FGMs

1.7 Relevance to Present Work

The concept of FGM has been used in the current study to manufacture a five-layered graded leaf spring plate using Al 7075-B_4C alloy. Higher reinforcement (16 wt. %) of the outer layers offers better stiffness and wear resistance whereas the inner layer has lower B_4C (8 wt. %) to give ductility and toughness. This type of gradation plan contributes to the stiffness to weight ratio, reduces residual stresses and provides long fatigue life-key performance to lightweight, high-performance suspension systems.

1.7.1 Integration of FGM Concept with Al 7075/B_4C System

The Functionally Graded Material (FGM) concept in conjunction with the Al 7075/B_4C system is a strategic path forward in dealing with the weakness of both monolithic alloys and homogeneous metal-matrix composites. Al 7075-T6 offers a

high strength/weight ratio, high corrosion resistance and excellent heat-treatability, whereas B_4C reinforcement offers superior hardness, wear resistance and low density. But in a case whereby the B_4C particles are evenly dispersed, the composite is likely to develop interfacial brittleness and localized stress concentration, which results in early crack initiation with cyclic loading. A graded distribution of B_4C through the plate thickness can be introduced to enable the upper layers to carry greater bending and compressive loads and leaving the inner layers in the green to have a ductile response, resulting in a balanced structural response and longer fatigue life. The incorporation of the concept of FGM and Al 7075/B_4C composite design has been demonstrated in figure 1.5.

Figure 1.5: Schematic depicting incorporation of the FGM concept into Al 7075/B_4C composite design.

1.7.2 Concept of Five-Layer Gradation

A five-layered gradation scheme was constructed to match the bending-stress profile of the leaf-spring plate with a reinforcement contents of 16/12/8/12/16 wt. B_4C contents from the top to the bottom surfaces. The top layers (16 wt. percent) are very rigid and wear resistant, the middle layers (12 wt. percent) guarantee stress transfer

continuity, and the bottom layer (8 wt. percent) maintain ductility and energy absorptive capacity. Such an arrangement provides a continuous modulus change and hardness, which prevents interfacial discontinuities and sharp drops in stiffness.

1.7.3 Expected Advantages of the FGM Leaf-Spring Design

The addition of the graded structure to the Al 7075 -B_4C system is likely to provide the following main performance improvements:

- *Less Deflection*: Stiffness of the outer layers increases to reduce the maximum deflection during both the static and dynamic loading.
- *Better Damping:* The difference in elastic modulus and particle dispersion is enhanced, which enhances the capacity of energy-dissipation and results in enhanced vibration control.
- *Best Fatigue Endurance:* Variation of the reinforcement produces gradual suppression of crack initiation and propagation that extends the fatigue life as compared to homogeneous MMCs.
- *Improved Residual-Stress Distribution:* The graded structure produces self-balancing compressive stress-tensile stress field, which prevents delamination and fatigue cracking.

Therefore, the FGM leaf-spring plate with Al 7075/B_4C alloys is an optimal solution of light weight, stiffness and durability as applied to sophisticated suspension systems.

1.8 Fabrication and performance challenges

The effective production of Al 7075/B 4C functionally graded composites by stir casting is an undertaking full of scientific as well as technological challenges that directly affect the microstructure, bonding strength and the ultimate mechanical property. A controlled gradation in reinforcement and maintenance of metallurgical soundness across the layers is only possible with a high level of control of the processing variables and post-treatment conditions.

1.8.1 Uniform Dispersion of B_4C Particles in Molten Al 7075

One of the foremost challenges during stir casting is obtaining a uniform dispersion of B_4C particles within the molten aluminium matrix. B_4C, being extremely hard and lightweight, tends to float on the molten surface or settle at the crucible base depending on the stirring energy and wetting conditions. The difference in density between Al (2.81 gcm^{-3}) and B_4C (2.52 gcm^{-3}) further complicates homogeneous distribution. Poor wettability between Al and B_4C can cause clustering or particle segregation, which degrades the mechanical performance of the composite. To diminish this, preheating of B_4C particles, surface activation using K_2TiF_6 flux, and argon gas shielding are adopted to enhance interfacial bonding and improve particle incorporation during mechanical stirring.

1.8.2 Maintenance of Metallurgical Bonding between Graded Layers

In functionally graded configurations, maintaining metallurgical bonding between successive layers is a critical requirement. Each layer is poured at a controlled semi-solid temperature so that the previously cast layer partially remelts to form a diffused

interface. Inadequate bonding leads to micro-voids or weak transition zones that act as crack-initiation sites under cyclic stress. Thus, pouring temperature control, layer-solidification timing, and mould preheating are essential to ensure strong interlayer cohesion. Post-fabrication heat treatment further enhances diffusion bonding and relieves residual thermal stresses at the interfaces.

1.8.3 Control of Porosity, Agglomeration, and Density Gradient

Porosity and agglomeration are inherent risks in liquid-state processing. Entrapped gases from strong stirring or incomplete particle wetting can lead to pores, reducing load-bearing capacity and fatigue resistance. Similarly, excessive clustering of B_4C particles creates local density variations and micro-hardness gradients that compromise stress uniformity. A typical casting defects and their causes has depicted in figure 1.6. Optimization of stirring speed, duration, and particle feeding rate, along with degassing of the melt using inert gas purging, are crucial for minimizing these defects. Proper control of these parameters yields a smooth and consistent density gradient required for the desired functional gradation.

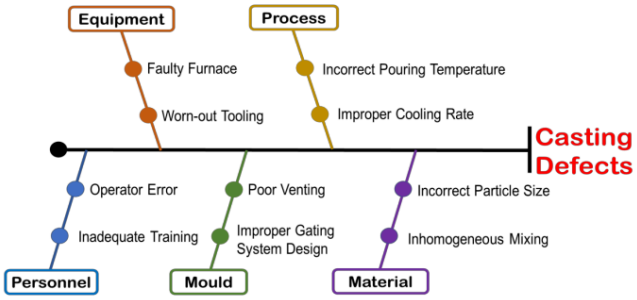

Figure 1.6: Typical casting defects and causes

1.8.4 Optimization of Casting Parameters and Heat Treatment Influence

Process parameters that determine the mechanical properties and microstructural integrity of the fabricated FGMs very strongly include stirring temperature, impeller speed, and dwell time.

Temperature: A low temperature level boosts viscosity and hinders incorporation of particles and a high temperature level leads to oxidation and entrapment of gases.

Speed and Time Stirring: Low stirring performance leads to lack of dispersion, and high stirring performance leads to the formation of vortices and oxidation.

Dwell Time: Determines suspension and bonding of uniform particles and interfaces.

Post-fabrication T6 heat treatment (solutionizing → quenching → artificial aging) greatly changes the microstructure, dissolving the precipitates and strengthening the matrix and increasing particle- matrix adhesion.

T6 process results in smaller precipitate distribution, enhanced hardness, and enhanced yield strength, hence enhanced performance of the graded composite.

1.9 Significance and Novelty of the Present Work

The current study has shown potential proof of a cost-efficient and scalable fabrication pathway producing functionally graded Al 7075/B_4C composites via a hybridized gravity-die + stir-casting technique. It allows the accurate control of reinforcement (16/12/8/12/16 wt % B_4C) in layers and still have metallurgical bonding by pouring and further T6 heat treatment. The method used is easier to process and cheaper as well as more appropriate on large structural components like automotive leaf-spring plates compared to conventional powder-metallurgy or

diffusion-bonding paths.

The microstructural (FESEM, EDS, XRD), mechanical, wear and dynamic-mechanical analyses along with finite-element and Taguchi optimization are combined in a complete experimental-computational method. This single process methodology authenticates the graded configuration and measures the relationship between process parameters and microstructure and performance.

The FGM leaf-spring plate developed has a better ratio of stiffness to weight, lesser deflection, and enhances damping and strength of fatigue than steel and uniform composites. Such improvements prove the usefulness of gradation to fit stiffness with the distribution of stress.

In general, the work offers a scientifically proven and productionally possible solution to lightweight, durable, and energy-efficient suspension parts and leads directly to the design of automobiles in the name of sustainability and national programs of the development of indigenous advanced-materials manufacturing.

1.10 Organization of the Thesis

The thesis consists of seven chapters, which logically cover the main issues of the fabrication, characterization, and optimization of the functional graded Al 7075/B_4C leaf-spring plate.

Chapter 1 provides the background, motivation, and need of lightweight, high-performance suspension materials. It demonstrates the gaps in the research, its goals and scope of the work, as well as the methodology used and the general outline of the thesis.

Chapter 2 gives a comprehensive literature review of the literature on the existent

knowledge on aluminium-matrix composites and the functionally graded materials. It critically analyzes the former fabrication techniques, mechanical and thermal behaviour research and optimization systems, and, therefore, pinpoints the particular research voids on which the current study is being founded on.

Chapter 3 explains experimental setup, raw materials and equipment involved in the fabrication of FGM leaf plate. It outlines the hybrid gravity and stir-casting process, gradient-evaluation process and entails T6 heat treatment parameters.

Chapter 4 reports the findings of the microstructural and phase study with the help of FESEM, EDS, and XRD in order to confirm the reinforcement distribution and interfacial bonding among graded layers.

Chapter 5 explains about the mechanical and dynamic behaviour of the fabricated composites once they have been heat treated. It associates process parameters with the hardness, tensile, impact and damping properties to determine the structure property associations.

Chapter 6 focuses on the computational modelling and optimization of the FGM leaf-spring plate. Finite-element simulations are used to evaluate stress, and deflection, while six possible models analyzed to identifies the optimal gradation configuration for improved performance.

Chapter 7 summarizes the major conclusions derived from the experimental and computational results and outlines the future scope for further extending the FGM concept to fatigue analysis and industrial applications in automotive suspension systems.

CHAPTER 2

LITERATURE REVIEW

2.1 Introduction

To make comfortable ride and to minimize various types of vibrations, bumps and impacts due to bad road conditions, springs play a crucial role in automobile industries. Leaf spring is the oldest suspension, used in automobiles. Revolution in design and manufacturing was introduced at the beginning of 19th century [1]. Leaf springs are fabricated as a stack of prismatic beams with longer lengths placed on top of each other. This design ensures that the spring is thicker at the middle to resist bending and thinner at the ends where it is attached to the vehicle body [2]. To improve load carrying capacity, these beams are initially pre-stressed [3]. The steels used for such leaf springs are primarily SAE 1095, SAE 5160, SAE 6150 and, SAE 9254 [3, 4].

During last few decades, automobile industries are attempting to use materials having high strength to weight ratio. This attempt will increase fuel economy of automobiles as well as meet the demands of natural resources conservation. The suspension leaf spring is one of the potential things for weight decrease in vehicles because it has 10 to 20 percent of the un-sprung weight [5]. Fortunately, fiber composites have excellent strength-to-weight ratio, higher natural frequency, superior fatigue strength which make them excellent for leaf spring [2-5].

However, demerits of fiber composite materials coming from discontinuous variation of properties at transition zone between two solids and delamination over a period of time. Demerits of fiber composite can be overcome by the use of low weight and high strength material i.e. metal matrix composite.

Metal matrix composites, particularly aluminum matrix composites, offer advantages like high strength, stiffness, thermal stability, low density, and improved wear resistance [6–9]. The metal matrix composites also provide better toughness and higher transverse properties compared to fiber composites. The group of metal matrix composites comprises different metals utilized as matrices like aluminum, magnesium, copper, and titanium. Different reinforcements have been utilized to accomplish desired properties. Albeit, each metal has remarkable applications best suit its properties however out of all, aluminium-metal matrix composites are the most broadly utilized composite materials [10, 11]. Aluminium matrix composites have striking properties, for example, lightweight, excellent corrosion resistance, high strength, low thermal expansion coefficient, great wear resistance, and simplicity of machining [12]. Aluminum7075, among various aluminium alloys, possesses the highest specific strength and toughness [13]. Similarly, in the reinforcement category Boron carbide is a charming reinforcement material because of its good chemical and thermal stability. Boron carbide has higher hardness and lower density compared to Silicon carbide and Aluminium oxide [14–16]. However, directional strength to weight ratio of aluminium matrix composites is lower than the fiber composites. It means that it is not a perfect replacement of fiber composite. Thus above discussions reveal that both aluminium matrix composites and fiber

composites will not be the perfect material for leaf springs. Although, aluminium matrix composites have one more advantage over fiber composite that its strength to weight ratio can be improved by tailoring in required direction this lead towards evolution of a modern material known as functionally graded material (functionally graded materials) using aluminium matrix composites.

Functionally graded materials are a class of microscopically heterogeneous materials in which the material compositions are designed to change material properties fluently over volume [17]. Generally solid based, liquid based and gas based methods are used to fabricate functionally graded materials [18]. There are various types of fabrication processes for producing functionally graded materials. Further, functionally graded materials can be divided majorly into two broad groups i.e. thin and bulk functionally graded materials. Coatings are considered into thin category; while bulk functionally graded materials have thick gradation, used for extreme environment. Bulk functionally graded materials are typically made out of two distinct materials, for example, metal and ceramic and they exploit the superior property from every constituent [17,19]. Bulk functionally graded materials are produced using powder metallurgy technique, slip casting, centrifugal casting method, gel casting, solid freeform technology etc. [20]. In addition to the diverse methods employed for the synthesis of functionally graded materials, various techniques have emerged, each possessing unique advantages and limitations. The versatility of functionally graded materials stems from their tailored composition, which changes gradually across the material, providing enhanced performance in specific applications. Beyond conventional methods like powder metallurgy and

chemical vapor deposition, several alternative approaches have gained prominence. A concise comparison to highlight the distinctive features of functionally graded materials fabrication techniques are presented in table 1.

Table 1: Comparative study of various methods for fabrication of functionally graded materials

Method	**Advantages**	**Limitations**
Powder Metallurgy	Widely established, cost-effective	Limited control over gradient profiles, fine-scale challenges
Chemical Vapor Deposition	High purity, precise composition control	Limited material compatibility, complex equipment
Additive Manufacturing	Customizable structures, intricate geometries	Material constraints, build size limitations
Electrochemical Deposition	Uniform coatings, controllable deposition rates	Limited to conductive materials, challenges in thickness
Spark Plasma Sintering	Rapid processing, high densification	Limited material compatibility, complexity in shapes

2.2 Applications of FGMs in Mechanical and Automotive

Functionally graded materials emerged to address limitations associated with laminated composites and monolithic alloys. They introduce a gradual variation of composition and microstructure across thickness, thereby reducing interfacial stresses, delamination and material discontinuities observed in classical composites [21]. The origin of FGMs is traced to aerospace and nuclear programs in Japan in the mid-1980s, where metal ceramic gradation was implemented to withstand large temperature gradients in rocket exhaust nozzles, space plane leading edges and turbine disks [22].

FGMs have revealed wide applicability in thermal, mechanical, and biomedical systems. They are used in turbine blades, combustion chambers, rocket nose cones and nuclear shielding exploiting their ability to suppress stress intensification and reorganize thermal and mechanical loads [22, 23]. In biomedical, graded implants allow modulus tailoring from a stiff core to a bone-friendly outer layer, modifying stress-defending and improving osteointegration [24]. Energy devices have applied FGMs in thermal barrier layers, heat exchangers, and thermoelectric devices, owing to their ability to maintain structural reliability under combined thermal-mechanical loads [25].

In the automotive, the FGMs have been studied for wear-intensive components including brake rotors, cutting tools, pistons, and suspension parts [26]. Their capability to combine a hard ceramic-rich surface with a ductile metallic substrate is advantageous in bending-dominated structures such as beams and leaf springs. Under cyclic loading, this graded configuration reduces peak von-Mises stress, delays crack initiation, and enhances fatigue strength relative to steel or polymer composites [27]. Additionally, numerical analyses have shown that FGM plates and beams present superior stiffness to weight ratios and more uniform stress distributions under static and dynamic loading when compared to homogeneous materials [28], confirming their suitability in lightweight suspension systems.

2.3 Development of Aluminium-Based FGMs

FGM development in aluminium structures has primarily focused on ceramic reinforcement particles (SiC, B_4C, Al_2O_3, TiC, etc.) due to their high hardness, modulus, and wear resistance. Research confirms that aluminium-based functionally

graded metal matrix composites improve flexural rigidity, hardness, and fatigue life while preserving ductility [29]. Multiple fabrication methods have been established, each with unique advantages and limitations.

2.3.1 Fabrication Techniques

The fabrication methods of FGMs are broadly categorized into four categories as shown in Figure 2.1. A brief literature review is present here as follows:

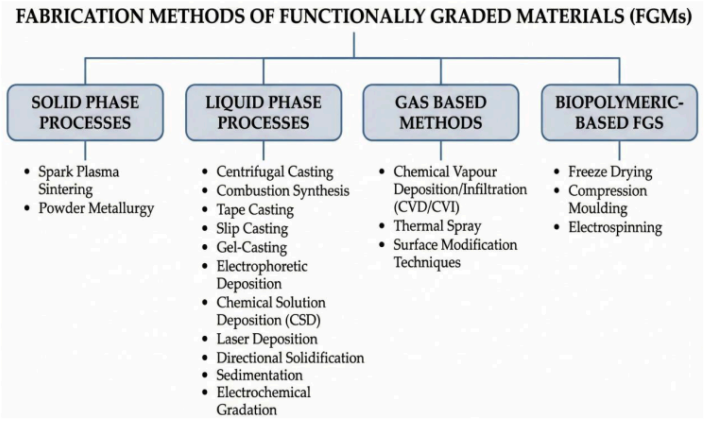

Figure 2.1: Classification for fabrication methods of FGMs

Powder Metallurgy (PM)

PM allows discrete or stepwise gradation by layering powders of different compositions followed by compaction and sintering. This approach has been successfully employed in Fe-Al, Ti-Mg, Al/Al_2O_3 and HA-Ti FGM systems, enabling density control and high interfacial bonding [30-32]. Vibration-assisted PM has also been used to homogenize Al-SiC mixtures and minimize sedimentation [33].

Spark Plasma Sintering (SPS)

SPS is widely used for high-density FGMs where local Joule heating produces strong metallurgical bonding and low porosity. ZrB_2/SiC/ZrO_2, Al_2O_3/Ti_3SiC_2 and Hap/Al_2O_3/YSZ FGMs achieved hardness in the 4 to 20 GPa range and exhibited crack-free interfaces [34 -37]. SPS also enables multimaterial functionally graded stacks in shorter sintering times [38].

Centrifugal Casting

This melt-based method creates natural gradation due to the density difference between molten aluminium and ceramic particles. It has been widely used in Al–SiC systems to concentrate ceramic reinforcement towards the outer surface, generating wear-resistant regions suitable for cylinder liners and heavy-duty bearings [39, 40]. However, its use is restricted to axisymmetric components and is difficult to apply to thin plates or curved leaf springs.

Stir Casting

Stir casting remains the most practical for industrial leaf springs and plates. Ceramic particles are incorporated into the molten aluminium, and mechanical agitation promotes dispersion [41]. Layer-wise distribution can be achieved through sequential particle feeding, melt superheat control, or mold-based gradient geometry. FGM-specific studies have shown controlled reinforcement distribution in Al–SiC and Al–B_4C composites, achieving enhanced surface hardness and flexural strength [7], [42].

Additive Manufacturing (AM)

Selective laser melting and directed energy deposition enable continuous thickness-wise gradation by varying reinforcement feed rates. These methods provide excellent

geometrical accuracy but face limitations including residual stresses, processing cost, and scalability [43].

2.3.2 Aluminium based FGMs

SiC reinforced Al matrix is high in stiffness, wear resistance and high fatigue behaviour. Centrifugal casting also produces a SiC-enriched surface that increases the resistance to bending and sliding wear [48, 44]. The graded Al/SiC beam models exhibited smaller deflection and no stress concentration like in homogeneous compositions [46]. Difficulties involve ceramic agglomeration and wettability, which is low because of elevated interfacial energy in molten aluminium [46].

B4C has been of special interest as a reinforcing element in aluminium alloys, particularly in Al7075 T6 MMCs, because of its outstanding characteristics, including low density, high thermal conductivity, high hardness, high Young modulus and high wear resistance [48-52]. Interestingly, B4C particles do not interact with aluminium, and thus, it is not possible to form a brittle reaction product at the interface between the reinforcement and the matrix [50, 53]. The comparative studies have shown that B_4C reinforced aluminium has better mechanical properties than other reinforcements such as TiC and SiC when prepared using the powder metallurgy route [47, 49]. These distinctive properties have influenced the extensive application of B4C in several ways such as engineering ceramics, automotive and aerospace parts and developing armour on land vehicles, aircraft and ship armour [54-56]. The major problem is the successful diffusion of B4C powder in the aluminium mesh when making these composites. It is at this point that the application of potassium titanium fluoride (K_2TiF_6) is essential because it drastically

increases the wettability of B_4C particles in the molten aluminium, which leads to the improved dispersion and high mechanical properties [57]. Wettability of reinforcements in the aluminium matrix has been of paramount interest in a number of studies with researchers investigating the different means of enhancing the interface between the matrix and the reinforcements [58, 59].

TiC has a high level of wettability and particle stability in aluminium melts. Al-TiC FGMMCs demonstrate a better hardness and compressive strength and do not tend to segregate in ceramics [60, 61]. Over reinforcement, on the other hand, is dangerous of brittle and hard to machine.

Nanocarbon reinforcements create multifunctional FGMs that have a stiffness, conductivity and damping enhancement. Gradation of CNTs in layers facilitates the development of lightweight beams, which have a higher modulus and damping, and industrial scaling is constrained [62].

2.3.3 Gradation Strategies and Processing Challenges

They are made by stepwise, layer-wise or continuous gradation and powder metallurgy is naturally conducive to discrete layers being stacked, centrifugal casting yields smooth radial gradients [30-33, 39, 40]. Instead, stir casting permits layer-wise melt feeding, and it is a cost-effective approach to automotive plates made of leaf springs [41-42].

Key challenges include:

- Unwetted metallic-ceramic (especially in Al–SiC and Al–B_4C) results in particle rejection and voids [46].
- Stress hotspots are caused by reinforcement clustering based on density differences [42], [44].
- Fatigue performance is reduced by porosity and off melt deformities [60].
- High reinforcement fractions are associated with low machinability and high brittleness which lowers service life [61].

2.4 Microstructural and Mechanical Characterization of FGMMCs

Microscopic characterization should be used to test performance in dynamic environments. The damping behaviour of the composites is studied by using Dynamic Mechanical Analysis (DMA). Vibration reduction and dissipation of energy is important in applications where damping properties are essential [63, 64]. It has been demonstrated in the past that B4C addition can create great effects on the damping behaviour of composites made of aluminium and that it could be an ideal compromise between mechanical strength and the damping capacity [63-66]. Further thermal cycling tests also support the fact that ceramics stabilize stiffness at high thermal temperature levels which is beneficial in the automotive or aerospace components that are in operation with varying thermal temperatures. The strength of the composites in terms of impact strength and tensile strength are also explored to get an idea of how the content of B4C can affect these characteristics. The interaction between B4C particles will be anticipated to increase the hardness, tensile strength,

and impact resistance of the Al 7075 matrix to be used in advanced structural applications where increased mechanical performance is demanded[67,68].

2.5 Numerical Modelling of FGMs and Leaf Springs

Functionally graded components, as numerical modelled, is no longer, like traditional homogeneous metallic leaf spring models. Classical spring analysis assumes that the leaf has constant material properties and bending stress is a function of geometry only and no load is applied [69]. This is inappropriate in FGMMCs where the stiffness changes with thickness and analysis of stress distribution needs to be done on a layer basis.

The initial theoretical formulation of graded structure is the continuous elasticity and variational formulations [17], which apply functional gradation as spatially dependent elastic fields. In the case of high-temperature multiphase composites, micromechanics-based homogenization is employed to determine the material reaction in the presence of thermal and mechanical loading [18]. These methods were then developed into more developed forms of computation where FEM is employed taking into consideration nonlinear geometry, residual stress and layer discontinuity.

The use of graded composites in oscillatory systems - including rotor shafts, as well as other systems, indicates that a change in the distribution of stiffness can change the behaviour of natural frequency and critical speed [71]. Equally, numerical analysis of composite leaf springs demonstrated that the layup or gradation must be

properly set up to achieve a considerable reduction in stress and a weight savings compared to steel springs [72].

Modelling is not just about stiffness in the contemporary world. Fail-safe analysis also has crack propagation behaviour, and damage prediction, where ceramic reinforcing enhances fatigue resistance, but local stress intensification needs to be controlled [73]. In the case of FGMMCs, the outer parts that are made of ceramic material endure high bending stress and the ductile inner part endures catastrophic fracture. These layer definitions have been incorporated in numerical models that give more accurate predictions of the bending strain, spring eye strain as well as long-term durability with road spectrum loading.

2.6 Optimization Studies in MMC and FGM Systems

Traditional optimization of suspension components has been concerning weight reduction without compromising strength, durability and stiffness. The oldest design ideas were aimed at the metallic springs where the stress redistribution was conducted by geometry--driven strategies, with variable width, parabolic tapering, and eye-reinforcement means to minimize tensile loading on the surface fibres [1]. Subsequently, stress minimization was further achieved numerically and analytical models of spring stiffness and bending resistance were developed in the automotive industry.

As composite springs were invented, the optimization shifted to the not-only-geometric strategy but instead to the design of the ply, the fibre orientation and the order of stacking the laminates. Shokrieh and Rezaei [2] established that the

composite leaf springs optimized using analytical and finite element methodology result in significant stress and mass reduction with the same satisfying the limit of the technique of static deflection. Equally, Rajendran and Vijayarangan [74] used optimization on unidirectional composite springs, which reduced the weight 30-60 percent as compared to steel with the same or even greater strain capacity.

Experimental validation was later applied in optimization when the modeling strategies grew more complicated. Yamada and Kuwabara [4] gave detailed charts of mechanical performance of metallic springs and indicated that the distribution of the stiffness had a strong influence on the fatigue life when the distribution of stress was non-uniform. The use of hybrid reinforcement and gradation in modern MMC/FGM spring design became inspired by this industrial viewpoint, and the alternative, single-material, method was being supplanted.

The use of multidisciplinary algorithmic tools to design springs has been used in modern optimization strategies to help a designer navigate the multifaceted design space, utilizing the benefits of sophisticated computational frameworks. Methods that have been used to work with multi-objective optimization of composite springs and metal matrix composite (MMC) have been genetic algorithms, response surface methodologies, and evolutionary heuristics. These methods allow simultaneous assessment of competing performance criteria- including stiffness, weight reduction, fatigue life, and manufacturability to create spring designs that perform better than conventional ones structurally and functionally. An example is Tanabe et al. [5], where the geometric parameters of automotive springs are optimized to have better endurance strength and small peak tensile stress.

Subsequent investigations demonstrated that the reduction in critical stress concentration is further enhanced by material stiffness tailoring, as opposed to geometric variation only [38].

The material selection research found out through optimization that the proportions of ceramic reinforcements should be in balance between the stiffness and the ductility. Surappa [7] had found a non-linear strengthening response in aluminium MMCs, and too heavy reinforcement leads to brittleness and porosity. This favors gradient-based MMC strategies in which high reinforcement is applied in surface stress areas only.

Subsequently, Bains et al. [9] found out that MMCs strengthened with hard ceramic grains like B_4C or SiC enhance wear-resistance and micro hardness, which provides better surface resistance. This allows the functionally graded leaf springs to perform well in bending in combination with graded stacking.

Wang et al. [38], who demonstrated that the incorporation of ceramic particles into the structure changes the dynamic response of composite structures and decreases the speed of the propagation of the crack, support the effect of the effect of particulate dispersion on MMC performance as well. The design of FGM therefore focuses on optimization of damping, stiffness and resilience to damage through particle architecture.

Structural design Optimization in leaf springs has one major principle namely maximize stiffness in areas where the stress tends to be the greatest and maximize ductility in areas where strain recovery and elastic deformation tend to be most

important. All functionally graded suspension systems are based on this design rationale. In these designs, compressive and tensile loads are distributed into the outer layers which are rich in ceramic to resist surface cracking, stress concentrated loads and the metallic ductile core to delay cracking, enhance strain accommodation and elastic rebound. Optimization of MMC and FGMMC leaf springs is therefore not confined to geometry or standpoint process parameters; but it is a combined materials structure manufacturing strategy. These systems have better stress redistribution, lower fatigue sensitivity, and better long-term durability in cyclic automotive loading conditions with a strategic grading of reinforcement and stiffness.

2.7 Experimental Validation Techniques for FGMMCs

Experimental validation ensures that the theoretical and numerical assumptions of graded composites translate into actual mechanical behaviour. For FGMMCs, this starts with microstructure validation using optical microscopy, FESEM, EDX mapping. These methods detect dispersion, clustering, eutectic transformation, and internal discontinuity [75].

Phase stability is verified using X-ray diffraction (XRD), which can confirm the presence of B_4C, SiC or TiC in aluminium without undesirable intermetallic. Validation of thermal stability and particle reinforcement is crucial, as unbonded particles degrade fatigue and tensile performance [76].

Mechanical validation follows three primary test classes. Static mechanical behavior such as tensile and hardness strength measure strengthening effects of

particles and interface bonding [77]. Dynamic or thermo mechanical behavior such as DMA and storage modulus tests capture behaviour under cycling or heating relevant to vibration and automotive fatigue [78]. Further, energy absorption behavior which is impact testing identifies the role of ceramic layers in resisting surface fracture and redistributing crack energy [79].

Advanced validation includes fractographic assessment, where ductile-brittle mixed fracture indicates correct gradation balance [80], and thermal cycling, which examines rheological stability and stress migration in MMCs [81].

Laboratory validation must be complemented by structural validation. Leaf springs, rotors or other fatigue-driven components must undergo loading protocols that reflect real-world service cycles. Work on automotive springs has demonstrated the criticality of correlating mechanical tests to working loads and validating predicted deflection profiles in situ [82].

2.8 Outcome of Literature Review

After a comprehensive literature survey on development, characterization, modelling, and optimization of aluminium-based MMCs and functionally graded structures, the following observations are made:

- A significant body of research exists on polymer composite and steel leaf springs, while functionally graded metal matrix leaf springs remain largely unexplored in the automotive suspension domain.
- In aluminium composites, reinforcement studies are predominantly limited to homogeneous MMC beams, or small laboratory specimens, whereas full-

scale graded leaf geometries with practical stress profiles have rarely been addressed.

- Existing studies on FGMs emphasize thermal gradients, vibration, resonance, or biomedical applications, but very limited attention is given to bending-dominant suspension components, where surface tension/compression cycles demand dual stiffness–ductility combinations.
- The effect of reinforcement distribution on microstructure, residual stresses, crack initiation, and long-term fatigue performance of FGM aluminium leaf springs requires in-depth investigation to establish reliable design guidelines.
- Research on manufacturing functionally graded MMCs highlights wettability, particle agglomeration and interfacial degradation as key fabrication challenges, yet process-driven gradation control for large flat structures such as leaf plates remains insufficiently demonstrated.
- While extensive numerical research is available on theoretical FGM beams or plates using ideal power-law gradation, experimental validation of real graded components with measured properties is limited, especially for automotive springs.
- A combined methodology integrating material fabrication, microstructural characterization, mechanical testing, finite element modeling, and optimization is rarely reported in existing studies, resulting in a knowledge gap that hinders the industrial application of metal-based FGMs.

The above gaps collectively indicate the need to develop a systematic approach for functionally graded aluminium leaf springs, considering fabrication feasibility, material behaviour, and realistic engineering loading conditions.

2.9 Problem Statement

A reliable and application-specific methodology is required for the design, fabrication, and analysis of functionally graded aluminium leaf springs that can sustain high bending stresses while maintaining elastic recovery and long service life. Existing approaches either rely on homogeneous MMC structures, by which brittle fracture is suffered at high-stress surfaces, or on composite laminates, which are prone to interlaminar delamination, environmental degradation, and manufacturing complexity.

Therefore, the present research is planned to conduct a systematic investigation that involves:

i. Development of graded aluminium-based MMC leaf plates using a feasible fabrication route,
ii. Characterization of their microstructure, mechanical properties, and residual stresses, and
iii. Analytical and numerical modelling of their structural performance under suspension loading.

A practical way is aimed to be established by this study for the production of lightweight, high-strength leaf springs plate with controlled gradation of reinforcement and validated structural modelling.

2.10 Thesis Objectives

- To select and fabricate the functionally graded materials for leaf spring Plate.
- To characterize physical properties of functionally graded materials for leaf spring plate.
- To carry out computational analysis of a FGM leaf spring plate for improved structural performance.
- To optimize the functionally graded materials for leaf spring plate.

Summary of present chapter has been conferred in a nutshell in next section.

2.11 Summary

The literature reveals that although MMCs and FGMs have been successfully developed for various structural and thermal applications, their deployment in automotive leaf springs remains largely unexplored. Existing fabrication routes struggle to achieve controlled reinforcement gradation, uniform interfacial bonding, and defect suppression in large plate-type components. Most mechanical and microstructural studies are limited to small coupons, while numerical investigations often assume ideal material distributions without experimental validation. Furthermore, optimization research remains fragmented, focusing either on geometry

or material selection rather than integrated fabrication–characterization–modelling approaches. These gaps clearly indicate the need for a comprehensive methodology to design, fabricate, test, and simulate functionally graded aluminium leaf springs for real suspension environments.

CHAPTER 3

FABRICATION METHODOLOGY

3.1 Introduction

The most important stage in development of any composite of functionally graded composite or Material (FGM) is fabrication stage. Fabrication stage plays role of foundation of the desired functional and mechanical properties in the component. The properties of the FGM leaf spring mainly depends on accuracy achieved and uniformity in the fabrication process. The distribution of the reinforcement particles, the quality of bonding between the matrix and reinforcement greatly influence the structural integrity of the composite. In event of any discrepancy during the fabrication process can result in issues such as porosity, poor quality interfacial bonding and / or uneven gradation resulting in poor mechanical behaviour and life of the component.

For developing required gradation and tailoring property variations in the entire thickness of the leaf plate, selection of appropriate fabrication technique and appropriate material is of utmost important. The selection of proper reinforcing material and matrix material directly influences density, stiffness, strength and wear resistance, whereas fabrication method greatly affects microstructural homogeneity and defect control. Current work is focussed on aluminium alloy (Al7075-T6) due to its high strength to weight ratio and good resistance to corrosion. Micro-sized boron carbide (B_4C) as a reinforcement was chosen due to its excellent hardness, low

density and thermal stability. Controlling the distribution of B_4C particles as reinforcement material in B_4C particles through optimized fabrication process is of utmost importance to get desired gradation in mechanical properties.

The primary objective of the fabrication phase in this study is to develop a functionally graded Al7075/B_4C composite leaf spring plate with systematically varying reinforcement content along its thickness. The process aims to ensure strong metallurgical bonding, minimal porosity, and uniform dispersion of B_4C particles in each graded layer. Additionally, the study seeks to establish an effective stir-casting-based fabrication route followed by T6 heat treatment to enhance the mechanical performance and reliability of the fabricated FGM leaf spring plate for lightweight automotive suspension applications.

3.2 Materials Selection

In the present work, the matrix material was selected as commercial grade Al7075T6 alloy. Micro particles of B4C were used as reinforcement. The selection of matrix and reinforcement material has done on the basis of fatigue strength and density of the material. To fabricate low weight and high fatigue leaf spring plate, selection was performed by using software (CES EDU PACK 2019). Figure 3.1, shows fatigue strength vs. density diagram of different materials. In figure 3.1, state (a) on density axis has showed that density of both reinforcement and matrix are approximately same whereas, state (b) and state (c) on fatigue axis have represented that the fatigue strength of reinforcement is much higher than the matrix material. Thus, the literature reviews and the software have confirmed that matrix Al7075T6 and reinforcement B4C are suitable material for leaf spring.

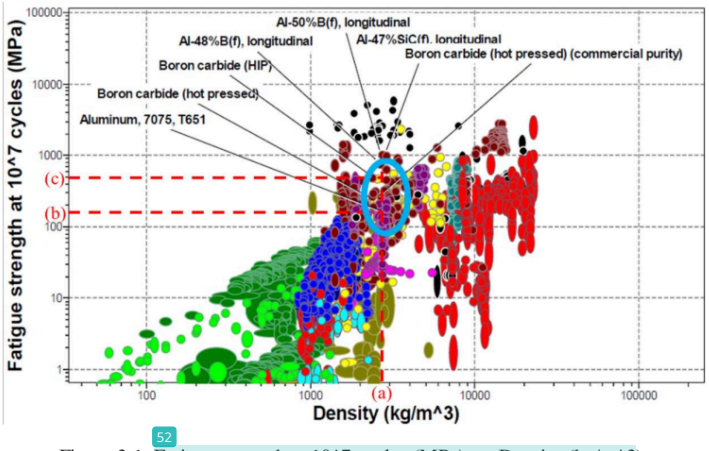

Figure 3.1: Fatigue strength at 10^7 cycles (MPa) vs. Density (kg/m^3)

3.2.1 Matrix material

In the present work, the matrix material was selected as commercial grade Al7075 T6 alloy. The chemical composition of matrix material has been investigated through spectroscopy test as per ASTM E 1507 standards shown in Table 3.1. Aluminium 7075 T6 is an alloy known for its outstanding combination of mechanical and thermal properties [25]. Aluminum 7075 has high strength, stiffness, wear resistance, excellent corrosion resistance, creep resistance and good fatigue behaviour, can be heat treated and widely used in structural applications.

Table 3.1 Chemical composition of Al7075

Elements	Zn	Mg	Cu	Mn	Cr	Si	Fe	Ti	V	Al
Weight %	5.950	2.590	1.630	0.239	0.236	0.140	0.371	0.053	0.005	Bal.

3.2.2 Reinforcement Material

In the present discussion, boron carbide was used as reinforcing material, Table 3.2. Micro-sized of B4C were used in this investigation. It is one of the hardest artificial materials and is black in colour in the form of thin lamellae or prisms. Due to its high hardness, it is used as a grinding and cutting material.

In the present investigation the B4C reinforcement particles shows the Zeta potential value 27mV (Table 3.2) which comes under the good stability regime. The good stability regime Zeta potential enhances the particle dispersion and minimizes the agglomeration in the Al7075-T6 matrix during the composites development. Further it results in the fair distribution of the particles in the matrix material. The solubility of reinforcement particles within the matrix material shows the extent of interfacial reactions and bonding. Further, the low solubility of B4C reinforcement particles exhibited the minimal dissolution and low density of the reinforcement particles.

Table 3.2: Properties of selected boron carbide

Parameters	Values
Density	2.52 g/cc
Purity	>99%
Zeta Potential	27mV
Solubility	Insoluble in water
Crystal structure	Hexagonal

3.2.3 Particle Size Estimation of Reinforcement and Wetting Element

The particle size of reinforcement (boron carbide) and wetting element (K_2TiF_6) have investigated with the help of their micrographs and image J analyzer. Further, origin 2017 was used to obtain average particle size and to generate histogram with normal distribution curve. Each particle of boron carbide was

measured from its field-emission scanning electron microscopy image, Figure 3.2(a). The average particle size of boron carbide was 3.9019 μm, Figure 3.2(b). Similarly, image J analyzer was used on field-emission scanning electron microscopy image of K_2TiF_6 particles to evaluate size of each particle, Figure 3.2(c). The average particle size of K_2TiF_6 was 1.00655 μm, Figure 3.2(d).

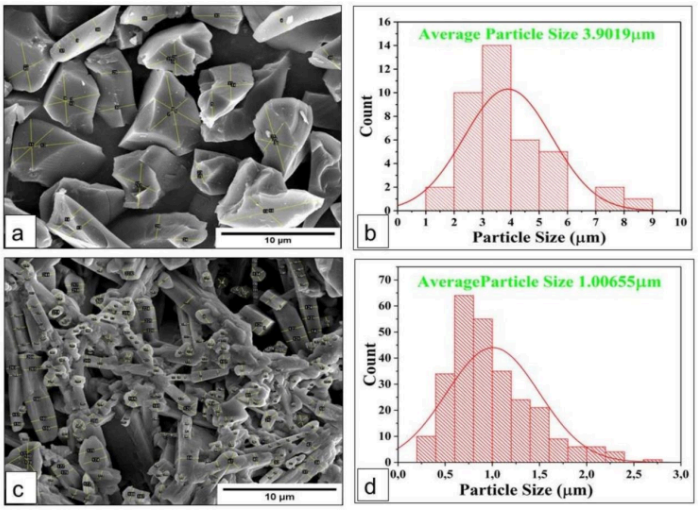

Figure 3.2: (a) FESEM of B4C particles (b) Crystallite size distribution of B4C particles (c) FESEM of K2TiF6 particles (b) Crystallite size distribution of K2TiF6 particles

3.3 Design of the FGM Leaf Spring Plate

3.3.1 Concept of Gradation and Property Tailoring along Thickness

The concept of gradation in a functionally graded material (FGM) is to achieve a gradual variation in composition and structure across the section, which results in corresponding changes in material properties. In the present work, stepwise gradation

was adopted during the fabrication of the FGM leaf spring plate to tailor the mechanical properties along its thickness. A five-layer gradation pattern was designed in the central portion of the leaf, while the remaining portions near both ends of the plate were maintained with the same composition, as shown in Figure 3.3(a).

The gradation pattern was decided based on the stress distribution along the plate thickness and the influence of reinforcement on the mechanical properties. According to bending theory, the maximum bending stresses are developed at the top and bottom layers of the plate, while the minimum stresses occur at the mid-thickness region, as illustrated in Figure 3.3(b). The shear stresses are maximum at the neutral axis and decrease towards the surfaces (Figure 3.3(c)). Therefore, to counteract the high bending stresses at the outer layers, a higher percentage of reinforcement (B_4C) was provided at the top and bottom layers, whereas the middle layer was designed with a lower percentage to maintain ductility. Accordingly, 8 wt%, 12 wt%, and 16 wt% B_4C compositions were selected to achieve a symmetric variation (16/12/8/12/16) from the surface to the mid-thickness.

Additionally, to resist twisting moments acting near both ends of the plate [2, 34] and to maintain uniformity in mechanical performance, the same composition as the top layer was used for both plate ends. This gradation pattern ensures that the outer layers provide high strength and stiffness, while the central region offers improved flexibility and toughness, resulting in a balanced stiffness-to-weight ratio and enhanced fatigue life.

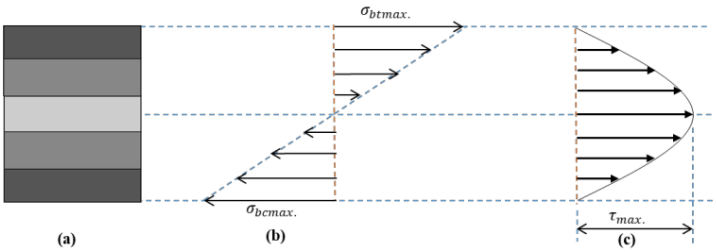

Figure 3.3: (a) cross-sectional view of fabricated leaf (b) Theoretical Distribution of bending Stresses (c) Shear stress distribution

3.3.2 Dimensions of the Leaf Plate and Design Considerations

In this research, the second leaf from the top of the rear suspension system of the TATA LPT 3518 model was selected as the reference component for the fabrication of the functionally graded material (FGM) leaf spring plate. This second leaf experiences substantial bending and torsional loads due to the fact that it supports eye ends and supports major portion of the vehicular load. A large number of literature have verified that maximum bending moment occurs at central portion of semi-elliptical leaf spring, making this region the most vulnerable for failure. The main objective of study was therefore, to impart strength at central region. This was done using controlled gradation in reinforcement material along the thickness. This gradation is focussed on strengthening strength to weight ratio and improving load bearing performance.

The second leaf of the TATA LPT 3518 rear suspension was taken as reference and FGM plate was designed. The dimensional data was taken using ZEISS Calypso Coordinate Measuring Machine (CMM) to ensure high accuracy.

The modelling was done using this data and mould was fabricated. The parameters of reference leaf obtained are presented in Table 3.3.

Table 3.3: Dimensions of the Reference (Second) Leaf of TATA LPT 3518 Rear Suspension System

Leaf Dimension	In mm
Span of Leaf	805
Radius of Curvature	1862
Width	80
Total Thickness	12

These parameters are taken as base dimensions and were used to prepare the mould. The boundary conditions for the computational model developed in ABAQUS/CAE also used this data. The central region of the leaf plate was modified with five layer reinforcement gradation and fabricated. It was ensured that compatibility with existing suspension assembly and external geometry to the reference leaf was maintained.

A detailed review was conducted for different manufacturing methods for FGM fabrication. The fabrication method was selected by weighing the ability to achieve precise gradation, operation simplicity, value for money, reproducibility and metallurgical bonding between layers. The best three techniques selected were powder metallurgy, centrifugal casting and stir casting. Further, due to die size and limitations of compaction for large size powder metallurgy was ruled out. Also, due to high power setup requirement for large curvature radius of leaf centrifugal casting was also ruled out. Stir casting was identified as most suitable process due to its simplicity, scalability and efficiency in liquid state processing.

It has been already demonstrated that efficient reinforcement dispersion and uniform property control at optimized key process parameters such as stirring speed, pouring temperature and blade angle [21,22] are key to mechanical performance and integrity. Therefore, the present work employs the stir casting technique for developing the Al7075/B_4C-based FGM leaf spring plate.

The novelty of this study lies in implementing a reinforcement gradation across the thickness at the central zone of the leaf spring plate, an approach that has not been previously reported for such applications. Five layer gradations has provided by using 3 composition of Al7075/B4C as shown in figure 3.4. The gradation design was further verified experimentally and computationally to determine the required material quantity for each layer, ensuring uniform layer thickness and accurate distribution during fabrication.

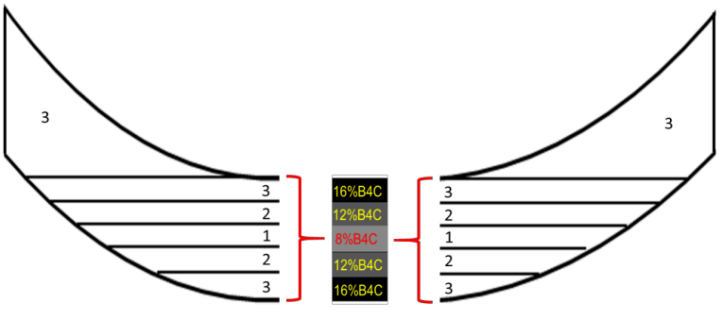

Table 3.4: Layer-wise distribution of reinforcement in the Al 7075/B_4C FGM leaf-spring plate.

3.3.3 Experimental and Computational Evaluation of Material Distribution for Different Gradation Layers

To determine the actual amount of material required for maintaining uniform thickness in each graded layer at the central portion of the FGM leaf spring plate, both experimental and computational evaluations were carried out.

3.3.3.1 Experimental Evaluation

An experimental study was conducted to estimate the volume of material required for each gradation layer. Initially, 6 kg of white Portland cement, water, and a pattern of the leaf spring plate were used to fabricate a mould. The cement and water were mixed thoroughly to form smooth slurry. Using this mixture, a mould of the leaf spring plate with one open side was prepared. The open surface of the mould was covered with a glass plate, and to ensure a seamless joint and prevent liquid absorption, the inner mould surface was coated with a thin polymer microfilm.

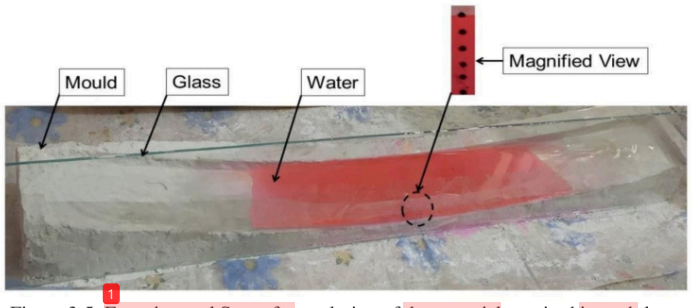

Figure 3.5: Experimental Setup for evalution of the material required in each layer

Five equal partition marks were made along the thickness representing five graded layers in the central region of the pattern. The placement of the mould in the pattern

was done carefully ensuring marked side faced the glass surface. As shown in Figure 3.5, coloured water was poured into the mould gradually using sealed measuring cup. The volume required to fill each partition was recorded. To minimize experimental error and ensure repeatability for more accurate average results this was repeated five times. The data recorded represented the quantity of material required during casting of FGM plate for each layer.

3.3.3.2 Computational Evaluation and Validation

The experimentally determined volume of the material was also validated by a computational study. This process of evaluating the molten material requirement involves rigorous comparison and benchmarking to ensure accuracy of data.

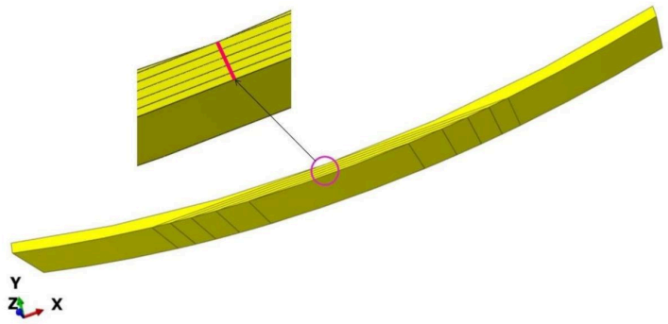

Figure 3.6: A 3-D model for investigation of required material in each gradation computationally

A coordinate measuring machine (CMM) was employed for measuring critical dimensions of the reference spring plate. The dimensions of the fabricated pattern was also measured. The data obtained was compared for dimensional accuracy. A CAD model was then prepared using three dimensional CAD modelling

software (ABAQUS). As discussed earlier the central thickness was divided into five equal partitions also shown in Figure 3.6. The volume was then evaluated using analytical tools in the software.

The experimental process was repeated 5 times as discussed earlier. The average volume of each layer was found to be 63.6 ml, 130.2 ml, 168.4 ml, 250 ml and 449 ml respectively from bottom to top layers. These values were also evaluated computationally and compared with experimental results. It was found that the experimental results were slightly on the higher side than computational values by 2 %. This can be attributed to the small errors during preparation of mould or liquid handling.

Table 3.4: Amount of composites required in different gradation at center part of the leaf spring plate

Gradation Number from Bottom to Top of the Leaf	Amount of liquid required (ml)							Average value (ml)	Amount selected with 2% additional allowance (ml)
	Experimental Readings						Computational result		
	1	2	3	4	5	Average			
1	64	64	61	65	64	63.6	61.3	62.5	63.7
2	132	132	124	130	133	130.2	133.0	131.6	134.2
3	169	173	170	165	165	168.4	167.6	168.0	171.4
4	247	253	245	250	255	250.0	248.7	249.4	254.3
5	450	454	445	446	450	449.0	450.1	449.6	458.5

The computational software provides approximate but reliable data. The average of experimental and computational results was thus adopted as the optimum

material requirement for each gradation layer. An additional 2% allowance was included to account for material losses in gating systems during casting. The final calculated values are summarized in Table 3.4.

3.4 Fabrication Methodology

A functionally graded material (FGM) leaf spring plate was fabricated using controlled stir casting and gravity die casting. This hybrid approach ensured uniform reinforcement distribution, strong metallurgical bonding and precise dimensional control. The process involved:

(i) stir casting of Al7075-B_4C composites

(ii) fabrication of functionally graded layers

(iii) post - casting operations.

3.4.1 Stir Casting Technique

Stir casting was used to prepare Al7075–B_4C composites with varying reinforcement weight percentages. Mechanical stirring and gravity die casting were combined to achieve homogeneous particle dispersion and form the graded leaf structure.

3.4.1.1 Pattern and Mould Preparation:

A mould was prepared using a wooden pattern based on TATA LPT 3518 second leaf design dimensions. The pattern dimensions included allowances for machining (1 mm), shaking (1 mm), shrinkage (2.5%) and a 1° taper. The mould cavity used green sand mixed with 1.5 wt.% coconut shell ash and camphor powder for permeability and strength [37, 38].

3.4.1.2 Melting of Matrix Alloy:

Melting of matrix alloy is done in using three stir casting setup. This setup contains graphite crucible with stirrer and speed controller. This is done by melting Al7075 alloy (2 kg per batch) at 800 °C in a resistance furnace in argon gas atmosphere to prevent oxidation.

3.4.1.3 Preheating of Reinforcement and Wetting Agent:

Preheating of Boron carbide (B_4C) powders in muffle furnace was done to remove moisture and improved wettability. 8 wt. %, 12 wt. %, and 16 wt. % were preheated for making test specimen along with wetting agent potassium titanium fluoride (K_2TiF_6) flux (purity 99.9%). Flux and reinforcement in equal amount were mixed before addition to the molten alloy.

3.4.1.4 Stirring Process:

Preheated reinforcement and flux mixture was added gradually in the molten matrix when the matrix material reached the desired temperature. Vortex was created using three-blade graphite impeller rotating at 550 rpm. This vortex promotes desirable uniform particle dispersion. To ensure through and homogenous mixing without clustering and particle sedimentation of B_4C, the stirring operation was continued for a sufficient duration. The setup of speed control unit to regulate stirring rate is shown in Figure 3.7(a), whereas the schematic of complete stir casting setup is presented in Figure 3.7(b).

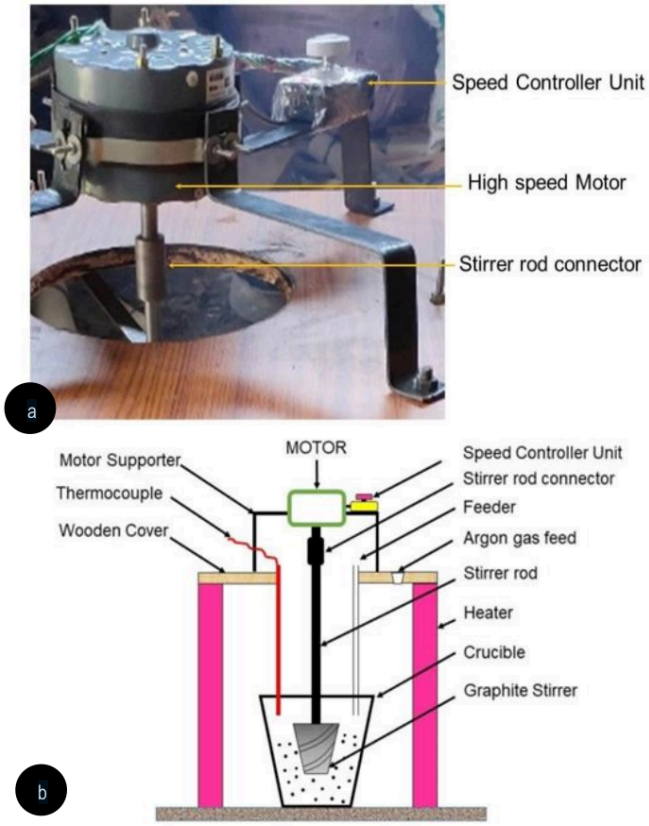

Figure 3.7: (a)Stirrer with a speed controller (b) Schemetic of Stir-Casting Setup

3.4.1.5 Pouring of Melt:

A gravity mould was prepared containing central runner. The molten composite was poured after stirring. The process was completed within one minute to avoid premature solidification. Specimen were casted from the remaining molten

composite for mechanical testing. Table 3.5 illustrates process parameters with optimized conditions and their effects.

Table 3.5: Process parameters with optimized conditions and their effects

Parameter	Optimized Condition	Purpose
Stirring Speed	550 rpm	Ensures uniform dispersion without vortex instability
Stirring Time	8 minutes	Allows homogeneous mixing of reinforcement
Melt Temperature	800 °C	Maintains fluidity and minimizes gas entrapment
Reinforcement Preheating	450 °C	Improves wettability and removes moisture
Pouring Temperature	720–740 °C	Prevents premature solidification
Mould Composition	Green sand + 1.5 wt.% coconut shell ash & camphor powder	Provides permeability and surface finish

3.4.2 Fabrication of Functionally Graded Layers

The FGM leaf plate was fabricated by dividing the composite into five layers, each layer with a specific reinforcement composition. The layers followed a symmetric pattern of 16/12/8/12/16 wt.% B_4C. This results in a stiffer outer layer and a more ductile core.

Experimental evaluation yielded liquid metal requirements for each gradation. Liquid requirement increased from bottom to top layer which reflects layer volume variation. As discusses earlier, computational results averaged experimental findings, with <2% deviation. A 2% allowance accounted for gating losses (sprue, runner, etc.), ensuring material adequacy.

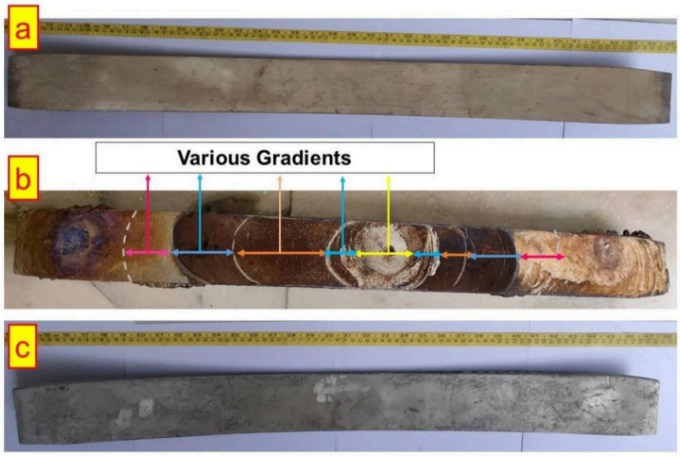

Figure 3.8: (a) Pattern of spring plate (b) Stir casted functionally graded materials leaf (c) Finished functionally graded materials leaf spring plate

All three allowances (machining, shaking, shrinkage and draft) were applied in pattern and mould fabrication respectively. The wooden pattern of the leaf plate is shown in Figure 3.8(a). A visible colour variation along the rear surface was seen in the stir-casted FGM leaf as shown in Figure 3.8(b). This clearly indicates successful gradation formation. After machining, this visual gradation disappeared due to surface removal clearly observed in Figure 3.8(c). To confirm gradation microscopic analysis was performed at the central portion of the leaf. Uniform distribution of B_4C reinforcement within each layer with strong metallurgical bonding at the interfaces was validated through microscopy. The controlled sequential casting and solidification process ensured uniform distribution. Mould temperature was maintained by controlled cooling between 200-250°C before pouring. To minimize residual stresses and porosity natural air cooling was also done post casting.

3.4.3 Post-Casting Operations

Post-processing operations such as removal of the casted FGM leaf spring plate and test specimens from the mould, followed by cleaning, grinding and lastly machining. Next operation was to clean castings remove sand, flux and oxides. Bench grinder and abrasive tools were used to remove excess flash. The plate was machined to ASTM designed dimensions. Visual inspection and dimensional verification was carried out on FGM leaf spring plate to ensure design adherence.

3.5 Heat Treatment of Fabricated Leaf Plate and Samples

Three step heat treatment (T6) was done on FGM leaf plate to improve mechanical and structural properties. The first process was solution treatment, followed by quenching and then artificial aging. To achieve three step heat treatment, they were heated in range of 465 - 480 °C for 3 hours to get a uniform solid solution. Followed by quick quenching in water to lock in the alloying elements. Finally, they were artificially aged at 120 °C for 24 hours to strengthen the material to enhance hardness, tensile strength and wear resistance. Detailed process for T6 heat treatment cycle is illustrated in Figure 3.9.

As shown in Figure 3.9, the FGM leaf plate and samples were put in a furnace for uniform heating. The solution heat treatment started at 465 °C for 2 hours, dissolving alloying elements into the aluminium matrix and forming a solid solution. Then, the temperature was bumped up to 480 °C for 1 hour to complete the solutioning process and ensure the alloying elements diffused evenly across the layers.

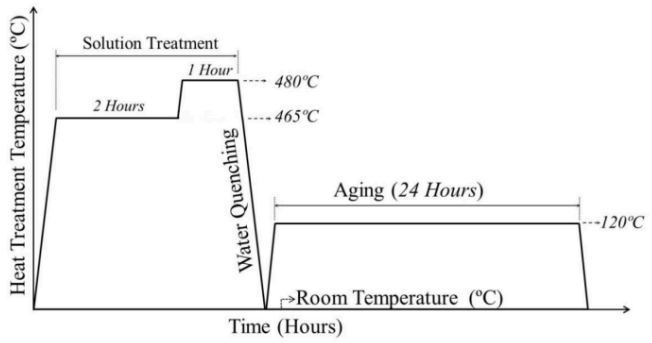

Figure 3.9: *The detailed schematic of the T6 heat treatment cycle*

After solution treatment, the samples were quickly dunked in water at room temperature. This rapid cooling trapped the alloying elements, preventing them from precipitating out too soon and setting the stage for the aging process. The quenched samples were then artificially aged at 120 °C for 24 hours to get the T6 temper. This controlled aging process created fine, evenly distributed strengthening precipitates, boosting hardness, tensile strength and wear resistance.

The T6 heat treatment was a game-changer for the FGM leaf plate. It refined the microstructure, strengthened the bonds between the layers and boosted mechanical performance. This made the component a top contender for demanding applications, like automotive suspension systems, where high load-bearing capacity, fatigue resistance and durability are crucial. The treated FGM leaf plate is ready to take on tough challenges and deliver reliable performance.

3.6. Conclusions

- Al7075-T6 was selected as the matrix material due to its high strength-to-weight ratio, fatigue resistance, and corrosion resistance.
- Micro-sized B_4C was chosen as reinforcement because of its high hardness, low density, and thermal stability, while its 27 mV zeta potential ensured good particle stability and reduced agglomeration.
- A five-layer symmetric gradation (16/12/8/12/16 wt.% B_4C) was designed based on bending and shear stress profiles to maximize stiffness at outer layers and maintain ductility at the core.
- The leaf geometry was replicated from the second leaf of TATA LPT3518, and dimensional accuracy was ensured using CMM measurements.
- Experimental (water-fill) and computational (CAD) methods were used to determine material volume for each layer, showing good agreement with only 2% deviation.
- Stir casting with gravity die casting was adopted to fabricate the FGM leaf, using K_2TiF_6 as a wetting agent to enhance B_4C dispersion, improve matrix–reinforcement bonding, and ensure scalable manufacturing.
- Controlled casting parameters (550 rpm stirring, 8 min mixing, 800 °C melt, 720–740 °C pouring) minimized porosity, clustering, and gas entrapment.
- T6 heat treatment (solutionizing, quenching, artificial ageing) improved hardness, tensile strength, and wear resistance, enhancing overall structural performance.

Chapter 4

Microstructural and Phase Characterization

4.1 Introduction

Characterization of microstructures and phase is very important in determining quality and homogeneity of functionally graded composites and their general efficacy. The characteristics of performance of such materials are distinguished by the evenness of the reinforcement particles distribution and the integrity of the interface between the matrix and reinforcement, and the phases formed in solidification and the following heat treatment. The internal structure is also analyzed in detail giving useful information on the effect of the gradation of reinforcement as to the mechanical properties, wear resistance and thermal stability of the composite system.

In the current work, the prepared Al7075-B4C functional graded metal matrix composite plates were subjected to extensive microstructural and phase examination to comprehend the effect of reinforcement content and gradation. The main goals of this characterization are to determine the graded distribution of the B 4 C particles in the graded layers, assess the interfacial bonding between the ceramic reinforcement and the aluminium matrix, and determine any secondary phases or reaction products generated during the processing. The analyses also allow to affirm that a graded

structure was formed successfully and to have the grounds to correlate the features of microstructures with the mechanical behaviour discussed in the following chapters.

Various methods of analysis were used in order to meet these goals. The general morphology of the grains and the distribution of B 4 C particles in the matrix were determined by means of Optical Microscopy. The information about the dispersion of reinforcement, porosity, and interfacial features was accumulated in greater in detail by Field Emission Scanning Electron Microscopy (FESEM). The elemental composition and bonding nature could be ensured at the matrix-reinforcement interface by the use of Energy Dispersive Spectroscopy (EDS) that allows avoiding the presence of undesired reaction products. Moreover, as a validation of the crystalline phases of the composite and the estimation of crystallite size, X-Ray Diffraction (XRD) analysis was undertaken to determine the effect of reinforcing content and heat treatment on the formation and enhancement of the crystalline phase.

In general, this chapter is a composite assessment of the microstructural and phase properties of the manufactured Al7075-B4C FGM composites, which creates an adequate picture of how the degree of gradation and reinforcedness influence the internal structure and the level of bonding of the material.

4.2 Sample Preparation

In order to characterize them microstructurally, representative specimens were cut with care on various regions on the fabricated plate of Al7075-B4C functionally graded composite at 8 wt.%, 12 wt.%, and 16 wt. B4C reinforcement level. All the

samples were removed to clearly reflect the difference in content of reinforcement amongst the graded layers and its effect on the microstructure and integrity of the interface.

A precision cut of the specimens was done via a Wire Electrical Discharge Machining (Wire EDM) process to achieve high dimensional accuracy and avoid any mechanical deformation or thermal damage which might change the inherent microstructural features. The samples were then sectioned, cleaned using acetone to wipe away all traces of dielectric fluid and debris and then mounted.

These specimens were then fixed in a thermosetting resin so as to make handling of them in the polishing process and further microscopic analyses simple. The samples mounted were subjected to standard metallographic preparation, which included grinding, polishing and etching in order to get a defect-free and reflective surface that is fit to be viewed under an optical microscope (OM) and field emission scanning electron microscopy (FESEM).

Grinding was done in series with silicon carbide (SiC) abrasive papers with grit sizes as 400- 2000 under a constant flow of water to reduce any heating and contamination of the surface. A rotating polishing cloth was used to polish the specimens with alumina and diamond suspensions (1 μm and 0.25 μm) until a mirror-like surface was attained, after grinding.

To identify the grain structure and particle distribution, the polished material was etched using the reagent of Keller (1.5 ml HCl + 2.5 ml HNO_3 + 1.0 ml HF + 95 ml distilled water). The etching time was maintained at 8-12 seconds to achieve

sufficient contrast without excessive etching of the aluminium matrix. After etching, the samples were washed with a lot of distilled water, dried with ethanol, and dried with warm air to avoid oxidation.

The prepared samples were then subjected to Optical Microscopy (OM) to observe the general morphology of the grains and the distribution of the particles, and the high-resolution images of the interfacial bonding, reinforcement dispersion and surface morphology of the different graded layers in the Al7075-B4C FGM composite were also taken under the Field Emission Scanning Electron Microscopy (FESEM).

4.3 Optical Microscopy

An optical microscopy was carried out to assess the morphology of the grains, particle distribution and gradation behaviour of the T6 heat-treated Al70757B4C functional graded composites. The sampling was accurately cut in the three areas of different grades through wire electrical discharge machining (EDM) to eliminate distortion of the microstructure or heat affected areas. The specimens were subjected to an optical microscope after conventional metallographic preparation (grinding, polishing and etching of the specimen by Keller). Figure 4.1(A–C) shows the representative micrographs of the 8 wt.%, 12 wt.%, and 16 wt.% B 4 C regions.

Figure 4.1(A) shows the Al7075 + 8 wt.% B4C region to have fairly coarse grains of the Al7075 matrix with the B 4 C particles being well dispersed both in the grains and at the grain boundaries. The distribution is even, and no signs of agglomeration can be noticed. The reinforcement particles are good in preventing the

grain boundary movement during solidification and heat treatment and this is also a contribution to grain refinement and higher strength. The red arrows point out the scattered particles of boron carbides that are resistant to the movement of dislocation, and therefore enhances the hardness and tensile strength of the composite.

The microstructure of Al7075 + 12 wt.% B4C region [Figure 4.1(B)], around the region is finer grained and with a higher density of reinforcement particles than the 8 wt.% zone. The higher concentration of B 4 C particles increases the nucleation sites in the solidification, which results in a higher refinement and efficiency of load transfer between the matrix and the reinforcement. But there is just a little local agglomeration of particles observed. Red arrows represent the B 4C particles that exist in the matrix and at the grain boundaries. The stronger and harder distribution is made, but when clustering begins, uniformity can be somewhat compromised.

The Al7075 + 16 wt.% B_4C region [Figure 4.1(C)], has a very refined grain structure with reinforcement particles dispersed densely. At this reinforcing stage, B_4C is highly concentrated, especially at grain boundaries (indicated in the yellow circle). This clustering limits the growth of the grain and offers the highest strengthening and wears resistance. The extreme agglomeration, however, also creates brittle and decreases ductile because of creation of solid clusters of particles that may serve as fracture initiation points during loading.

All in all, the optical microscopy results indicate a definite reinforcement distribution gradient and grain refinement between the 8 wt.% and 16 wt.% areas. The gradual augmented B_4C content augments the power and toughness because of fine grains and better load transmissions but it brings about localized agglomeration

at elevated reinforcement concentrations. Therefore, a perfect strength, wear resistance, and ductility ratio of Al7075-B_4C FGM leaf spring plate require an optimal percentage of reinforcements.

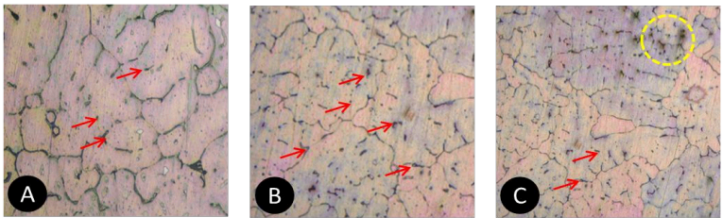

Figure 4.1: The microstructure of samples (A) Al7075-T6 /8wt. % B_4C (B) Al7075-T6 /12 wt. % B_4C (C) Al7075-T6 /16 wt. % B_4C

4.4 Field Emission Scanning Electron Microscopy (FESEM)

We performed Field Emission Scanning Electron Microscopy (FESEM) to investigate the reinforcement distribution, interfacial bonding and microstructural characteristics of the T6 heat-treated Al7075B_4C plate, which is a functional graded composite. Figure 4.2(a) demonstrates the sectioning of the samples of five different layers through the plate thickness, with each layer denoting a different concentration of the reinforcements between50g wt.% and50g wt.% B_4C. Figure 4.2(b-d) shows the FESEM micrographs of the various zones of reinforcement.

Reinforcement Distribution

As seen in the FESEM observations, the dispersion of the B_4C particles is dependent on the percentage of the reinforcement. The microstructure in the lower reinforcement zone (8 wt.% B_4C) [Figure 4.2(b)], exhibits a homogeneous and

homogenous distribution of the B 4 C particles in the Al7075 matrix. The small-scale distribution of reinforcement particles proves the efficient stirring and wetting of the fabrication process with insignificant porosity or aggregation of particles.

In the middle reinforcement level (12 wt.% B_4C), as illustrated in Figure 4.2(c) the distribution of the particles is quite homogenous, but there is a rather random pattern because the density of the particles is higher. The B4C particles serve as the nucleation sites during solidification, which refines the grains but elevates the probability of clustering in specific areas.

Figure 4.2(d) in the high reinforcement zone (16 wt.% B_4C) indicates that distribution of the particles is non-uniform, and the agglomeration can be observed, as well as small micro-pores. Such flaws are explained by the fact that it is harder to maintain uniform distribution at increased particle concentrations in the stirring and solidification processes.

Interfacial Bonding

The FESEM images reveal that there is excellent metallurgical bonding between the Al7075 matrix and the B_4C particles at all areas of reinforcement. The interfaces are kept clean with no cracks or interfacial voids in the 8 wt.% and 12 wt.% areas which indicates successful wetting of B_4C by the molten aluminium alloy during fabrication. Nevertheless, when the B_4C content is at 16 wt.%, some areas exhibit weak interfacial bonding and formation of micro voids around particle clusters, which may form potential sites of cracks initiation during the application of mechanical forces. These remarks indicate that increasing the content of

reinforcement improves hardness and wear resistance yet it can also reduce the interfacial integrity because of agglomeration of particles.

Microstructural Features of T6 Heat-Treated Samples

A micrographic examination of the T6 samples that are heat-treated shows that there is major refinement of grains throughout the layers of the grading. It is also seen that the uniform precipitation of strengthening phases ($MgZn_2$ and Al_2CuMg) in the matrix contributes to increased strength and hardness. The B_4C particles present practically inhibit grain boundary motion in the aging of materials to form refined and equiaxed grains. Nevertheless, in more reinforced areas (16 wt.% B_4C) localized micro-pores and interfacial segregation minimally lower the uniformity of the phase, meaning that the effect of the heat treatment is less homogeneous with a high reinforced rate.

Comprehensively, the FESEM examination proves that the Al7075 - B_4C FGM has a continuous compositional gradient, solid interfacial bonding, and fined microstructure post-T6 heat treatment. The reinforcement distribution becomes non-uniform at lower B_4C content levels and skewed to greater levels, which indicates that the best balance between dispersion uniformity, interfacial integrity, and mechanical performance is between the optimum reinforcement (12 wt.% B_4C) and higher reinforcement concentrations.

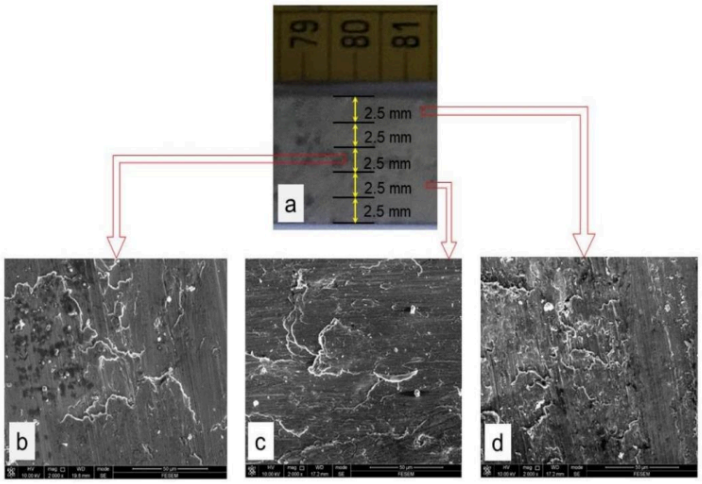

Figure 4.2: (a) sectioned FGM plate of 5 graded layers; (b) FESEM micrograph of 8 wt.% B_4C, (c) and (d) FESEM micrographs of 12 and 16 wt.% B_4C zones after T6 heat treatment.

4.5 Energy Dispersive Spectroscopy (EDS) Analysis

Energy Dispersive Spectroscopy (EDS) was performed and FESEM to identify the elemental composition of the reinforcement powders and the developed Al7075/ B_4C composites.

4.5.1 EDS of Reinforcement and Wettability Materials

Figure 4.3(A, B) EDS spectra of untreated B_4C particles indicates that the boron (B) and carbon (C) are as the dominant elements, which proves that they are highly pure before fabrication. On the same note, the wettability agent K2TiF6 (Figure 4.3 (C, D)) gives strong signals of titanium (Ti) and fluorine (F), showing that it has been appropriately chosen in improving the reinforcement-matrix interaction. Both

powders have no impurities and this makes them appropriate in the development of composite.

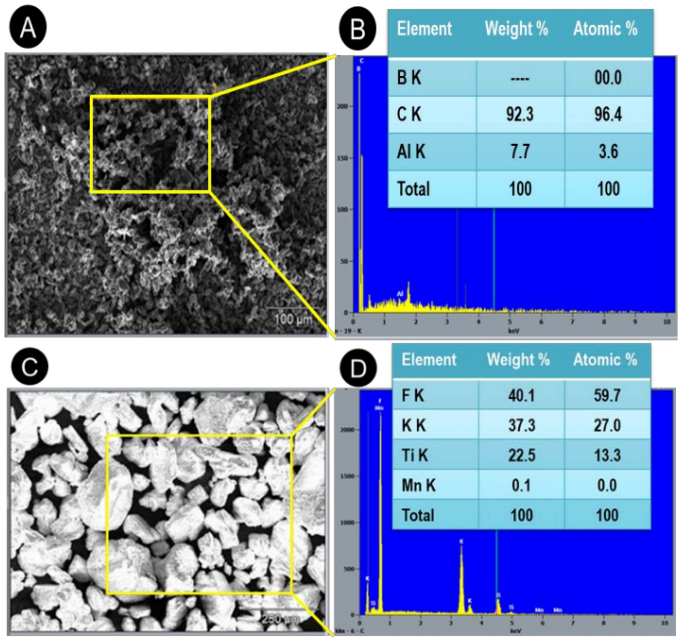

Figure 4.3: FESEM and EDS analysis of (a–b) B_4C powder, and (c–d) K_2TiF_6 powder.

4.5.2 EDS of Al7075/12 wt.% B_4C Composite

The EDS results for the composite containing 12 wt.% B_4C (Figure 4.4) confirm peaks of Al, Zn, Mg, and Cu from Al7075-T6 alloy along with distinct B and C peaks representing the reinforcement. These findings denote that the B_4C particles are successfully embedded into the aluminium matrix. Furthermore, no traces of undesirable reaction compounds, such as Al_4C_3, were observed, indicating strong chemical compatibility and an effective casting process.

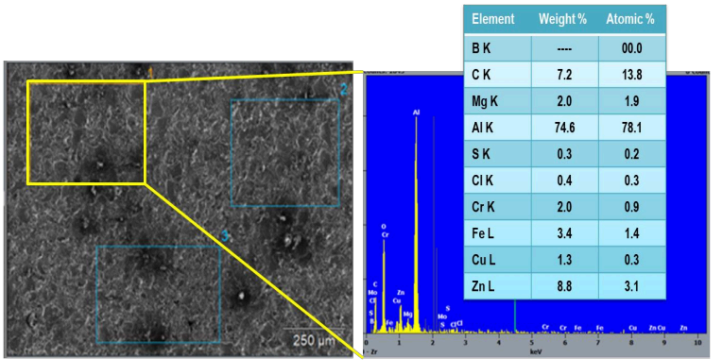

Figure 4.4: FESEM and EDS of Al7075/12 wt. % B_4C composite confirming successful reinforcement incorporation.

4.5.3 EDS Elemental Mapping of Al7075/16 wt. % B_4C Composition

A detailed elemental mapping for the 16 wt.% composite (Figure 4.5(a–n)) shows:

- Al uniformly distributed throughout the matrix
- B and C distributed across the scanned region, confirming reinforcement presence
- Slight agglomeration with increasing B_4C content, common at higher ceramic loading

Additionally, small traces of O, Mg, S, Cl, K, Cr, Fe, Cu, Zn, and Mo correspond to natural alloying constituents or minor impurities formed during melting. No localized elemental segregation was detected, indicating suitable interfacial bonding.

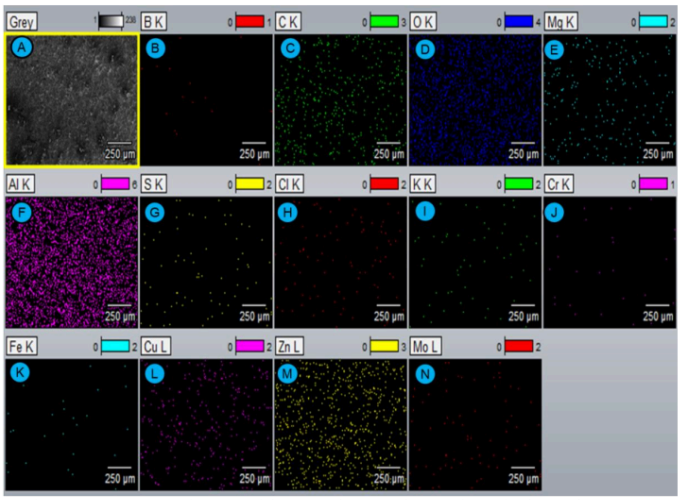

Figure 4.5: FESEM image with EDS elemental mapping of Al7075/16 wt.% B_4C composite showing spatial distribution of Al, B, C and minor elements.

4.5.4 Summary of EDS Findings

- The reinforcement and wettability materials used were chemically pure.
- B_4C particles were successfully incorporated into the Al7075-T6 matrix.
- Elemental distribution remained reasonably uniform despite increased clustering at higher reinforcement content.
- No harmful interfacial reaction products were detected, confirming strong metallurgical bonding.
- The microstructure verified through EDS directly correlates with the improved mechanical and damping performance at higher B_4C wt.% reported in the study.

Thus, the EDS analysis confirms that the fabricated composites possess the required chemical integrity and reinforcement consistency to support their application as high-strength, lightweight structural materials.

4.6 Phase Analysis Using X-Ray Diffraction (XRD)

X-ray diffraction (XRD) analysis was performed to determine the phase composition of the fabricated Al7075–B_4C composites used in the functionally graded leaf spring plate. The XRD patterns were plotted using Origin 2017 software. Each diffraction peak was fitted using the Gaussian peak fitting method to obtain accurate peak intensity and position values.

The XRD patterns of the composites reinforced with 8 wt%, 12 wt%, and 16 wt% B_4C, presented in Figure 4.6, confirm the coexistence of aluminum matrix (α-Al) and boron carbide particles. Peak identification was carried out by matching the diffraction signatures with the corresponding standard reference cards from the International Centre for Diffraction Data (ICDD). The major diffraction peaks were found to be consistent with ICDD card numbers 89-2837 and 07-0275 for Al7075 and B_4C phases, respectively.

It was observed that the intensity of B_4C peaks increases progressively with reinforcement content, indicating the presence of a larger volume fraction of B_4C in the higher reinforced layers. Prominent peaks of B_4C, especially at the (101) plane, exhibited a significant increase with increasing wt% of reinforcement. Additionally, a slight shift of aluminum peaks toward higher 2θ angles was detected. This shift may be attributed to the lattice strain and interfacial bonding effects caused by the addition of stiff ceramic particles into the metallic matrix.

Based on these observations, the XRD analysis confirms that:

- The dual-phase system (Al + B_4C) remains stable during fabrication.
- Reinforcement incorporation increases uniformly with composition.
- Higher reinforcement induces slight structural distortion, which supports improved mechanical properties.

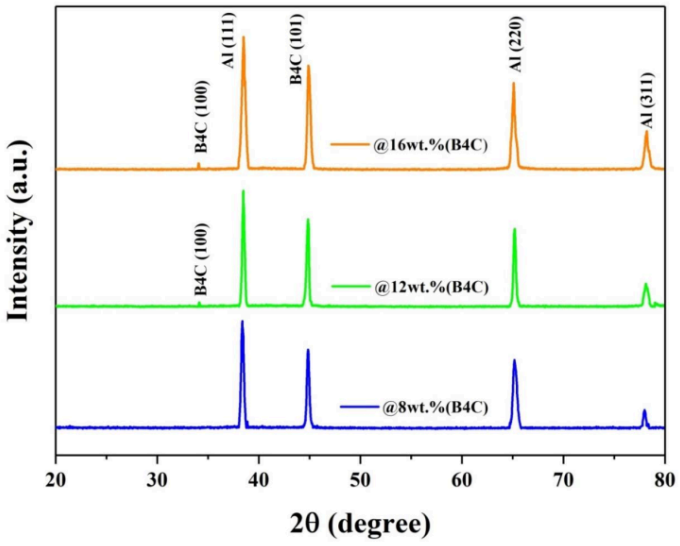

Figure 4.6: Cascade model of XRD pattern of compositions used in functionally graded materials plate

4.7 Grain Size Measurement

The crystallite size of the aluminium matrix in each composite composition was evaluated from the XRD data using the Full Width at Half Maximum (FWHM) of the fitted peaks. The Scherrer equation was used for the calculation:

$$D = \frac{K\lambda}{\beta \cos\theta} \quad (4.1)$$

In equation 1, D is crystallites size in (nm), K is Scherrer constant (0.94), λ is wave length of copper K-alpha radiation (0.15406 nm), β is full width at half maximum and θ is peak position (Bragg angle) in radians.

The calculated crystallite sizes for the three composites are shown in table 4.1

Table 4.1: Crystallite sizes of all three compositions

Composite Composition	Crystallite Size (nm)
8 wt% B_4C	29.71
12 wt% B_4C	28.15
16 wt% B_4C	26.55

It was observed from the XRD plots that FWHM values increase with increasing 2θ, and therefore, the crystallite size decreases with higher scattering angles for all compositions. The reduction in crystallite size with increasing reinforcement percentage indicates:

- Restriction in grain growth due to B_4C particles
- Improvement in internal structure and lattice integrity

These results confirm that the higher reinforced region (16 wt% B_4C) possesses a more refined crystalline structure, contributing directly to enhanced strength, hardness, and load-bearing capability of the composite.

4.8 Residual Stress Measurement

To evaluate the internal stress distribution across the functionally graded Al7075–B_4C composite layers, residual stress measurements were carried out using X-ray

diffraction. Before testing, the surface of each sample was chemically etched at 100 °C for 7 minutes to remove surface contamination and machining effects.

Residual stress was measured using an X-ray residual stress measuring machine, as shown in Figure 4.7, which operates based on the cos α method using Chromium K-alpha radiation. During testing, the setup parameters were:

- Tube voltage 30 kV,
- Tube current 1 A,
- Radiation wave length (λ) of chromium K-alpha: 2.909 A^0
- Incident angle (ψ_0) 35
- Detector: 2-dimensional imaging plate

This technique is highly efficient, giving results in approximately 3 minutes per exposure.

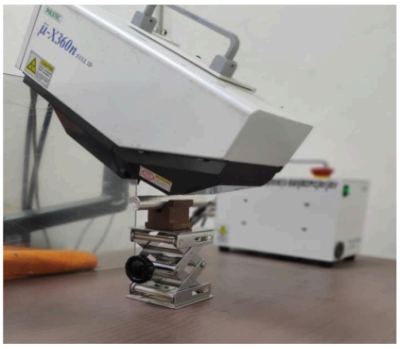

Figure 4.7: X-ray residual stress measuring machine

Principle of Measurement (cos α Method)

Residual stress measured by cos α method is a very simple and quick technique. In this method the stress is measured within 3 minutes in a single

exposure and it provides more accurate result. The imaging plates were used to collect strain data around the circumference of debye-scherrer ring. The imaging plates placed normal to the X - ray and at azimuthal angle α, Figure 4.8. The value of strain (ε_α) for a known diffraction angle θ, equation 2 is as following [34].

$$\varepsilon_\alpha = \frac{\cos^2 2\theta}{2L\cos\theta}(r_\alpha - r_0) \qquad (4.2)$$

where L is the distance between the specimen and the imaging plate, r_α is the radius of the debye ring at the azimuthal angle α and r_0 is the radius of stress-free crystals [34-36]. The relation between strain and cos α was used to determine the magnitude and the nature of stress. When the rotation angle is 0°, the stress is determined from the slope of the strain and cos α.

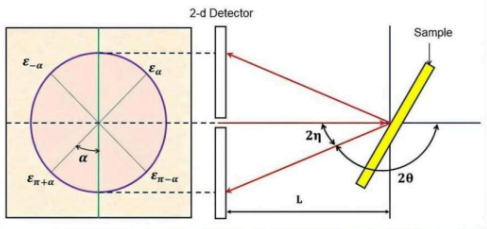

Figure 4.8: Strain measurement in debye-scherrer ring in cosα method

Debye-scherrer ring profiles shows with distortion of all temper 6 heat treated samples under normal incidence of X rays on imaging plate, Figure 4.9.

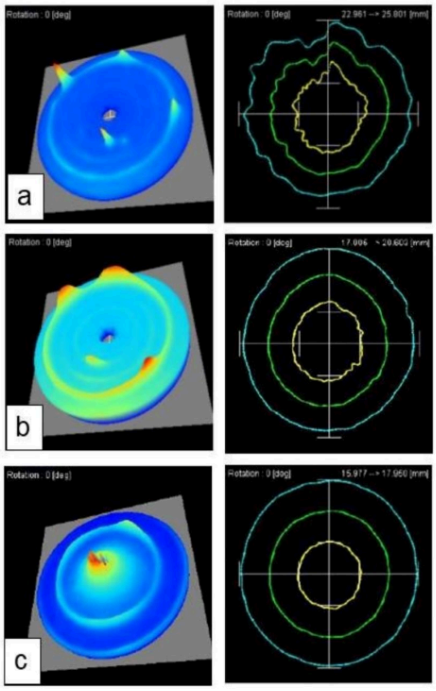

Figure 4.9: 3-D debye-scherrer ring and distortion for (a) Al 7075 8wt% B4C, (b) Al 7075 12wt% B4C, and (c) Al 7075 16wt% B4C

Figure caption also shows full width at half maximum average around the circumference of debye ring. Comparison between debye rings shows that the smoothness and uniformity of debye ring and distortion profiles increases towards higher weight percentage of reinforcement, Figure 16. With the increase in weight percentage of reinforcement, distorted ring as well as debye-scherrer ring becomes more uniform which reveals that grain refinement increases with the increase of reinforcement [35, 36].

Coarse grain composite having tensile residual stress and with the increase in weight percent of reinforcement the magnitude of residual stresses increases in compressive nature, which reveals that fatigue property increases with the increase in weight percentage of reinforcement, Table 4.2.

Table 4.2: Residual stress for different weight percent of reinforcement

Material Composition	Residual Stress (MPa)
Al 7075 + 8wt% B4C	-24
Al 7075 + 12wt% B4C	-73
Al 7075 + 16wt% B4C	-144

4.9 Results and Discussions

The microstructural and phase characterization results presented in this chapter provide clear evidence of the successful fabrication of functionally graded Al7075–B_4C composites with varying reinforcement levels (8 wt%, 12 wt%, and 16 wt% B_4C). The reinforcement was incorporated effectively through the stir-casting route, and the T6 heat treatment further enhanced the structural refinement across the composite.

The analysis of optical and FESEM proved the gradual growth of the reinforcement density of the bottom (8 wt% B_4C) and the top (16 wt% B_4C) layers. The 8 wt% area had a homogenous and well bonded interface with no significant defects, but the 16 wt% area had localized cluster of particles with micropores, which was due to the higher number of contacts between particles and difficulty in dispersing the ceramic completely. This notwithstanding, good wettability and

compatibility between molten Al7075 and B_4C particles were confirmed by the interfaces in all the layers being metallurgically in sound shape.

The results of the XRD showed that only Al and B_4C phases were formed and no other undesired reaction compounds, like Al_4C_3 existed, which indicates that the interfacial bonding is not unstable. The gradation of reinforcement as intended was confirmed by the increasing intensity of B_4C peaks particularly in the (101) plane. The increase in the B_4C content produced a slight peak shift to higher 2 theta positions which indicates the internal strain in the lattice by thermal disparity and structural limitations within the ceramic particles.

The analysis of crystallite size exhibited a downward trend (29.71 nm to 26.55 nm) with an increase in reinforcement. These add refinement is associated with B_4C pinning of grain boundaries and solidification through better nucleation, which leads to high strength and hardness via the HallPetch effect.

The above findings were supported by residual measures of stress. The 8 wt% B_4C layer had reduced compressive stress (-24 MPa) with slight Debye ring distortion, which signified comparatively coarse grains and restrained strain hardening. However, the compressive stress (-144 MPa) and uniformity/stress distribution in the Debye-Scherrer ring were much higher in the 16 wt% layer. This decrease in lower- to higher-compressive stresses proves that reinforcement level is directly proportional to fatigue resistance, and stronger influence of crack-closure on higher B_4C loading.

In general, the tendencies discussed in table 4.3, explicitly demonstrate that there is mechanically optimized structure present in the developed FGM plate due to the reinforcement gradation:

Table 4.3: Relationship among reinforcement gradation, the development of microstructure, residual stress behaviour, and the functioning performance of the Al7075-B4C FGM leaf spring plate

Reinforcement Zone	Microstructure	Residual Stress	Functional Effect
8 wt.% B_4C	Coarse grains, uniform dispersion	Low compressive (−24 MPa)	Provides elastic flexibility
12 wt.% B_4C	Fine grains, balanced dispersion	Moderate compressive (−73 MPa)	Optimal strength–ductility balance
16 wt.% B_4C	Highly refined, dense particles	High compressive (−144 MPa)	Maximum hardness & fatigue life

4.10 Conclusions

The multi-level microstructural and phase characterization of the Al7075/B_4C functionally graded composites give the following main conclusions:

Effective Formulation of Ranked Structure

The stir-casting process preceded by T6 heat treatment was able to effectively create a functional graded Al7075-B_4C composite plate with the reinforcement content of 8 wt%, 12 wt%, and 16 wt%. The reinforcement dispersion through the thickness is well-regulated and gradual, which proves the efficiency of the fabrication technique.

Microstructural Gradation and Distribution of Reinforcement

Optical and FESEM observations showed that B_4C particles concentration gradually increased as the lower and upper layers of the plate were observed. The 8 wt percent zone had homogenously dispersed and coarse grain particles whereas the 16 wt percent zone had finer grains and greater density of particles with slight agglomeration. The 12 wt Percent region was the most homogeneous providing a balance between particle dispersion and quality of interface.

Interfacial Stability and Phase Interface

FESEM and EDS measurements showed that there was a good metallurgical bond between the aluminium matrix and B_4C reinforcement. There was no detected presence of deleterious intermetallics like Al_4C_3 and was therefore chemically compatible. XRD confirmed the presence of only alpha-Al and B_4C phases which correspond to the ICDD card nos. 89-2837 and 07-0275, which means that the phase remains stable during solidification and aging.

Crystallite-Size Refinement

XRD data fitted to the Gaussian process exhibited a systematic reduction in crystallite size, 29.71 nm (8 wt%) to 26.55 nm (16 wt%) when assessed by the Scherrer equation. Grain-boundary pinning and increased nucleation offered by the ceramic reinforcement lead to the reduction in crystallite size and hence, improved strength is produced by the Hall-Petch mechanism.

Residual-Stress Evolution

The cos α method of X-ray residual-stress measurement revealed that low compressive stress (-24MPa) in the 8 wt% layer was changed to high compressive

stress (-144MPa) in the 16 wt% layer. More reinforcement content improves grains, increases internal lattice strain and produces good compressive stress which prevents the formation of cracks and increases fatigue strength.

Structure–Property Correlation

The overall findings indicate that reinforcement gradation provides an effective method of microstructure and internal stress field customization.

The lower-reinforcement zone (8 wt %) provides flexibility and ductility.

The middle reinforcement zone (12 wt%) offers moderate strength and hardness.

The maximum hardness, wear resistance and fatigue life are found in the high-reinforcement zone (16 wt%).

Overall Outcome

The processed Al7075-B_4C FGM has high structural integrity, refined grains, consistent interfacial bonding, and favorable compressive residual stresses. These properties verify the fact that the material architecture obtained in this chapter presents a valid basis of the high-order mechanical and dynamic performance described in Chapter 5.

CHAPTER 5

MECHANICAL AND DYNAMIC PROPERTY EVALUATION

5.1 Introduction

Structural integrity and service performance of functionally graded aluminium matrix composites (FGAMCs) can be critically evaluated in mechanical characterization, especially when the material is to be used in load-bearing and vibration-damping components like automotive leaf springs. The mechanical behaviour assessment offers measurable data regarding tensile strength, hardness, impact toughness and viscoelastic behaviour that are a combination of the ability of the material to sustain complex loading conditions and fatigue stresses in the working environment.

The systematic research on the mechanical performance of Al 7075 reinforced with micro boron carbide (B_4C) particles has been conducted in the current research to identify its applicability in lightweight suspension components. The grading of the distribution of B_4C in the plate thickness allows gradual change of mechanical properties which gives high strength and stiffness in the outer plates and high ductility in the core. This type of gradation provides good stress transfer, localization inhibition of strain, and better overall stiffness-weight ratio of the composite, which is important in fatigue resistance and structural integrity in leaf-springs.

The presence of B_4C particles helps to provide significant enhancement to the mechanical properties by the following mechanisms: load-transfer strengthening, Orowan looping, and refining of the grain. The well-developed grain structure and ceramic-metallic interfaces contribute towards hindrance of dislocation movement and also improves the modulus of elasticity and damage tolerance of the material. In order to measure these effects, a complete set of testing, tensile, Vickers hardness, Charpy impact and dynamic mechanical analysis (DMA) was performed. These experiment findings confirm the mechanical integrity of the developed Al 7075-B_4C functional gradient system and present a base upon which it is to be performed under the simulated service conditions.

5.2 Tensile Test

Tensile behaviour of the developed Al7075-B_4C functionally graded composites was tested in order to ascertain the effect of reinforcement percentage on strength and deformation behaviours. The tensile characteristics play a vital role in guaranteeing the safe load-carrying capacity of the leaf springs under static and dynamic service loading conditions.

To obtain accurate, consistent, and repeatable testing of tensile strength of composite specimens, tensile test was tested under ASTM E8 standard. This standard entails information about the way of specimen preparation, dimensions, and test conditions. A CNC lathe machine was used to prepare the specimens. In addition, the paper 1200 grit was used to finish the surface of the specimens as in Figure 5.1A. Figure 5.1B represents the schematic diagram of the circular tensile test specimens (36 mm gauge length and 6 mm diameter).

Figure5.1: (A) Tensile test specimens (B) Dimensions of tensile test specimen (in mm)

Five tensile samples of all compositions were made. Also, tensile properties were examined with the help of 100 kN BiSS Universal Testing Machine presented in Figure 5.2(A). The data of load (W) against extension (l) of tensile test were then plotted against the engineering stress (σ_e) against engineering strain (ε_e), as in Figure 5.2(B), by the relationship equation represented by Equations 5.1 and 5.2. The rate of strain of 10^{-3} s^{-1} was chosen according to the usual rate of strain experienced in quasi-static loading terms and this enabled an overall analysis of the mechanical properties of the material under usual testing circumstances. The bilinear stress-strain curve which is identified in this study can be explained by the microstructural properties of this composite namely the interaction of the B_4C reinforcement and the Al 7075 T6- matrix. The first linear region is the change in elastic deformation of the composite and the second linear region at a lower slope may be the start of plastic deformation.

$$\sigma_e = \frac{W}{A} \tag{5.1}$$

$$\varepsilon_e = \frac{\delta l}{l} \qquad (5.2)$$

Where A and l represents the cross-sectional area (mm^2) and the change in length (mm), respectively.

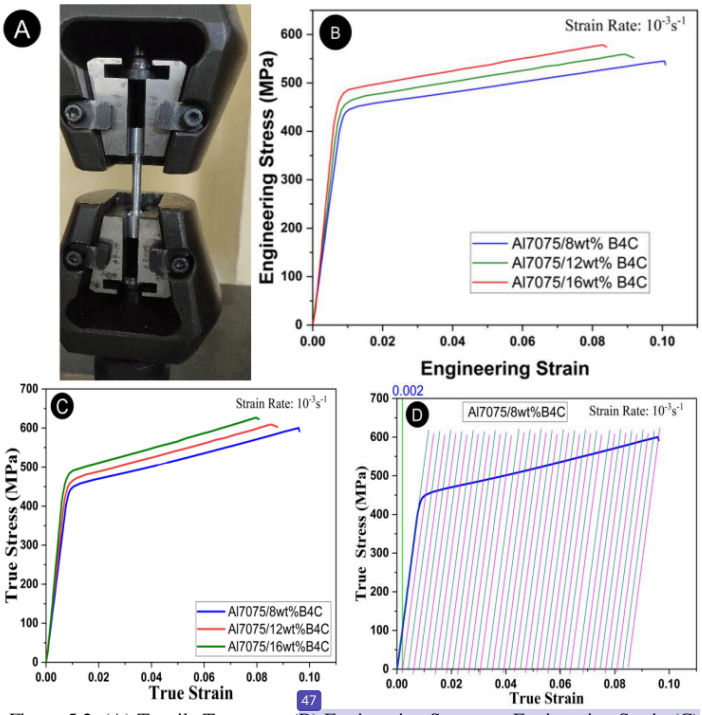

Figure 5.2. (A) Tensile Test setup (B) Engineering Stress vs. Engineering Strain (C) True stress vs. True strain. (D) Data reduction from true stress vs. True strain to True Strain

Furthermore, the engineering stress (σ_e) versus engineering strain (ϵ_e) data is converted into true stress (σ_t) versus true strain (ϵ_t) using Equations 5.3 and 5.4, as shown in Figure 5.2(C).

$$\sigma_t = \sigma_e(1 + \varepsilon_e) \quad (5.3)$$

$$\varepsilon_t = \ln(1 + \varepsilon_e) \quad (5.4)$$

The σ_t versus ε_t data is ultimately reduced to σt versus true plastic strain (ε_p) by removing the elastic component of strain, as shown graphically in Figure 5.2D. The relation of the total true strain (ε_{ts}) with true elastic strain (ε_{es}) and the true plastic strain (ε_p), as expressed in Equation 5.5

$$\varepsilon_{ts} = \varepsilon_{es} + \varepsilon_p \quad (5.5)$$

The equation is rewritten as:

$$\varepsilon_p = \varepsilon_{ts} - \varepsilon_{es} \quad (5.6)$$

Equation (5.6) is expressed as follows:

$$\varepsilon_p = \varepsilon_{ts} - \left(\frac{\sigma_t}{E}\right) \quad (5.7)$$

Here E is young's modulus in MPa. Equations (5.5-5.7) are used for the estimation of plastic low behaviour of all composites.

5.3 Hardness

The hardness of the fabricated Al7075-B_4C composites were determined in accordance with ASTM E384 using a Digital Vickers Hardness Tester (Make: ASI, Model: HVT-100ADL). The instrument features an automatic turret with closed-loop load control, eliminating the need for mechanical dead weights, ensuring high repeatability and precision. A test load of 60 kgf and a dwell time of 15 s were employed for each indentation, and the results were expressed as HV 60/15.

Before testing, the machine calibration was verified using a certified reference block, and the measurement uncertainty was maintained within ±1 HV (k = 2). For each composite composition (8 wt %, 12 wt %, 16 wt % B_4C), five indentations were

taken at uniformly spaced locations across the surface and mid-thickness regions of the functionally graded plate to capture the hardness variation arising from reinforcement distribution. The average of these readings was taken as the representative hardness value for that composition.

5.4 Flexural Strength

The flexural strength of the fabricated Al 7075–B_4C composites was evaluated using a three-point bend test on a 10 kN universal testing machine (UTM) under quasi-static loading conditions. The test followed the ASTM E855 standard for metallic and composite materials.

Rectangular specimens with dimensions 56 mm × 7 mm × 1.75 mm were sectioned from the heat-treated FGM plate using wire-cut EDM, ensuring precise geometry and minimal edge deformation. Each specimen was placed horizontally on two lower rollers at a support span (L) = 40 mm, while a centrally located upper roller applied load at a cross-head speed = 0.5 mm min^{-1}.

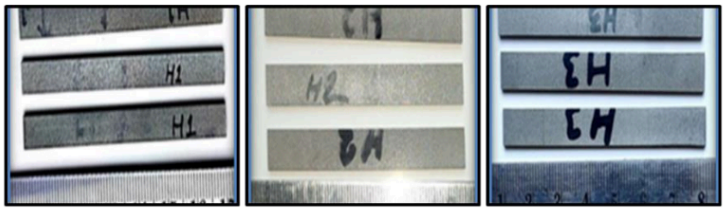

Figure 5.3: T6 Heat-treated test specimens for 8, 12, and 16 wt. % B_4C

The applied load (P) and mid-span deflection (D) were continuously recorded. The flexural stress (σ_f) and strain (ε_f) were computed using the equation 5.8 and 5.9 respectively:

$$\sigma_f = \frac{3PL}{2bd^2} \quad (5.8)$$

$$\varepsilon_f = \frac{6Dd}{L^2} \quad (5.9)$$

where b and d are the specimen width and thickness, respectively. Figures 5.3 show the machined test specimens for 8, 12, and 16 wt. % B_4C, while Figure 5.4 illustrates the UTM setup and loading configuration.

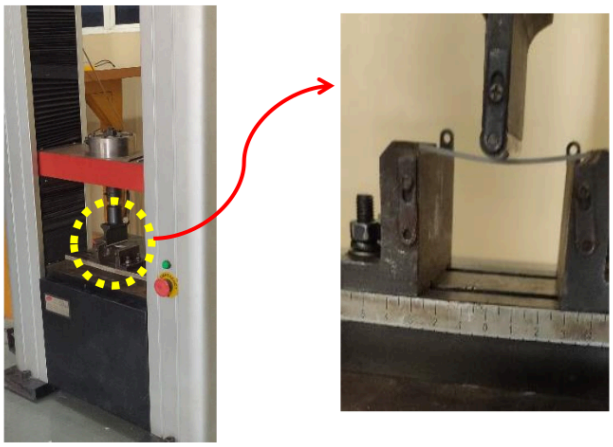

Figures 5.4: UTM setup and loading configuration

5.5 Impact Strength

The impact toughness of the fabricated Al 7075–B_4C composites was evaluated using the Charpy impact test in accordance with ASTM A370 and IS: 1586 P-1 (2018) standards. Standard V-notch specimens of size 55 mm × 10 mm × 10 mm, with a 2 mm notch depth and a 0.25 mm notch-tip radius were prepared as per standard specifications. The test specimen geometry is illustrated in Figure 5.5,

showing the schematic of the V-notched sample dimensions used for all compositions.

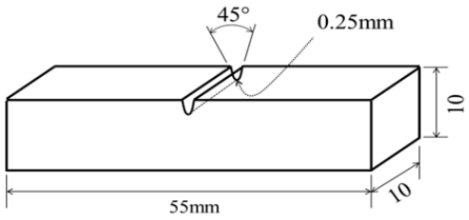

Figure 5.5: Schematic of the Charpy V-notch specimen

A Wire Electrical Discharge Machining (Wire-EDM) process was used to cut the composite bars into accurate blanks of equal dimensions so they could be notched. The residual stresses caused by machining were reduced to a minimum by the Wire-EDM method, and a high-quality surface finish was obtained on the specimen faces. The precision milling cutter was then used to machine final V-notches in order to obtain an accurate geometry and smooth surface finish.

Each specimen was positioned horizontally on the anvil supports with the notch facing opposite to the direction of the pendulum strike, as recommended by the standard procedure. The absorbed energy (in Joules) was recorded directly from the impact machine dial after fracture. Tests were carried out at room temperature, and five specimens were tested for each reinforcement composition (8 wt. %, 12 wt. %, and 16 wt. % B_4C) to obtain the mean impact energy values. Representative sets of untested V-notched samples for the three compositions are shown in Figure 5.6 (a)-(c).

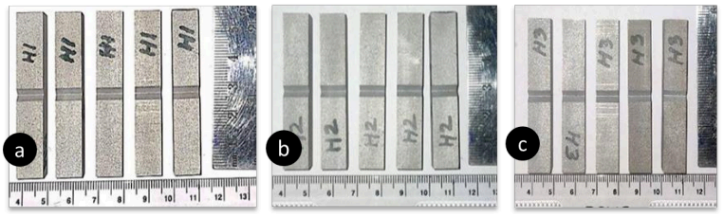

Figure 5.6 (a–c): Standard Charpy V-notch specimens for 8 wt %, 12 wt %, and 16 wt % B_4C composites before testing.

5.6 Dynamic Mechanical Analysis

Five samples of each composition were examined for their damping behaviour using DMA 8000 (Perkin Elmer). The machining process must adhere to ASTM E855 standards to ensure accurate and reliable mechanical property evaluation. The specimen dimensions are carefully selected to maintain an appropriate span-to-thickness ratio, ensuring uniform stress distribution during testing. Specimens of dimensions 20 mm x 7 mm x 1.75 mm were clamped in three-point bending position as shown in Figure 5.7(a). To achieve high precision and consistency, wire-cut EDM is preferred and maintains a machining tolerance of ±0.05 mm. A smooth surface finish is essential to reduce stress concentrations; therefore, fine grinding or polishing with 1000-grit SiC abrasive paper is performed to achieve a surface roughness (Ra) of ≤0.8 µm. Specimen edges are chamfered (0.2 mm) to prevent premature failure under bending loads as shown in Figure 5.7(b). To eliminate machining debris, final cleaning is conducted using ultrasonic cleaning composites in ethanol. These precise machining details ensure high accuracy and repeatability in DMA testing of Al7075T6/B_4C. Each sample was investigated under

gradual loading at a constant frequency (10Hz). The experiments were performed at a constant heating rate of 3 ºC per minute. Dynamic mechanical analysis was investigated for the temperature range started from room temperature to 350 ºC.

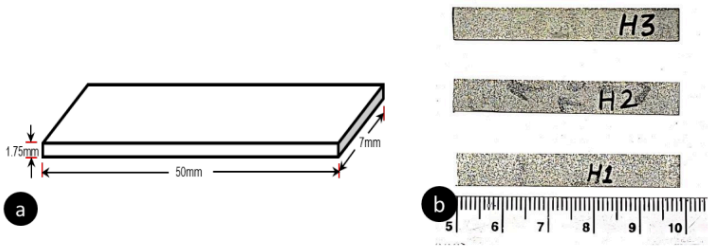

Figure 5.7: (a) Dimensions of specimens (b) DMA specimens of all three compositions

The grips used for the three-point bending test in the DMA 8000 (Perkin Elmer) machine are mechanical-type grips, specifically designed for flexural testing. To ensure consistent clamping pressure at the top and bottom grips during the testing of Al7075T6/B4C composites, several factors were controlled. Precision-designed fixtures ensured even force distribution, with a fixed lower support (two contact points) and an upper loading nose (one contact point), shown in figure 5.8. Alignment and calibration were performed before testing to prevent misalignment and uneven force application. A controlled clamping mechanism allowed for precise positioning, and pre-test calibration using a force gauge ensured consistent pressure.

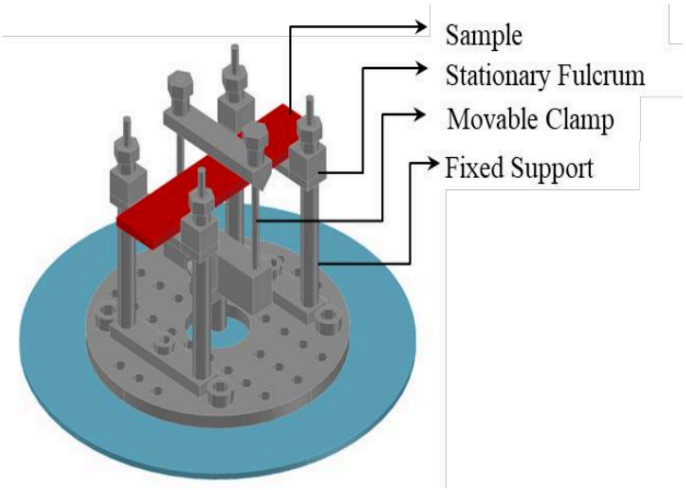

Figure 5.8: DMA three-point bend test fixture

Additionally, load monitoring was conducted to verify uniform force application. Proper specimen preparation, including uniform thickness and surface quality, minimized variations in clamping pressure. The DMA test was conducted within a temperature range of room temperature to 350°C, at a frequency of 10 Hz, with a temperature ramp rate of 3°C/min, using specimens of 50 × 7 × 1.75 mm, and each test lasted approximately 2 hours. These measures ensured reliable and reproducible three-point bending test results.

5.7 Results and discussions

5.7.1 Tensile strength

5.7.1.1 Effect of Reinforcement on Yield Strength and UTS

In developed composites, it is important to understand the effect of the weight percentage of the reinforcement on the tensile properties. The data shown in Figure

5.9 show the yield strength and ultimate tensile strength (UTS) of Al7075 alloy reinforced with different weight percentages of boron carbide (B4C). The analysed composites were Al7075 reinforced with 8 wt%, 12wt% and 16 wt%B4C.

From Figure 5.9, it is clear that increasing the weight percentage of B4C reinforcement in the Al7075 alloy increases the yield strength. Generally, the yield strength increases from 450.80645 MPa for Al7075/8wt%B4C to 483.65874 MPa for Al7075/16wt%B4C. This increase in yield strength indicates that the material is more resistant to plastic deformation with higher B4C content. This means that higher B4C percentages can withstand higher stress levels before deformation begins, increasing performance and durability under load bearing conditions. The data shows a similar trend for UTS as observed for yield strength. The UTS increases from 600.17659 MPa for Al7075/8wt%B4C to 626.64555 MPa for Al7075/16wt% B4C. This trend signifies that the overall tensile strength of the material is enhanced with the addition of B4C reinforcement

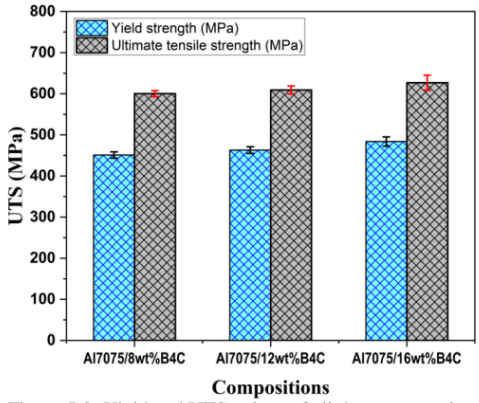

Figure 5.9: Yield and UTS values of all three composites

5.7.1.2 Effect of reinforcement on the strain hardening

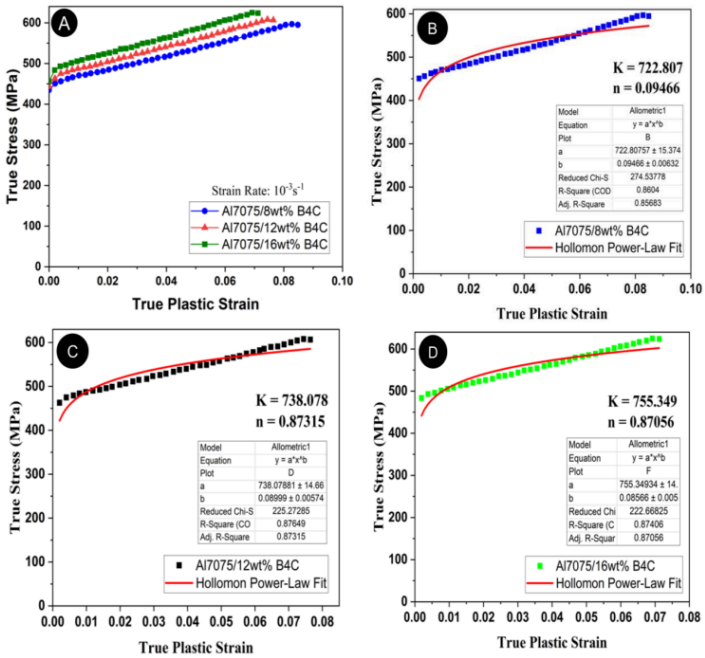

Figure 5.10: (A) True stress–true plastic strain curve; (B–D) Hollomon power law fitting for Al7075/8 wt.%, 12 wt.%, and 16 wt.% B_4C composites, respectively.

The true plastic strain behaviour with respect to true stress was determined with the help of equations (5-7) and the curve between these are plotted with the help of data obtained from figure 5.2(D) as shown in Figure 5.10(A). Furthermore, Hollomon establishes a power-law relationship between true stress (σ_t) and true plastic strain (ε_p) in the plastic deformation region. The true stress versus true plastic strain for each composition is plotted in Figure 5.10(B-D) and fitted to the power-law equation 5.10.

$$\sigma_t = K\varepsilon_p^n \quad (5.10)$$

here K represents the strength coefficient and n represents the strain hardening exponent.

The numerical results are in good agreement with the experimental results. However, 5% variation was observed between experimental and numerical results. Through the Hollowmon power law fitting the values of the strength coefficient and strain hardening exponent have been obtained. The data presented in Table 5.1 highlights the effect of B4C reinforcement on the strain hardening exponent (n) and the strength coefficient (K). The three compositions considered in this study include Al7075 reinforced with 8wt%, 12wt%, and 16wt% B4C. The variation of strain hardening exponent (n) with respect to strength coefficient (K) for all three composites are shown in Figure 5.11(A).

Table 5.1: Hollomon Power-Law fitting parameters for Al7075-B_4C composites

Composite Composition	Strength Coefficient (K)	Strain Hardening Exponent (n)	R-Square (COD)	Adjusted R-Square	Reduced Chi-Square
Al7075/8wt%B4C	722.807 ± 15.374	0.09466 ± 0.00632	0.8604	0.8563	274.5378
Al7075/12wt%B4C	738.078 ± 14.66	0.08999 ± 0.00574	0.8749	0.8731	225.2728
Al7075/16wt%B4C	755.349 ± 14.00	0.08656 ± 0.0056	0.87406	0.87056	222.6682

It is evident from the data that an increase in the weight percentage of B4C reinforcement results in a consistent decrease in the strain hardening exponent. Specifically, the strain hardening exponent decreases from 0.09466 for the Al7075/8wt%B4C composition to 0.08566 for the Al7075/16wt%B4C composition. This trend indicates that as the proportions of B4C in the composite increases, the

material's capacity to strain harden diminishes. In practical terms, this reduction implies that the composite becomes less capable of enhancing its strength through plastic deformation, which could influence its performance in applications requiring significant plastic work. Conversely, the strength coefficient (K), which represents the overall strength of the material, shows a positive correlation with the weight percentage of B4C reinforcement. The strength coefficient increases from 722.807 for the Al7075/8wt%B4C composition to 755.349 for the Al7075/16wt% B4C composition. This increase suggests that the addition of B4C reinforcement effectively enhances the inherent strength of the Al7075 alloy. Higher strength coefficients are indicative of a material that can withstand greater loads, making these composites potentially more suitable for applications demanding high strength.

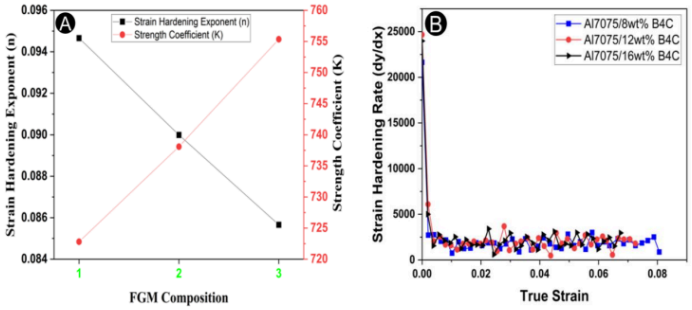

Figure 5.11: (A) Strain hardening exponent vs. Strain coefficient vs. composite compositions (B) Strain hardening rate vs. True plastic strain.

5.7.1.3 Effect of weight percentage of reinforcement on strain hardening rate:

The strain hardening rate (dy/dx) versus true strain of Al7075 alloy with different weight percentage of boron carbide (8wt%, 12wt%, and 16wt) is explained

in the graph in Figure 5.11(B). This discussion offers useful information as far as the degree of B4C reinforcement is concerned by how the hardening behaviour of the material is affected by deformation. The data show that the three compositions have a strong first peak in the strain hardening rate at the beginning of the deformation. This high initial rate indicates considerable dislocation interactions and work hardening as the materials start deforming.

Strain hardening rates of the various compositions are comparable which implies that early deformation response is comparable across all levels of the B4C reinforcing. The strain hardening rate of each composition after the first peak is much lower meaning that the initial strain hardening stage changes over to a regime of very low strain hardening rate. Beyond this drastic decrease, the rate of strain remains constant and tends to vary within the real range of strain to a small extent of about 0.08. Such stability implies that the material attains a condition where strain hardening proceeds at a slow and constant rate.

Through the comparison of the compositions, it is possible to observe that Al7075/8wt% B4C exhibits very different strain hardening behaviour after the peak, whereas the strain hardening behaviour of Al7075/16wt% B4C exhibits a behaviour strain hardening. This implies that an increase in B4C content can help facilitate a greater response during a continuous change. These differences are not as significant as the strain hardening rates of the different compositions are similar following the initial peak-value, which means that the extent of reinforcement has less effect on the rate of strain hardening in the later parts of the cycle.

5.7.2 Hardness Measurement

The hardness values of five sites in each composite are recorded in Table 5.2 and the average values are plotted in Figure 5.12. The degree of hardness was found to increase consistently with the proportion of reinforcement in the form of B4C with the hardness increasing to 141.2HV at a weight ratio of 8wt% B4C to 166.6HV at 12wt% B4C and reaching 202.4 HV for 16 wt %. This is a rough 43 percent increase in surface hardness over the lowest reinforcement structure, which proves the enhancing influence of ceramic particle incorporation.

Table 5.2: Vickers hardness values of Al 7075–B_4C composites at different measurement locations.

Material Composition	Vikers Hardness Values at Different Locations (VHN)					Mean (HV)
	1	2	3	4	5	
Al 7075/8wt% B4C	137	145	141	143	140	141.2
Al 7075/12wt% B4C	175	170	162	160	166	166.6
Al 7075/16wt% B4C	201	190	210	203	208	202.4

The hardness enhancement can be attributed to several concurrent mechanisms. The homogeneous dispersion of B_4C particles within the aluminium matrix serves as an effective obstacle to dislocation movement, thereby contributing to dispersion strengthening and promoting Orowan looping mechanisms**.** Additionally, the thermal mismatch between the Al matrix and B_4C particles during solidification induces geometrically necessary dislocations at the interface, further contributing to work hardening. The presence of fine, uniformly distributed particles also results in grain refinement, thereby increasing resistance to localized plastic deformation.

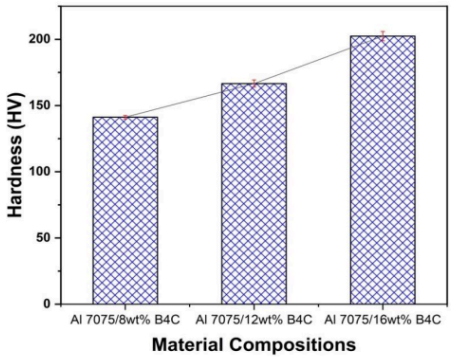

Figure 5.12: Variation of hardness of Al 7075–B_4C composites with reinforcement percentage.

The hardness percentage increases with reinforced percentages which show that the load bearing ability and wear resistance increase with the amount of B4C. Localized concentration of particles and natural microstructural heterogeneity of cast composites explain minor differences between indentation sites as can be seen in Table 5.2. In general, the trend supports the fact that functionally graded architecture gives a more favourable gradient of hardness, which is more intense at the outer layer (16 wt% B4C) and moderate at the core of the structure, providing both stiffness and toughness to the leaf-spring performance.

5.7.3 Flexural Strength Measurement (Three-Point Bend Test)

The outcomes of the bending test are shown in Table 5.3 and the trend of the flexural strength in Figure 5.13. Measured average strengths improved with reinforcement content, 541 MPa with 8 wt% B4C, 558 MPa with 12 wt%, and 594 MPa with 16 wt%. The positive effect of B4C reinforcement on the load-bearing capacity and

interfacial integrity is corroborated by the 10 percent improvement in the lowest and highest compositions.

Table 5.3: Mean flexural strengths of all compositions

FGM Composition	Mean Flexural Strength (MPa)	Std. Dev.
Al7075/8% B_4C	529.7	8.16
Al7075/12% B_4C	548	8.4
Al7075/16% B_4C	573.8	14.59

The trend observed is in line with the findings by Baradeswaran and Perumal (2013), who found that the addition of B4C particles into an Al7075 matrix significantly improves flexural and hardness characteristics due to the reinforcement of the grains by the particles and good bonding between the matrix and the reinforcers. In the same fashion, Venkatesh et al. (2018) revealed that B4C reinforced Al7075 composites exhibit better bending strength than Al_2O_3 filled systems because of increased stiffness and strength at the interfaces.

The increment in strength with the increase in the wt % B4C in the current study can be attributed to the load-transfer mechanism whereby, the stress is distributed efficiently between the aluminium and the hard ceramic reinforcement. Moreover, the dislocations, which are geometrically required, emerge at the particle/matrix boundaries due to the difference in the thermal expansion coefficients of Al and B4C, making plastic flow in bending more difficult.

The load-deflection behaviour was linear in its elastic phase and then gradually operated in the non-linear yielding direction to fracture, which corresponded with the behaviour of Azzam and Li (2014), who found that interfacial

adhesion and uniformity of the microstructure control the stiffness and the initiation of failure in composite laminates during three-point bending. Microscopic observation of the fractured surfaces showed that there was a slight deflection of cracks and bridging with ceramic particles, which proved the successful interfacial bonding that was obtained with the help of ideal stir-casting and T6 treatment

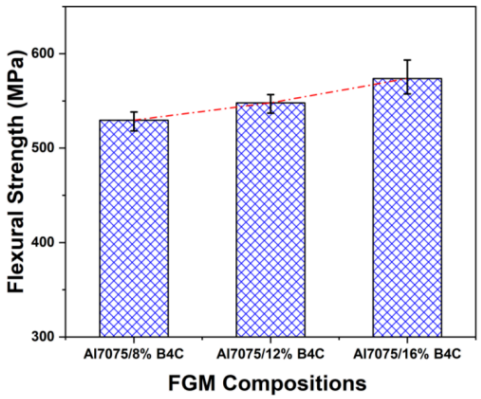

Figure 5.13: Flexural strength of all three compositions of FGM leaf

Interpretation and Implications

The increase in flexural strength was found to be closely consistent with the results of aluminium-based B4C composites by Baradeswaran and Perumal (2013) and Manjunatha et al. (2018) which showed an augmentation of the bending stiffness and fatigue resistance of the material with the rise in the reinforcement ratios during cyclic loading. The highest percentage of bending stress occurs on the outermost layers containing 16 wt% B4C to resist crack formation, and the core layer

containing 8 wt% B_4C to remain ductile and energy-absorbing in the context of the functionally graded plate.

Therefore, the test of three point bending proves the integrity of the structure and the optimization of the strength of the plate of FGM made. The results confirm the appropriateness of the developed Al 707-B4C FGM system to leaf-spring and suspension applications, which are characterized by high stiffness, fatigue endurance, and lightweight efficiency in comparison with traditional steels.

5.7.4 Impact Strength Assessment

The findings in Figure 5.14, reveal that the impact strength of the reinforcement material reduces with increase in its reinforcement content. The variants 12 wt percent and 16 wt percent of B4C were less effective in energy absorption, hence the Al7075/8 wt percent B4C with the highest energy absorption of approximately 18 J. The steadily decreasing effect strength in increasing concentration of B4C has been explained by the increased brittle nature and decreasing ductility of the matrix which is caused by the presence of hard ceramic particles that serve as micro-stress concentrators.

At a reduced reinforcement (8 wt % B 4C) the plastic deformation ability of the aluminium matrix is not reduced, and consequently, more energy is absorbed before fracture occurs. The overall effect of raising the B 4 C fraction is the creation of more rigid interfaces and restriction of the plastic flow of the aluminium, which induces early crack initiation and propagation.

Similar behaviour has been observed in other Al-based metal-matrix composites, where higher ceramic content improves hardness and strength but diminishes

toughness. The observed reduction in impact energy therefore reflects a trade-off between strength enhancement and loss of ductility.

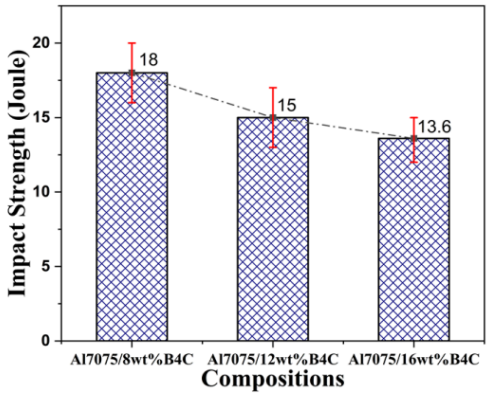

Figure 5.14: Impact strength of Al7075–B_4C composites with different reinforcement levels.

5.7.5 Damping Characteristics

Dynamic mechanical analysis was performed to investigate the damping behaviour of the newly developed composites, utilizing storage modulus, damping factor and loss modulus measurements across a wide temperature range. It was exciting to compare the findings, resulting from changes in the reinforcement weight percentage in the composite materials with the interpretations presented in the literature. The induced strain response for the applied sinusoidal stress was measured by mechanical spectroscopy. Total stress (σ) and total strain (ε) equations are given by equations 11 and 12.

$$\sigma = \sigma_{\circ}\exp(iwt) \quad (5.11)$$

$$\varepsilon = \varepsilon_{\circ}\exp(iwt - \delta) \quad (5.12)$$

The respective terms: $\sigma_\circ$ represent amplitude of applied stress; $\varepsilon_\circ$ represent Strain response, δ represent phase shift between the applied stress and the resulting strain and, ω angular frequency of vibration. Further by dividing equation 5.11 with equation 5.12, a result in young's modulus (E) is given by equation 5.13.

$$E = \frac{\sigma_\circ}{\varepsilon_\circ}(\cos\delta - i\sin\delta) = E' - iE'' \tag{5.13}$$

The material's damping capacity is defined as the ratio between the two moduli shown in equation 5.14.

$$Damping\ Capacity\ (\tan\delta) = \frac{E''}{E'} \tag{5.14}$$

Figure 5.15 represents variation of storage modulus and internal friction (tan δ = E"/E′) as a function of temperature during heating for all three composites. For the Al 7075/8% B4C composite, the storage modulus revealed a minimum value of 48.67383 GPa at 349.375°C, showing significant stiffness reduction at raised temperatures as shown in Figure 5.15(A). The highest storage modulus was 59.47132 GPa at 25.75°C, demonstrating enhanced mechanical properties at lower temperatures. This temperature-dependent behaviour highlights the potential limitations of this composite in high-temperature applications. Al 7075/12% B4C composite showed similar characteristics. The minimum storage modulus was 48.87307 GPa at 379.5°C, and the maximum value was 62.42296 GPa at 30.4°C, as interpreted in Figure 5.15(B). Increasing the B4C content improved the stiffness of the composite at lower temperatures, but the stiffness did not decrease significantly at higher temperatures. In Al 7075 /16wt% B4C composite, the minimum storage capacity is 52.3858 GPa at 379.3125°C and the maximum is 66.9682 GPa at 29.3 °C as shown in Figure 5.15(C). The higher B4C content resulted in the highest storage

modulus values in the composites studied, indicating a strong reinforcing effect. However, the temperature dependence continued and the modulus decreased significantly at higher temperatures.

The tan delta analysis provides insight into the damping behaviour of the composites, as interpreted by Figure 5.15(A-C). For the Al 7075 T6 and 8% B4C composite, the lowest tan delta is 0.00317 at 125.3375°C, indicating little loss of strength. The highest tan-delta at 349.375 ºC is 0.00919, indicating better damping behaviour at higher temperatures. Al 7075 with 12% B4C composite is 0.00153 at 80.7ºC and a maximum of 0.0118 at 379.1ºC. A smaller tan-delta indicates a decrease in energy dissipation and an increase in stiffness at lower temperatures, while a larger tan-delta indicates an increase in damping at high temperatures. For Al 7075 and 16% B4C composite, the minimum tan delta is 0.00132 at 52.275ºC and the maximum is 0.01539 at 379.3125ºC. The lowest tan delta among the compounds indicates the highest stiffness and the least loss of strength (energy dissipation) at low temperatures. A large increase in tan-delta at high temperatures indicates highest energy absorption capacity (highest damping).

Finally, the tan delta findings for all three compositions revealed that at low temperatures, energy dissipation (loss of strength) and stiffness are high, whereas at high temperatures, the damping capacity increases. With the increase in weight percentage of B4C, stiffness and energy dissipation of the composites improve at low temperatures and damping at high temperatures.

Damping properties are affected by lattice misalignments, such as point defects, and dislocations. Zhang et al. were among the first to illustrate the potential

mechanisms governing damping in metal matrix composites (MMCs). At low temperatures, the difference in the coefficients of thermal expansion (CTE) between the matrix and dispersoids leads to dislocation damping. At elevated temperatures, grain boundary sliding and interface effects become critical for damping. According to Granato–Lucke's (G-L) dislocation theory, the movement of dislocations between the matrix and dispersoids can be described by equations 5.15, 5.16 and, 5.17.

$$\tan\delta = \frac{C_1}{\varepsilon} exp\left(\frac{C_2}{\varepsilon}\right) \quad (5.15)$$

$$C_1 = \frac{\rho F_B L_N^3}{6bEL_C^2} \quad (5.16)$$

$$C_2 = \frac{F_B}{bEL_C} \quad (5.17)$$

The terms are defined as follows: E is Young's Modulus, ε is the strain, ρ represents dislocation density, C_1 and C_2 are specific constants of material, b is the Burger's vector, F_B represents the cohesive force between weak pinning points and dislocations. Mean dislocation distances between strong pinning point to weak pinning point are represented by L_N and L_C The results reveal a clear interrelationship between the storage modulus and tan δ. As the B4C content increases, both stiffness (indicated by the storage modulus) and damping behaviour (indicated by tan δ) improve. However, this improvement is more pronounced at lower temperatures. At higher temperatures, all compositions exhibit a reduced storage modulus and an increased tan δ, indicating a shift from stiffness to enhanced damping behaviour.

Among the composites, Al7075/16 wt% B4C shows the highest storage modulus for the entire temperature range, indicating increased stiffness due to the higher B4C content shown in Figure 5.15(D). This shows that integrating a higher percentage of B4C particles notably improves the stiffness of the composite material. In contrast, Al7075/8B4C shows the lowest storage modulus, indicating that a lower B4C content results in a less stiff material.

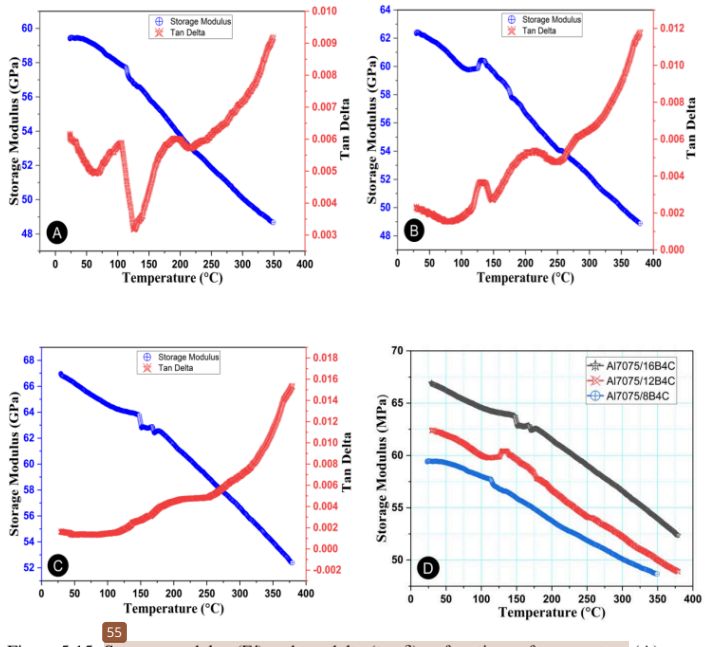

Figure 5.15: Storage modulus (E′) and tan delta (tan δ) as functions of temperature (A) Al7075/8B4C composite (B) Al7075/12B4C composite (C) Al7075/16B4C composite (D) Storage modulus as function of temperature of all three composites

The slight variations between the modulus values could be explained by the various phases of the material change; however, a large drop in the stiffness is evident as the temperature rises. The findings indicate that B_4C reinforcement can be used to improve the structural rigidity of Al7075 composites, which can be applied in high stiffness jobs at high temperature. The fact that the values of the initial storage modulus are high at low temperatures shows that the T6 heat treatment has been effective in improving the rigidity of the composite. But with rise in temperature, the

strengthening effect of B_4C particles and T6 treatment is conquered and gradual stiffness reduction takes place.

The tan delta (tan δ), or the damping factor, is a quantification of the energy dissipation properties of a substance, the ratio of the energy lost to the energy stored per cycle of deformation. Figure 5.16(A) shows the values of tan delta of the Al7075/B_4C composites versus temperature. The three composites have an increasing tan delta with increasing temperatures and that means, the more compliant the materials, the higher the energy dissipation. The tan delta values of Al7075/8B_4C composite (8% B_4C) are higher than the other two composites at lower temperatures. This implies that the composite is lower in B_4C content and therefore has better damping properties at such temperatures. Higher energy dissipation can be used in applications where it is necessary to have vibration damping. Nevertheless, the value of tan delta converged to all the composites as the temperature rose above 200°C, which is a sign of a high-temperature damping behaviour. This mixture demonstrates a lesser reliance on B_4C material at a specific temperature. Peaks and variations observed in tan-delta curves can be associated with a wide range of thermal transitions in composites including glass transition temperatures and other softening processes. This type of transition is relevant to know the thermal and mechanical characteristics of composites in different operating conditions.

Loss Modulus Analysis

The loss modulus of Al 7075 composites reinforced with 8, 12% and 16% B4C was investigated in the temperature range room temperature to 400°C. The results show a significant dependence on temperature and B4C content. The

composite of Al 7075 with 8% B4C showed an initial fatigue strength of around 100 MPa, which increased continuously and reached 450 MPa at 375 ℃. The Al 7075 with 12% B4C composite started with a higher initial critical point of around 150 MPa and reached a maximum of 500 MPa at 350 ℃. The Al 7075 & 16% B4C composite demonstrated the highest performance, beginning at 200 MPa and reaching up to 800 MPa at 375°C as shown in Figure 7(B) . This trend illustrates that higher B4C content significantly enhances the composite's energy dissipation capacity, particularly at elevated temperatures.

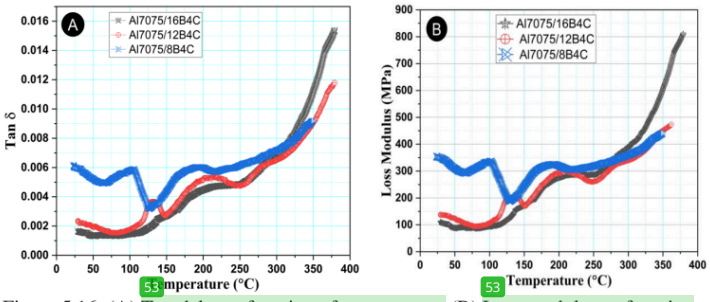

Figure 5.16: (A) Tan delta as function of temperature (B) Loss modulus as function of temperature

The combined DMA results confirm that both stiffness (E′) and damping (tan δ) behaviour depend strongly on temperature and reinforcement level. At lower temperatures, dislocation-based damping dominates due to mismatch in the coefficients of thermal expansion (CTE) between aluminium and B_4C, whereas at higher temperatures, grain-boundary sliding and interfacial friction govern the damping process. According to the Granato–Lücke dislocation theory, the movement

of dislocations between strong and weak pinning points explains the observed dependence of damping on reinforcement and temperature.

The increase in B_4C content up to 16 wt% raises both the initial stiffness and the high-temperature damping capacity of the composites. This dual improvement validates that the developed Al7075-B_4C system combines rigidity with enhanced energy-absorption characteristics, making it highly suitable for dynamic components such as FGM leaf springs subjected to fluctuating loads.

5.8 Conclusions:

Mechanical and dynamic characterization of the fabricated Al 7075/B_4C functionally graded composites showed uniform enhancement of the strength, stiffness and damping behaviour with the increase of reinforcement content. According to the experimental research, the following conclusions are made:

Tensile Behaviour:

The tensile tests revealed that there was a gradual increase in yield and ultimate tensile strength as reinforcement increased. The yield strength rose to about 483.6 MPa with 16 wt% B_4C compared to 8 wt% B_4C and the ultimate tensile strength also rose by about 626.6 Mpa which is a 4.4 percent increment compared to 5.7 percent increment in 8 wt%. This enhancement is credited to efficient load transfer of the hard B_4C particles with the aluminium matrix, dislocation blocking by the Orowan looping and grain refinement processes.

Strain Hardening Response:

The power-law analysis using the Hollomon method showed that the strain-hardening exponent (n) decreased to 0.0857 and the strength coefficient (K) increased to 755 MPa as the reinforcement concentration (8 wt% to 16 wt%) increased. The decreased n value is the indication of the decreased work-hardening capacity and the increased K value is the indication of the raised intrinsic strength. The strain-hardening rate showed a sharp peak and a flat plateau which agreed with the fact that the rate of deformation is the same in all compositions.

Hardness:

The reinforcement content was found to raise the Vickers hardness gradually, with a 16 wt% sample of 202.4 HV, and 8 wt% sample of 141.2 HV, which is a total improvement of about 43. The improvement is due to the dispersion strengthening of the particles, looping of Orowan, and the generation of dislocation by thermal mismatch. The graded distribution offered hardness gradient that was useful in hardness at the outer layers and toughness at the center.

Flexural Strength:

The three-point test showed that flexural strength rose by the same 10 percent, between about 529.7 MPa of 8 wt% and 573.8 MPa of 16 wt%. This is aided by the existence of effective stress sharing between the reinforcement and the matrix and good interfacial bonding generated by an optimized stir casting and T6 heat treatment. The graded structure was necessary to ensure that the outer layers withstood bending stresses with the core being ductile.

Impact Toughness:

The enhancement of impact strength with the increase in the level of reinforcement was noted to be 18J at 8 wt% and 13J at 16 wt% due to the rigid nature of B_4C inclusions that created brittle characteristics. This is the trade-off between strength and toughness, which is characteristic of particle reinforced metal matrix composites, and is acceptable within the limits of structural applications in which stiffness is a major consideration.

Dynamic Mechanical Analysis:

Storage modulus (E') was found to increase with reinforcement which proved higher rigidity at lower temperatures. The highest E' was increased to approximately 59.5 GPa to 66.9 GPa respectively. As temperatures increased, E′ decreased as a result of the softening of the matrix and the damping factor (tan 6) and loss modulus also rose, indicating enhanced energy-dissipation ability. The minimum tan δ and maximum tan δ were reduced by approximately 52 percent and 14 percent in the first and second reinforcement increments respectively, and the maximum tan δ was increased by 28 percent and 30 percent respectively, with consequent improvements in the high-temperature damping performance.

Overall Behaviour:

The overall mechanical and dynamic performance proves that the functionally graded material system of Al7075-B4C has an ideal balance of high stiffness, strength and damping performance. The outer layers consist of 16 wt% B4C that enables it to be stiff in nature and have high load bearing capacity, and the core consists of 8 wt% that still has ductility and the ability to absorb energy. The following attributes render the developed composite to be very suitable in

lightweight structural applications like functionally graded leaf spring plates in automotive suspension systems.

Chapter 6

FINITE ELEMENT ANALYSIS AND OPTIMIZATION OF AN FGM LEAF SPRING PLATE

6.1 Introduction

40

The finite element method (FEM) is a go-to tool for testing how structural components will behave before they're even made. In this study, finite element analysis to put the functionally graded Al7075/B_4C leaf spring plate through its paces. The main goal was to figure out which gradation scheme would deliver the best stress and deflection performance. The main aim was to identify the optimal combination for best structural performance.

Simulations under static bending conditions using ABAQUS 2018 Explicit solver, mimicking the real world loading and support setup was performed. Results were analysed considering Von-Mises stress distribution and end deflections to quantify leaf spring plate's structural integrity and stiffness.

6.2 Finite Element Modelling Strategy

6.2.1 Geometric Modelling

A 3D model of the functionally graded leaf spring plate using ABAQUS 2018 was created basing its dimensions on precise measurements from a coordinate measuring machine (CMM) as illustrated in Figure 6.1. The developed model had a five layer

graded core with aluminium layers at both ends. This layout directly replicated the fabricated specimen and served as the reference model for subsequent simulations.

Figure 6.1: Measurement of leaf spring geometry using CMM.

6.2.2 Assignment of Material Properties

Each graded layer was assigned elastic properties such as Young's modulus, Poisson's ratio, and density, according to its reinforcement level (8, 12, and 16 wt.% B_4C). Aluminium 7075-T6 served as the base matrix material. The B_4C content was modelled as a compositional gradient along thickness to mimic the fabricated FGM structure.

6.3 Gradation Schemes for FEA

Only six feasible gradation combinations exist for a five-layered FGM section due to symmetry at both ends of the plate. These schemes are listed in Table 6.1 and

labelled M-M6 for clarity. The matrix material was Al7075-T6, while micro-sized B_4C particles were used as reinforcement.

Table 6.1: Reinforcement gradation patterns (top-to-centre).

FGM Gradation of leaf from top to centre or bottom to centre	Model Name
16/12/8	M 1
16/8/12	M 2
12/16/8	M 3
12/8/16	M 4
8/12/16	M 5
8/16/12	M 6

6.3.1 Visual Representation of FGM Layout

The central gradation of the fabricated Al7075-T6/B_4C leaf spring plate is illustrated in Figure 6.2. The graded section comprises five layers, where the reinforcement percentage is varied to tailor stiffness and improve bending performance. Three gradation families (A, B, and C) were evaluated, each maintaining uniform reinforcement at both ends of the leaf and applying a mirrored layer-wise distribution across the central region.

Configuration A: 16 wt.% B_4C at top, bottom and ends, with central layers following 16/12/8/12/16 or 16/8/12/8/16. This setup boosts tensile resistance at the outer surfaces, where bending stresses are highest.

Configuration B: 12 wt.% B_4C at ends, with central gradation following 12/16/8/16/12 or 12/8/16/8/12. This helps assess how mid-layer reinforcement inversion affects performance.

Configuration C: 8 wt.% B_4C at ends, with central region adopting 8/12/16/12/8 or 8/16/12/16/8. This checks if reinforcing the core makes up for lower surface stiffness.

These grading setups are useful in evaluating the impact of reinforcement positioning on stiffness, stress and deflection in the functionally graded leaf spring, clearly illustrated in Figure 6.2.

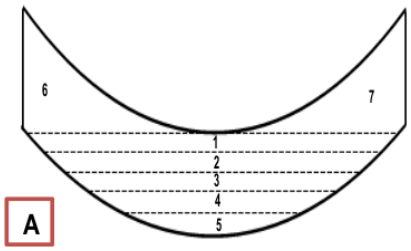

Numbering	Corresponding Composition	
	M1	M2
1	Al7075T6/16wt% B4C	-
2	Al7075T6/12wt% B4C	Al7075T6/8wt% B4C
3	Al7075T6/8wt% B4C	Al7075T6/12wt% B4C
4	Al7075T6/12wt% B4C	Al7075T6/8wt% B4C
5	Al7075T6/16wt% B4C	-
6	Al7075T6/16wt% B4C	-
7	Al7075T6/16wt% B4C	-

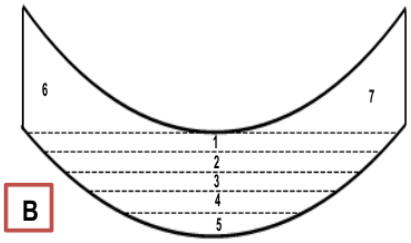

Numbering	Corresponding Composition	
	M3	M4
1	Al7075T6/12wt% B4C	-
2	Al7075T6/16wt% B4C	Al7075T6/8wt% B4C
3	Al7075T6/8wt% B4C	Al7075T6/16wt% B4C
4	Al7075T6/16wt% B4C	Al7075T6/8wt% B4C
5	Al7075T6/12wt% B4C	-
6	Al7075T6/12wt% B4C	-
7	Al7075T6/12wt% B4C	-

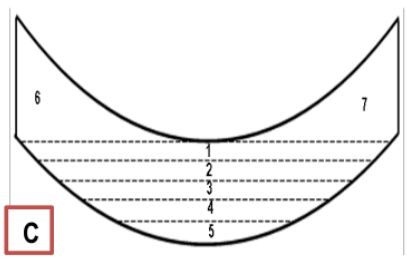

Numbering	Corresponding Composition	
	M5	M6
1	Al7075T6/8wt% B4C	-
2	Al7075T6/12wt% B4C	Al7075T6/16wt% B4C
3	Al7075T6/16wt% B4C	Al7075T6/12wt% B4C
4	Al7075T6/12wt% B4C	Al7075T6/16wt% B4C
5	Al7075T6/8wt% B4C	-
6	Al7075T6/8wt% B4C	-
7	Al7075T6/8wt% B4C	-

Figure 6.2: Central gradation schemes of the composite leaf spring.(A) 16-based arrangement; (B) 12-based arrangement; (C) 8-based arrangement.
Each scheme maintains uniform reinforcement at the two plate ends.

6.4 Boundary Conditions and Simulation Setup

The leaf spring was fixed in the central region in all translational and rotational degrees of freedom to simulate the actual clamping condition. Symmetric vertical bending loads were applied at both free ends to represent vehicle suspension loading.

A structured mesh of 8-node linear brick elements (C3D8R) was generated, providing accurate representation of stress gradients across layers. Mesh density was refined near interfaces to capture potential stress localization, Figure 6.3.

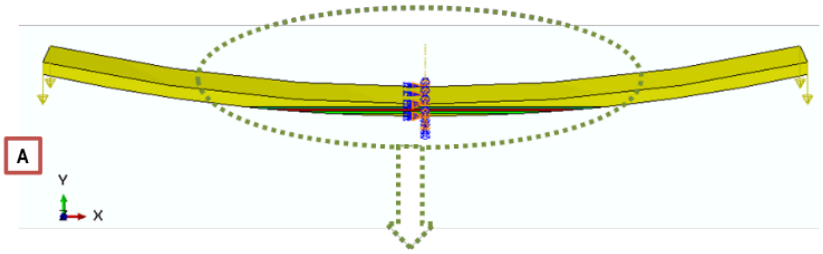

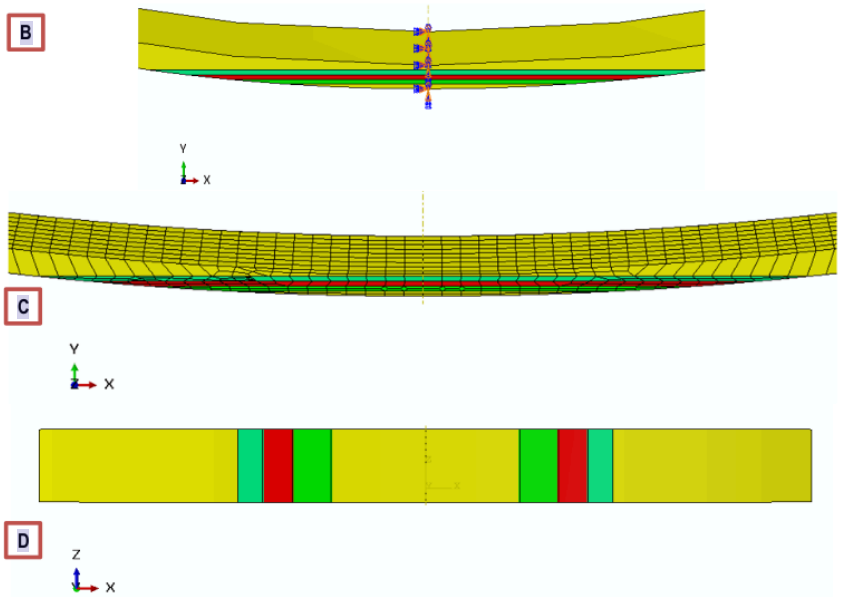

Figure 6.3: FGM plate FE model configuration. (A) Applied loading at free ends, (B) Fully fixed central region, (C) C3D8R meshing strategy, (D) Bottom view of 5-layer gradation.

6.5 Numerical Results and Discussion

6.5.1 Stress Distribution Analysis

The mechanical response of the functionally graded leaf spring plate was analysed using ABAQUS 2018. The central region of the plate was fully constrained, while symmetrical bending loads were applied at both free ends to reproduce realistic in-service conditions. This method of loading ensures transfer of load through bending and mirrors operational behaviour of leaf springs.

The von Mises stress contours for the six gradation models (M1-M6) are shown in Figure 6.4. The detailed description of various are Model summarized below.

Model M1 (16/12/8): Stress is uniformly distributed evenly across the span, with moderate levels in the central fixed region and peaks near the loaded ends. The smooth gradation is helping to transfer stresses efficiently, reducing hotspots.

Model M2 (16/8/12): Stress concentration is near the central fixation zone, likely due to stiffness discontinuity. This could lead to premature cracking under cyclic loading.

Model M3 (12/16/8): Stress magnification at layer interfaces is more pronounced than in M1.

Model M4 (12/8/16): Central low-reinforcement layer creates sharp stress peaks, potentially reducing durability and increasing fatigue risk.

Model M5 (8/12/16): Stress accumulates in thicker end layers, leading to uneven stress transfer and possible non-uniform deformation.

Model M6 (8/16/12): High stress concentrations near the constrained region and significant non-uniformity.

35

M1

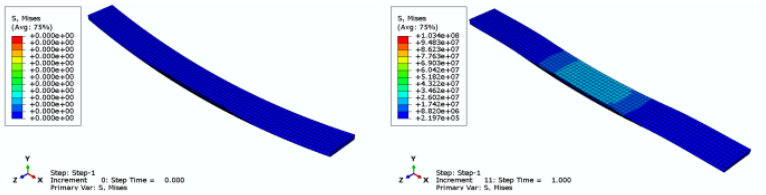

M2

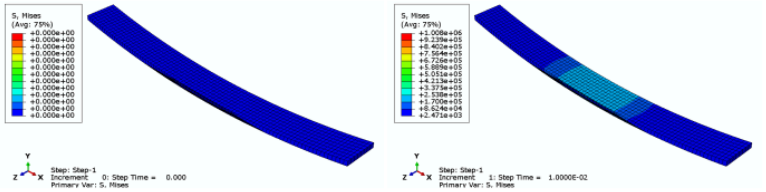

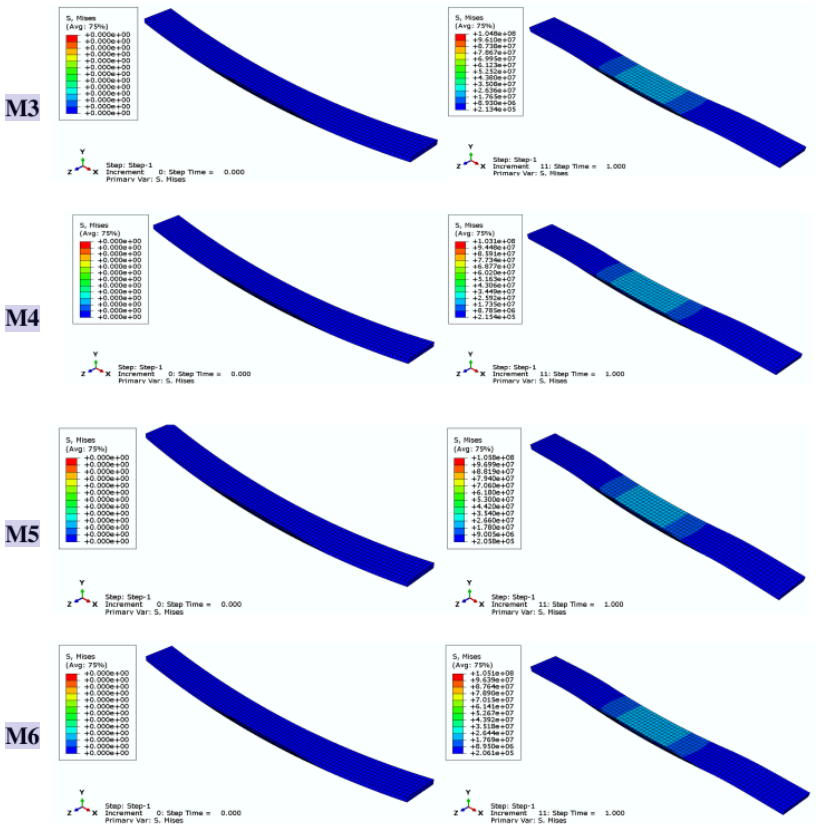

Figure 6.4: Von Mises stress contours for models M1–M6.

It can be concluded that 16/12/8 gradation (M1) is the best; Stress distribution is uniform and minimal concentrations in the critical fixed region. On the other side, setups like 8/16/12 (M6) had severe stress localization that could lead to material failure. These results clearly highlights the importance of strategically placing reinforcement to optimize load distribution and enhance the structural performance of functionally graded leaf springs.

M1

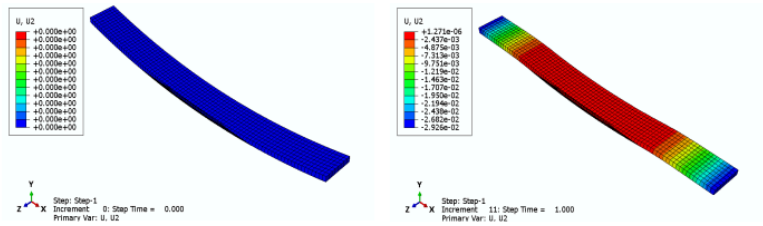

6.5.2 Deflection Analysis

ABACUS was used to simulate and evaluate the deflection behaviour of the functionally graded composite leaf spring plate. The Central portion of the plate was fixed and a bending load was applied symmetrically at both ends. Six configuration, M1–M6, were analysed; These layers incorporate 8 wt.%, 12 wt.% and 16 wt.% B_4C as shown in Figure 6.5 within five-layer structure.

The deflection of configuration depicted by Model M1 (16/12/8/12/16) is lowest. The 16 wt.% B_4C outer layers resists tensile stresses, whereas the 12 wt.% layer helps in transfer stress and the 8 wt.% layer provides a gradual stiffness transition.

The deflection of configuration of Model M2 (16/8/12/8/16) is slightly higher due to the weaker 8 wt.% middle layer whereas the 16 wt.% outer layers still compensation.

For Model M3 (12/16/8/16/12) relatively low deflection was observed. The 16 wt.% reinforcement near the mid-thickness boosts central stiffness. However, the lower outer reinforcement moderates its performance compared to M1.

.

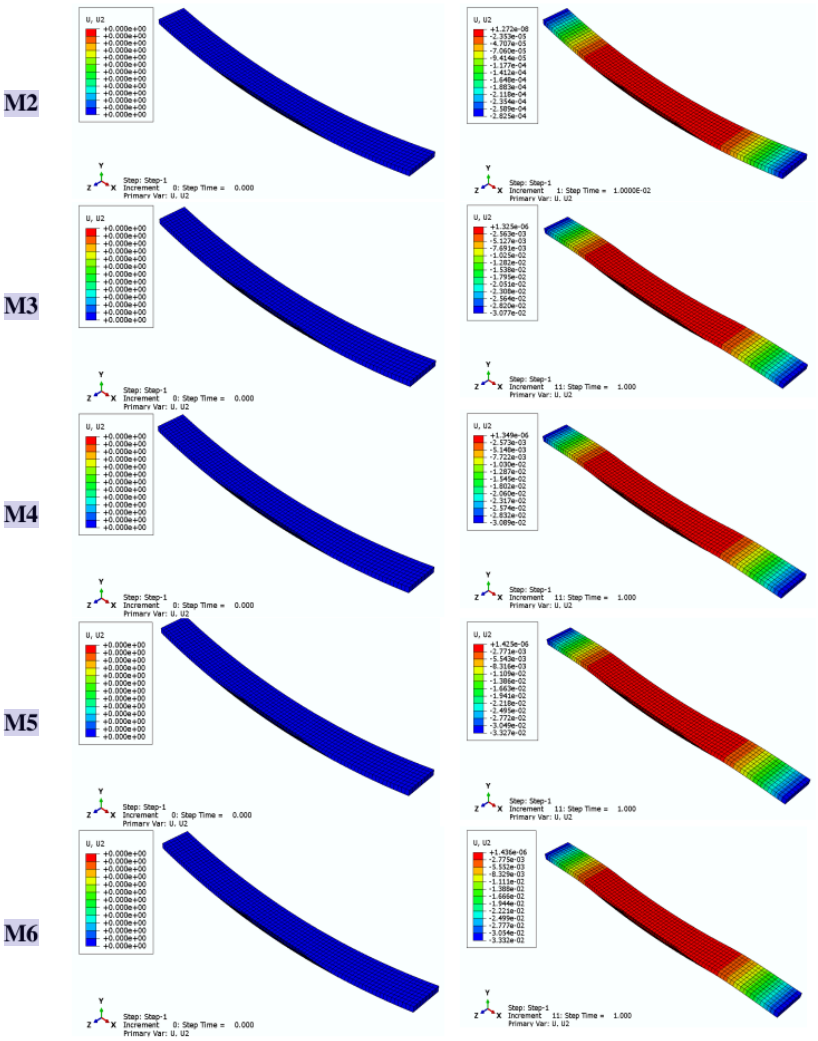

Figure 6.5: Vertical deformation for FGM models M1-M6.

Model M4 (12/8/16/8/12) showed higher deformation because the 8 wt.% central layer weakens the load path. Even though the 16 wt.% layer is present, its effect is insufficient to stabilize bending.

Model M5 (8/12/16/12/8) exhibited further increased deflection, as weaker outer surfaces and mid-level reinforcement produce non-uniform stiffness across thickness.

Model M6 (8/16/12/16/8) displayed the maximum deformation among all configurations. The low-stiffness outer layers and inconsistent reinforcement distribution lead to poor load-bearing capability and reduced structural integrity under bending

6.6 Layer-wise Stress and Deflection Analysis

To investigate the influence of reinforcement gradation through the thickness, the von Mises stress and vertical deflection were evaluated at five layers (L1–L5) of the composite leaf spring. The results are presented with respect to the leaf mid-span, which is the point of maximum bending under symmetric loading. Since the bending response is inherently symmetric about the centre, the plots are referenced to the midpoint rather than absolute coordinates. This representation isolates the mechanical effect of reinforcement positioning without being influenced by geometric distance.

6.6.1 Layer-wise Von Mises Stress

Layer-wise von Mises stress distribution of the FGM leaf spring for 16/12/8, 12/16/8 and 8/12/16 wt.% B_4C gradations under symmetric bending shown in figure 6.6.

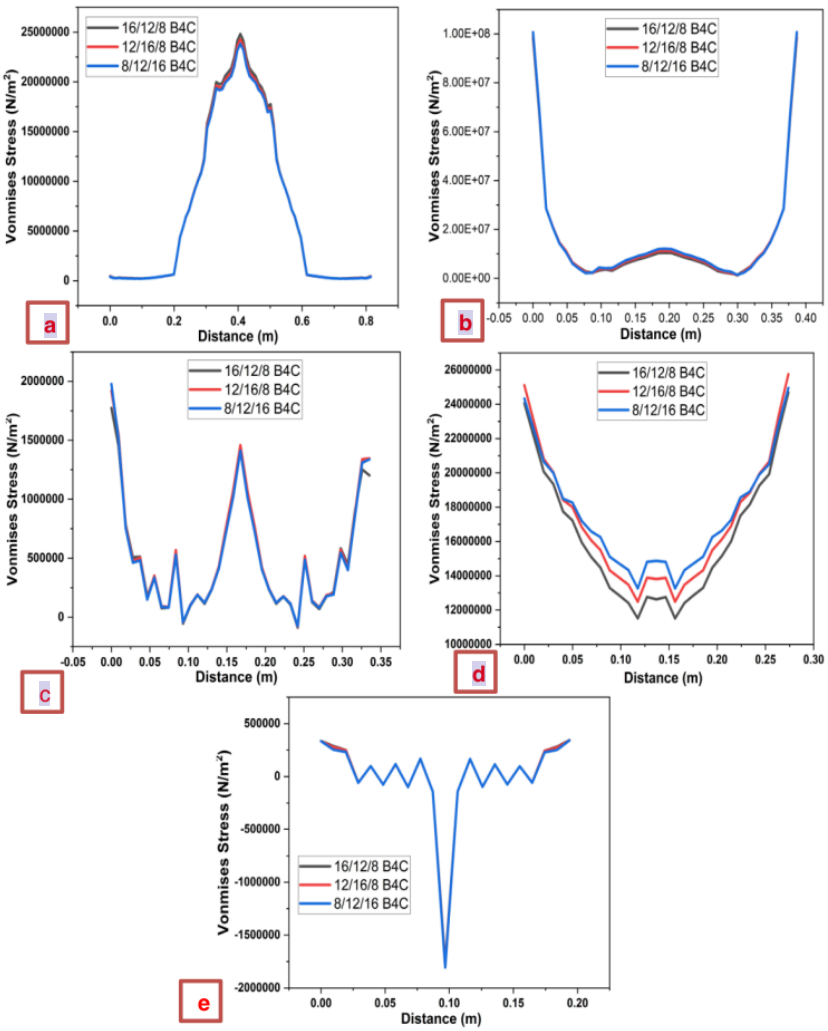

Figure 6.6: Layer-wise von Mises stress distribution (L1–L5) of the FGM leaf spring for 16/12/8, 12/16/8 and 8/12/16 wt.% B_4C gradations under symmetric bending.

Layer L1 (top tensile surface): The stress profiles exhibit a bell-shaped trend, with peak stress at the midpoint and a gradual reduction toward the ends. All gradations, but 8/12/16 follow similar trends. Gradation, 8/12/16 shows slightly higher peak values. This clearly indicates reduced tensile resistance at the outer

surface. Also, gradation, 16/12/8 demonstrates marginally lower stress. This confirms the benefit of higher reinforcement at the top layer. Top layer directly carries tensile bending loads.

Layer L2: U-shaped response is observed for layer L2. Ends shows higher stresses and reduced magnitudes of stress around the centre. Lowest stress is exhibited by 16/12/8 configuration, whereas shows highest stress values. This clearly indicates, improvement in stress abatement by reinforcement placement in sub surface region.

Layer L3: Localized oscillations observed in for all configurations. The 8/12/16 gradation exhibits larger fluctuations and local peaks. This clearly reflects poor stress uniformity across mid-depth layers whereas, for gradation 16/12/8 smoother distribution is observed.

Layer L4: Stresses start picking up again towards the centre. The configuration 16/12/8 is best with the lowest stress levels, whereas the configuration 8/12/16 exhibits higher stresses. This clearly indicates that flipping the reinforcement (low on top, high in core) doesn't make any difference in the structure. Stress intensities begin to increase again toward the centre. The configuration 16/12/8 yields the lowest stress, while 8/12/16 shows consistently higher magnitudes, reinforcing the observation that inversion of reinforcement (low on top, high in core) degrades structural response.

Layer L5 (bottom surface): The arrangement 8/12/16 exhibits sharp stress drop. This indicates unstable stress transfer near the compression side. The configurations 16/12/8 and 12/16/8 exhibit smoother profiles. Smoother profiles indicates more uniform stress redistribution toward the lower layers.

To conclude, we can clearly state that 16/12/8 gradation demonstrates superior stress uniformity and lowest peak intensities, whereas 8/12/16 exhibits higher concentrations and layer sensitivity.

6.6.2 Layer-wise Deflection Behaviour

The deflection curves for all layers are symmetric about the centre, with maximum displacement at the mid-span and minimum values at the edges shown in Figure 6.7. This pattern corresponds to classical bending deformation of simply supported or centrally constrained beams.

Across L1–L5, the same trend is observed:

- 8/12/16 B_4C: lowest deflection (highest stiffness)
- 12/16/8 B_4C: moderate deflection
- 16/12/8 B_4C: highest deflection (lowest stiffness)

The reduced deflection in 8/12/16 arises from reinforcement concentration around the neutral plane, which increases bending rigidity. Conversely, 16/12/8 places higher stiffness at outer layers, yielding more favourable stress distribution but slightly lower flexural rigidity.

Although differences across layers are small, they are systematic: deflection magnitude decreases from surface (L1) towards mid-depth layers (L4–L5), reflecting the transition from dominant tension/compression to neutral-axis behaviour.

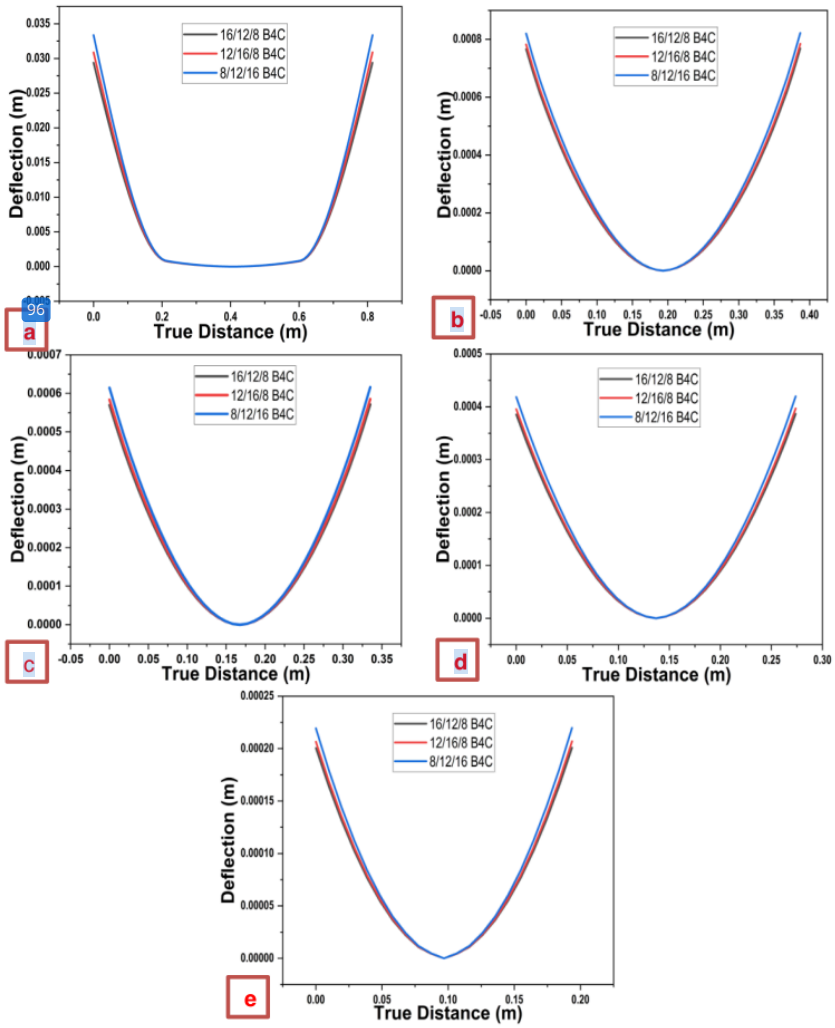

Figure 6.7: Layer-wise vertical deflection profiles (L1–L5) of the FGM leaf spring for 16/12/8, 12/16/8 and 8/12/16 wt.% B_4C gradations under symmetric bending.

6.6.3 Interpretation

The layer-wise results confirm that reinforcement positioning governs the mechanical response of the FGM leaf.

- Gradations favouring outer layers (16/12/8) reduce stress peaks and improve fatigue reliability.
- Gradations centred toward the core (8/12/16) enhance stiffness but induce stress instability and larger gradients along thickness.

Therefore, 16/12/8 provides the best balance of stress uniformity and structural safety, whereas 8/12/16, despite reducing displacement, increases local stresses and is less desirable for long-term service loads.

6.7 Optimization of Gradation

The optimization of the reinforcement gradient in the functionally graded Al7075–B_4C leaf spring plate was carried out using the validated finite element model developed in this chapter. Unlike conventional uniform composite plates, the mechanical performance of a graded plate depends not only on the reinforcement weight fraction but also on the sequence and positioning of reinforcement layers across the thickness. The main goal is to find the graded configuration for that configuration which minimizes stress concentration in the critical central region and maintains sufficient bending stiffness under operational loading.

The optimization is not targeted at maximizing a single parameter in isolation. Instead, it considers the dual design requirements of a suspension leaf spring:

(I) Low stress to improve fatigue life and avoid crack initiation, and

(II) Low deflection to ensure stability during vertical load fluctuations and to maintain the desired ride comfort.

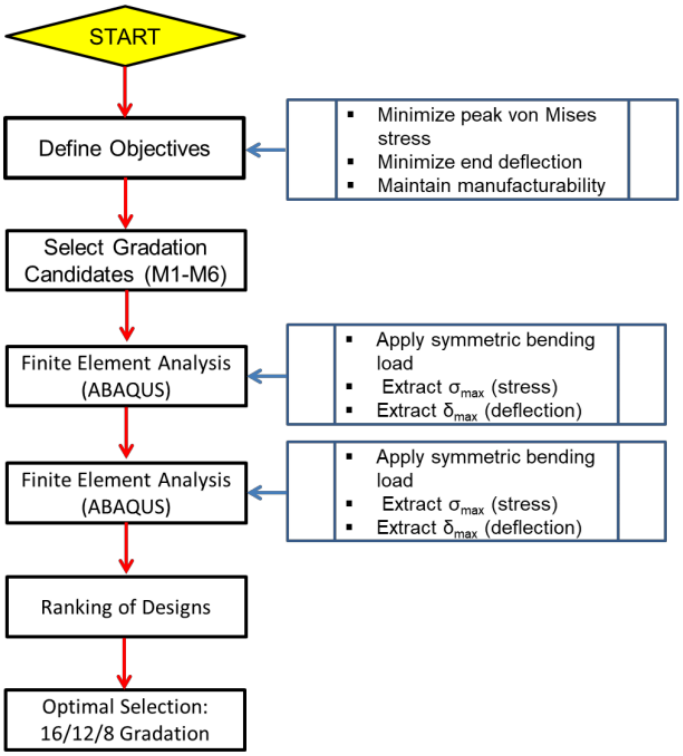

Figure 6.8: Flowchart of the optimization methodology for reinforcement gradient selection in the FGM Al7075–B_4C leaf spring.

These two performance indicators are strongly interdependent in functionally graded materials. A gradient that increases stiffness may also increase stress concentration, while a gradient that reduces stress may allow greater compliance. Therefore, a performance-balanced optimization approach is adopted. The methodology adopted for the optimization of reinforcement gradient selection in the FGM Al7075–B_4C leaf spring shown in figure 6.8.

6.7.1 Objectives

The objective of gradient optimization is to determine the reinforcement distribution that produces the most favourable mechanical response under bending.

The optimization targets are as follows:

- Minimize peak von Mises stress at the central fixed region and layer interfaces.
- Minimize end deflection of the leaf spring under service loading.
- Maintain manufacturability, ensuring the gradient configuration can be realized through the adopted fabrication route (five-layer casting with uniform ends).

These objectives directly reflect operational requirements. Peak stress governs durability and crack initiation sites, whereas excessive deflection leads to instability, increased damping demands, and reduced performance in suspension systems.

6.7.2 Evaluation Metrics

Comparative analysis of six model / gradations was done. Each model features five graded layers at the centre with uniform reinforcement at both ends. Following data were taken from the finite element simulations:

- Maximum von Mises stress in the plate.
- Maximum vertical displacement at the free ends.
- Stress distribution uniformity, assessed qualitatively through contour smoothness and concentration band patterns.

These responses were selected because they capture the key performance indicators of graded structural members. Von Mises stress represents multiaxial failure

behaviour. End deflection indicates bending rigidity. The stress – deflection response with reinforcement layer ordering varies significantly, opposite to mass or volume, which remains constant for all models.

6.7.3 Ranking of Designs

All the six gradient configurations manifested distinct mechanical properties. A summary of stress and deflection responses is provided in Table 6.2.

Table 6.2: Numerical ranking of design candidates:

Model	Max bending stress (N/m^2)	Max deflection (m)	Rank
M1 (16/12/8)	1.034×10^{8}	2.926×10^{-2}	Best
M3	1.048×10^{8}	3.077×10^{-2}	2
M4	1.031×10^{8}	3.089×10^{-2}	3
M2	1.041×10^{8}	3.003×10^{-2}	4
M5	1.058×10^{8}	3.327×10^{-2}	5
M6 (8/16/12)	1.051×10^{8}	3.332×10^{-2}	Worst

Model M1 (16/12/8/12/16) exhibited the lowest peak stresses and a smooth stress field across thickness. Stress concentration at the central fixed region was minimal, and layer-wise stress oscillations were reduced. Although its deflection was slightly higher than some core-dominant schemes, it remained within acceptable bounds.

Model M3 (12/16/8/16/12), showed moderate stress attenuation and deformation. The elevated reinforcement near the mid-thickness improved stiffness but reduced the ability of outer layers to resist tensile bending stresses.

Model M2 and M4 exhibited unbalanced behaviour, where reduced reinforcement in the inner layer intensified stress gradients. The 8 wt.% core layer

produced discontinuities, amplifying local stress regions and increasing deflection sensitivity.

Configurations in Model M5 and M6, with highest reinforcement at the internal layers and lowest reinforced layers on external layer, exhibited below par performance. Localised hotspots near fixed region and bending surfaces were clearly shown in stress contours. It was found that deflection was less comparatively but at the expense of reduction in reliability and higher risk to structure. For applications in which long term fatigue and safe stress transfer dominates, stress driven ranking has high priority than stiffness alone, such as suspension systems.

6.7.4 Selection of Optimal Configuration

The reinforcement gradation (M1- 16/12/8) was selected as the optimal configuration considering dual objectives and manufacturing constraints. This configuration is arranged such that it places strongest B_4C concentration in the tensile and compressive layers. This placement enables efficient stress redistribution during bending. Interlayer stress accumulation is reduced and stiffness transition is mediated by intermediate 12 wt.% layer. The abrupt stiffness is prevented by inner layer with 8 wt.% concentration which prevents mixed compliance.

The 16/12/8 configuration demonstrates a favourable combination of low peak stress, smooth stress transfer and acceptable deflection. This makes it a mechanically stable arrangement. This configuration is also compatible with the fabrication process employed for the physical leaf spring. The strategic placement of lower reinforcement levels within the core and higher reinforcement levels at the surfaces aligns with bending mechanics principles, where outer fibres are subjected to

maximum stress. Due to which the optimization results suggest that gradient positioning exerts a more significant influence on structural performance than the absolute reinforcement percentage in functionally graded structures.

6.8 Discussion

The mechanical performance of the FGM leaf spring strongly depends on reinforcement placement relative to the bending neutral axis. Upper-layer enrichment (16 wt.%) improves tensile resistance, reduces stress peaks, and enhances stiffness. Lower-dominant gradations (8/12/16) confirmed poor uniformity and undesirable deflection trends.

The results also confirm the value of distributing higher reinforcement to outer layers and moderate reinforcement centrally to maintain stress transfer competence.

6.9 Conclusions

This chapter presented a comprehensive finite element investigation of the fabricated functionally graded Al7075-B_4C leaf spring plate. The geometry, layering scheme, and material compositions were modelled to replicate the actual fabricated specimen, ensuring consistency between numerical and experimental studies. The simulation approach accurately represented the bending conditions of a real suspension system, with the central region constrained and symmetric vertical loads applied at both free ends. This configuration enabled realistic evaluation of stress transfer, stiffness, and deformation modes.

The analysis revealed that the reinforcement gradient strongly manages the structural response, more than the absolute amount of B_4C used. Gradations enriched

at the outer tensile and compressive surfaces (16/12/8/12/16) produced smoother stress contours, minimized peak von Mises stress near the central fixation, and reduced layer-wise stress fluctuations. In contrast, core-dominant gradations (M5 and M6) generated sharp local stress peaks, non-uniform stress waves, and higher layer sensitivity, making them mechanically susceptible under cyclic loading. The layer-wise stress plots demonstrated that higher reinforcement near the surface layers improves bending resistance and reduces interface discontinuities.

Deflection results complemented the stress findings. While core-reinforced configurations (8/12/16 and 8/16/12) yielded lower overall deformation, they did so at the expense of stress uniformity. The 16/12/8 gradation achieved the most balanced behaviour, combining acceptable stiffness with reduced stress intensities. This arrangement aligns with bending theory, where the outer layers of a flexural member carry the maximum tensile and compressive stresses, and thus benefit from higher reinforcement content. Placing intermediate reinforcement in the sub-surface layers further promotes smooth stiffness transitions, reducing the possibility of interlayer cracking.

Considering performance, durability and manufacturing feasibility, the 16/12/8 gradation was identified as the optimal configuration. This gradient not only reduces structural risk in critical regions but is also friendly with the hybrid stir–gravity casting route employed in the current fabrication. The findings demonstrate that reinforcement sequencing is a decisive design variable and properly engineered gradation can significantly enhance the reliability of lightweight FGM suspension components.

CHAPTER 7

CONCLUSIONS, FUTURE SCOPE AND SOCIAL IMPACT

7.1 Conclusions

The current study designed, developed and tested in functional capacity Al7075/B4C metal matrix composites in the automotive automobile leaf springs. The significant conclusions given by this work are as follows in brief and clear statements.

7.1.1 Material Selection and Development

- Al7075 alloy was selected due to the high specific strength and the fact that it can be used in lightweight structural components.
- The choice of B4C reinforcement was due to its low density, high elastic modulus, and thermal stability with aluminium alloys.
- A five-layer graded structure (16/12/8/12/16 wt.% B4C) was developed to offer strength in the outer areas and ductility in the middle area.
- The combination of stir casting and gravity die casting in a melt-route fabrication method was effectively attempted and the graded leaf spring plate made without any defects.

7.1.2 Microstructural and Phase Observations

- The desired variation of reinforcement across layers was ensured by optical and FESEM inspection.
- The core 8 wt.% area exhibited more extensive grains and increased ductility whereas the outer 16 wt.% region exhibited more refined grains with a large number of hard particles.
- No harmful intermetallic phases at the interface were detected by EDS and XRD analysis.
- Grain refinement, Orowan strengthening, and load transfer mechanisms were observed.
- XRD residual stress values revealed that the compressive stress was on the rise with the increase in the B_4C content, which plays a part in the enhancement of crack resistance.

7.1.3 Mechanical Performance

- Tensile, hardness and flexural tests indicated that overall strength increased clearly with increase in reinforcement.
- The 12 wt.% B4C region was a good compromise between strength and ductility with the 16 wt.% region being the hardest.
- Central 8 wt.% layer proved to be tough enough to avoid brittle failure, enhancing the impact resistance.
- Impact testing revealed that the graded configuration retained energy absorption in the core and limited brittle fracture of the outer layers.

- Dynamic mechanical analysis indicated constant storage modulus and damping behaviour over the temperature range of automotive operation.

7.1.4 Computational Validation and Optimization

- Application of FEA with central clamping and symmetric loading simulated service-like boundary conditions.
- The 16/12/8/12/16 gradient yielded the lowest deflection, the most homogenous stress distribution and the least concentration around restricted areas.
- Designs that had weaker outer layers resulted in high deformation at mid-span and concentrated stress.
- The chosen graded architecture hence has better stiffness-life ratio compared to homogenous MMC plates.

7.1.5 Overall Outcome of the Research

- Result: A fully developed and verified FGM leaf spring plate was created, which provides better stiffness, stress distribution, and weight reduction.
- The study created a methodological system of material selection, gradation design, experimental characterization and computational validation.
- The suggested FGM spring design offers better flexural performance and lifespan, which may be appropriate to vehicle suspensions.

7.2 Future Scope

- Do fatigue and durability tests to establish long-term behaviour when loaded with road-profile.
- Study thermal fatigue, creep and temperate dependent damping with braking and high heat conditions.
- Explore inter-leaf wear, fretting behaviour, and lubrication in full leaf-spring assemblies.
- Research better production pathways like semi-solid casting, automated graded feeding, and shot-peening.
- Apply the principle to multi-leaf assemblies and hybrid FGM polymer systems, as well as other lightweight suspension parts.

7.3 Social and Industrial Impact

- ***Economic benefit:*** The decrease in weight decreases the fuel and maintenance expenses of commercial vehicles.
- ***Safety improvement:*** Enhanced stress distribution will slow down the creation of cracks and decrease unexpected failures.
- ***Sustainability:*** Reduced material consumption and extended component life enable efficient and sustainable production.
- ***Industrial applicability:*** The technology can be applied to the defence vehicles, mining trucks, agriculture machinery and freight transport systems.

Final Statement

This research demonstrates that functionally graded Al7075/B_4C leaf spring plates can be successfully designed, fabricated, and optimized to surpass conventional steel and homogeneous MMC springs. The combined insights from microstructure, mechanical testing, and FEA provide a strong foundation for future innovations in lightweight and high-performance suspension systems.

Final Thesis

ORIGINALITY REPORT

9%	4%	6%	1%
SIMILARITY INDEX	INTERNET SOURCES	PUBLICATIONS	STUDENT PAPERS

PRIMARY SOURCES

1	Ranjeet Kumar Singh, Ramesh Chandra Singh. "Evaluation of the mechanical and microstructural properties of an Al7075/B4C/Gr FGM plate fabricated using a stir casting process", Journal of Mechanical Science and Technology, 2024 Publication	2%
2	dspace.dtu.ac.in:8080 Internet Source	1%
3	Ranjeet Kumar Singh, Nagendra Kumar Maurya, Ambuj Saxena, Abhishek Pandey, Shailendra Kumar Verma. "Development and Characterization of Functionally Graded Al2024-Ni Metal Matrix Composite Leaf Plate under T3 Heat Treatment", MAPAN, 2025 Publication	<1%
4	Pathinettampadian Gurusamy, Murugesan Devarajan Vijayakumar, Sathiyamoorthi Ramalingam. "Advances in Additive Manufacturing Technologies - Proceedings of 6th International Conference on Advances in Additive Manufacturing Technologies (ICAAMT 2024), December 19-20th, 2024, Chennai,	<1%

India Shaping the Future of Digital Fabrication and Smart Manufacturing", CRC Press, 2026
Publication

5	"Composite Materials Engineering, Volume 2", Springer Science and Business Media LLC, 2018 Publication	<1 %
6	www.researchgate.net Internet Source	<1 %
7	Sushanta Ghuku, Kashi Nath Saha. "A Review on Stress and Deformation Analysis of Curved Beams under Large Deflection", International Journal of Engineering and Technologies, 2017 Publication	<1 %
8	idr.nitk.ac.in Internet Source	<1 %
9	worldwidescience.org Internet Source	<1 %
10	Aykut Çanakçı, Abdullah Hasan Karabacak, Müslim Çelebi, Serdar Özkaya, Kürşat Alp Arpacı. "A Study on the Optimization of Nano-B4C Content for the Best Wear and Corrosion Properties of the Al-Based Hybrid Nanocomposites", Arabian Journal for Science and Engineering, 2024 Publication	<1 %
11	deepblue.lib.umich.edu Internet Source	<1 %

12	Subhash Singh, Kaushik Pal. "Influence of Texture Evolution on Mechanical and Damping Properties of SiC/Li2ZrO3/Al Composite Through Friction Stir Processing", Journal of Engineering Materials and Technology, 2020 Publication	<1 %
13	link.springer.com Internet Source	<1 %
14	A. Gnanavelbabu, M Prahadeeswaran, E. Vinothkumar, Rajesh Jesudoss Hynes Navasingh, Jana Petru. "Investigating the influence of stir-ultrasonication-squeeze casting parameters on microstructure and mechanical performance of AA2014/nAl2O3 composites for aerospace applications", Materials & Design, 2025 Publication	<1 %
15	M. Hemanth Kumar, R. Saravanan, B. K. Naveen Kumar, Raman Kumar, T. Hemanth Raju, A. Bhowmik, Madeva Nagaral, Rashmi P. Shetty. "Synthesis of Aluminium-Ceramic Composites: Mechanical-Wear Characterization of Al7085 – B4C Micro Composites", Journal of Bio- and Tribo-Corrosion, 2025 Publication	<1 %
16	Piyush R. Thakre, Raman P. Singh, Geoffrey Slipher. "Mechanics of Composite, Hybrid and	<1 %

	Multifunctional Materials, Volume 5", River Publishers, 2025 Publication	
17	"Thermal Load", Encyclopedia of Thermal Stresses, 2014. Publication	<1 %
18	hdl.handle.net Internet Source	<1 %
19	River Rapids, Meredith Silberstein, Piyush R. Thakre, Raman Singh. "Mechanics of Composite and Multi-functional Materials, Volume 7", River Publishers, 2025 Publication	<1 %
20	jcpr.or.kr Internet Source	<1 %
21	Submitted to GL Bajaj Institute of Technology and Management Student Paper	<1 %
22	constellation.uqac.ca Internet Source	<1 %
23	Gomes, J.R., A.S. Miranda, L.A. Rocha, and Rui F. Silva. "Effect of Functionally Graded Properties on the Tribological Behaviour of Aluminium-Matrix Composites", Key Engineering Materials, 2002. Publication	<1 %
24	www.degruyter.com Internet Source	<1 %

25	Submitted to University of Plymouth Student Paper	<1 %
26	Submitted to Amity University Student Paper	<1 %
27	Urena. "Scanning and transmission electron microscopy study of the microstructural changes occurring in aluminium matrix composites reinforced with SiC particles during casting and welding: interface reactions", Journal of Microscopy, 11/1999 Publication	<1 %
28	www.springerprofessional.de Internet Source	<1 %
29	Qiumin Xie, Yunxin Wu, Tao Zhang, Shunli Peng, Zhongyu Yuan. "Effects of Quenching Cooling Rate on Residual Stress and Mechanical Properties of a Rare-Earth Wrought Magnesium Alloy", Materials, 2022 Publication	<1 %
30	Submitted to Higher Education Commission Pakistan Student Paper	<1 %
31	J.W. Simmons. "Influence of nitride (Cr2N) precipitation on the plastic flow behavior of high-nitrogen austenitic stainless steel", Scripta Metallurgica et Materialia, 1995 Publication	<1 %

32	Submitted to Northampton College, Northamptonshire Student Paper	<1%
33	S Sivakumar, KP Padmanaban, M Uthayakumar. "Wear behavior of the Al (LM24)–garnet particulate composites under dry sliding conditions", Proceedings of the Institution of Mechanical Engineers, Part J: Journal of Engineering Tribology, 2014 Publication	<1%
34	Wang, Xu, Sabu John, and He Ren. "A Study of Squeal Noise in Vehicle Brake System", Volume 8 Mechanics of Solids Structures and Fluids Vibration Acoustics and Wave Propagation, 2011. Publication	<1%
35	dspace.mit.edu Internet Source	<1%
36	researchonline.ljmu.ac.uk Internet Source	<1%
37	www.tandfonline.com Internet Source	<1%
38	Submitted to Maulana Azad National Institute of Technology Bhopal Student Paper	<1%
39	Sónia Simões. "Advances in the Design and Development of Lightweight Metal Matrix	<1%

	Composites: Processing, Properties, and Applications", Metals, 2025 Publication	
40	Xiao-Ling Zhao, Lili Hu. "FRP-Strengthened Metallic Structures", CRC Press, 2025 Publication	<1 %
41	journal.mtu.edu.iq Internet Source	<1 %
42	Submitted to Anna University Student Paper	<1 %
43	Md. Nehal Hasnain, Abdullah Haque, Abdul Wahid Chowdhury, Imran Hossain, M.J. Hosen, M.D.I. Bhuyan, Abdul Hannan. "Synthesis of a high-capacitance supercapacitor electrode material Pr2CoCrO6 and study of its structural, magnetic and optical properties", Results in Engineering, 2025 Publication	<1 %
44	Submitted to Phenikaa University Student Paper	<1 %
45	Submitted to Lehigh University Student Paper	<1 %
46	Nhu H.T. Nguyen, Ha H. Bui, J. Kodikara, S. Arooran, F. Darve. "A discrete element modelling approach for fatigue damage growth in cemented materials", International Journal of Plasticity, 2018 Publication	<1 %

47	Pushpendra Kumar Jain, Prashant Baredar, S.C. Soni. "Microstructure and mechanical properties of silicon carbide particle reinforced aluminium 6101 metal matrix composite produced by two-step stir casting", Materials Today: Proceedings, 2020 Publication	<1 %
48	Submitted to South Tyneside College Student Paper	<1 %
49	A. Agbossou, M. Lagache. "Fiber distribution effects in linear viscoelastic behavior of polymer matrix composites: Computation modelling and experimental comparison", Mechanics Research Communications, 1998 Publication	<1 %
50	Eujin Pei, Giselle Hsiang Loh, David Harrison, Henrique de Amorim Almeida, Mario Domingo Monzón Verona, Rubén Paz. "A study of 4D printing and functionally graded additive manufacturing", Assembly Automation, 2017 Publication	<1 %
51	Submitted to Florida State University Student Paper	<1 %
52	Submitted to Munster Technological University (MTU) Student Paper	<1 %
53	Samakande, A.. "Rheological properties of RAFT-mediated poly(styrene-co-butyl	<1 %

	acrylate)-clay nanocomposites [P(S-co-BA)-PCNs]: Emphasis on the effect of structural parameters on thermo-mechanical and melt flow behaviors", Polymer, 20090102 Publication	
54	eprints.utm.my Internet Source	<1 %
55	jukuri.luke.fi Internet Source	<1 %
56	mospace.umsystem.edu Internet Source	<1 %
57	123dok.net Internet Source	<1 %
58	Neal F. Enke. "Mechanics of Deformable Bodies", Eshbach s Handbook of Engineering Fundamentals, 01/12/2009 Publication	<1 %
59	Submitted to Texas A&M University, College Station Student Paper	<1 %
60	resolver.caltech.edu Internet Source	<1 %
61	www.mdpi.com Internet Source	<1 %
62	Mehrdad Khakbiz, Farshad Akhlaghi. "A Hybrid Artificial Intelligence and Tribological Approaches for Surface Characterization of	<1 %

	Nanocomposites", Tribology International, 2025 Publication	
63	Submitted to Panipat Institute of Engineering & Technology Student Paper	<1 %
64	digitallibrary.usc.edu Internet Source	<1 %
65	eprints.lancs.ac.uk Internet Source	<1 %
66	i-rep.emu.edu.tr:8080 Internet Source	<1 %
67	studentsrepo.um.edu.my Internet Source	<1 %
68	www.freepatentsonline.com Internet Source	<1 %
69	www.rsc.org Internet Source	<1 %
70	Ranjit Bauria, M.K. Surappa. " Processing and properties of Al–Li–SiC composites ", Science and Technology of Advanced Materials, 2007 Publication	<1 %
71	S.S. Nayak, V.H. Baltazar Hernandez, Y. Okita, Y. Zhou. "Microstructure–hardness relationship in the fusion zone of TRIP steel welds", Materials Science and Engineering: A, 2012 Publication	<1 %

72	Tomasz Trzepieciński, Sherwan Mohammed Najm. "Current Trends in Metallic Materials for Body Panels and Structural Members Used in the Automotive Industry", Materials, 2024 Publication	<1 %
73	archive.org Internet Source	<1 %
74	safem.info Internet Source	<1 %
75	www.aksteel.com Internet Source	<1 %
76	www.ijfrcsce.org Internet Source	<1 %
77	www.ir.nctu.edu.tw Internet Source	<1 %
78	www.mat.mines-paristech.fr Internet Source	<1 %
79	Amal NassaR, Eman NassaR. "Tensile behaviors of aluminum matrix composites in extrusion simulation experiments", 2012 2nd International Conference on Advances in Computational Tools for Engineering Applications (ACTEA), 2012 Publication	<1 %
80	M. Gupta, F. Mohamed, E. Lavernia, T. S. Srivatsan. "Microstructural evolution and mechanical properties of SiC/Al2O3	<1 %

particulate-reinforced spray-deposited metal-matrix composites", Journal of Materials Science, 1993
Publication

81	Onoro, J.. "High-temperature mechanical properties of aluminium alloys reinforced with boron carbide particles", Materials Science & Engineering A, 20090115 Publication	<1 %
82	Peter Domone, John Illston. "Construction Materials - Their nature and behaviour", Spon Press, 2018 Publication	<1 %
83	Shoogo Ueno. "Bioimaging - Imaging by Light and Electromagnetics in Medicine and Biology", CRC Press, 2020 Publication	<1 %
84	Song, Sihun. "Memristor-Based Control for Hardware Parameter Sensitivity Abatement in Power Electronic Converters", The Florida State University, 2025 Publication	<1 %
85	Ustinov, A.I.. "Effect of grain size on the damping capacity of quasicrystalline Al-Cu-Fe materials", Surface & Coatings Technology, 20080815 Publication	<1 %
86	Yalcin, B.. "Molecular origins of toughening mechanism in uniaxially stretched nylon 6	<1 %

	films with clay nanoparticles", Polymer, 20080317 Publication	
87	ajme.aut.ac.ir Internet Source	<1 %
88	dr.ntu.edu.sg Internet Source	<1 %
89	dspace.lib.cranfield.ac.uk Internet Source	<1 %
90	iopscience.iop.org Internet Source	<1 %
91	ntnuopen.ntnu.no Internet Source	<1 %
92	repository.dl.itc.u-tokyo.ac.jp Internet Source	<1 %
93	repository.tudelft.nl Internet Source	<1 %
94	J Simmons. "Strain hardening and plastic flow properties of nitrogen-alloyed Fe-17Cr-(8–10)Mn-5Ni austenitic stainless steels", Acta Materialia, 1997 Publication	<1 %
95	Zeng, Xiaohan. "Texture Evolution of Hot Rolled Titanium Alloys.", The University of Manchester (United Kingdom) Publication	<1 %

96	Dahal, Neelima. "Microwave Flow Cytometer for Single Cell Detection, Differentiation, and Drug Effect Study", Clemson University, 2025 Publication	<1%

Exclude quotes	Off	Exclude matches	Off
Exclude bibliography	Off		